DOCTORAL (Ph.D.) DISSERTATION

Polycyclic aromatic hydrocarbons (PAHs) in water and sediments of three major rivers: Spatial distribution, pollution source apportionment, ecological risks and human health impacts

DOI:10.18136/PE.2025.932

Thesis submitted for obtaining a Ph.D. degree in the Biochemical, Environmental and Chemical Engineering

Doctoral School of Chemical Engineering and Material Science

Faculty of Engineering

University of Pannonia

Written by:

Ruqayah Ali Naser Grmasha

MEngSc UNSW, Sydney, Australia in Environmental Engineering

Supervisor:

Prof. Dr. Csilla Stenger-Kovács

Faculty of Engineering, Center for Natural Science

Research Group of Limnology

Veszprém, Hungary

2025

Polycyclic aromatic hydrocarbons (PAHs) in water and sediments of three major rivers: Spatial distribution, pollution source apportionment, ecological risks and human health impacts

Thesis submitted for obtaining a Ph.D. degree in the Biochemical, Environmental and Chemical Engineering

Doctoral School of Chemical Engineering and Material Science

Faculty of Engineering

University of Pannonia

Written by: Ruqayah Ali Naser Grmasha

Supervisor: Prof. Dr. Csilla Stenger-Kovács

Propose acceptance (yes / no) .....

(Supervisor/s)

As a reviewer, I propose acceptance of the thesis:

Name of Reviewer:

..... yes / no .....

(Reviewer)

Name of Reviewer:

..... yes / no .....

(Reviewer)

The PhD-candidate has achieved .....% at the public discussion.

Veszprém

.....

(Chairman of the Committee)

The grade of the PhD Diploma ..... (.....%)

Veszprém

.....

(Chairman of UDHC)

Publications related to this dissertation

1- Grmasha, R. A., Stenger-Kovács, C., Al-Sareji, O. J., Al-Juboori, R. A., Meiczinger, M., Andredaki, M., ... & Al-Ansari, N. (2024). Temporal and spatial distribution of polycyclic aromatic hydrocarbons (PAHs) in the Danube River in Hungary. Scientific Reports, 14(1), 8318. **D1, IF=3.8**

2- Grmasha, R. A., Stenger-Kovács, C., Bedewy, B. A. H., Al-Sareji, O. J., Al-Juboori, R. A., Meiczinger, M., & Hashim, K. S. (2023). Ecological and human health risk assessment of polycyclic aromatic hydrocarbons (PAH) in Tigris River near the oil refineries in Iraq. Environmental Research, 227, 115791. **D1, IF=8.3**

3- Grmasha, R. A., Abdulameer, M. H., Stenger-Kovács, C., Al-Sareji, O. J., Al-Gazali, Z., Al-Juboori, R. A., ... & Hashim, K. S. (2023). Polycyclic aromatic hydrocarbons in the surface water and sediment along Euphrates River system: Occurrence, sources, ecological and health risk assessment. Marine Pollution Bulletin, 187, 114568 **Q1, IF=7.1**.

Abstract

Water is one of the planet's most critical and valuable resources, essential not only for sustaining human life but also for residential, agricultural, and industrial applications. Over recent decades, rapid industrialization and population growth have significantly increased water contamination through various pollutants, resulting in substantial declines in water quality and posing serious threats to aquatic ecosystems. These pollutants include, but are not limited to, an array of emerging organic compounds introduced globally at an accelerated rate each year. Among these compounds are pharmaceuticals, pesticides, personal care products, and polycyclic aromatic hydrocarbons (PAHs), which are widely utilized in industrial processes. PAHs, in particular, are hazardous compounds composed solely of carbon and hydrogen, structured in two or more interconnected aromatic rings arranged in linear, angular, or clustered forms. Over 100 types of PAHs have been identified, with 16 classified as hazardous by the United States Environmental Protection Agency (EPA). Due to their widespread presence in the environment (air, surface water, soil, and living organisms) many countries have imposed strict regulations concerning the toxic impacts of PAHs on ecosystems and human health. Human exposure to PAHs is associated with a range of toxic effects, including carcinogenicity, endocrine disruption, genotoxicity, neurotoxicity, immunotoxicity, and reproductive toxicity.

This thesis represents the first measurement of contamination levels of 16 PAHs in water and sediments along three major rivers in Hungary and Iraq: the Danube River in Hungary and the Tigris and Euphrates Rivers in Iraq. Sampling was conducted at six locations along the Danube River over a 12-month period, while 13 sites were monitored along the Euphrates River over five months. Additionally, PAHs levels in surface water and sediments near oil refineries along the Tigris River were examined, with samples taken both upstream and downstream from the refinery. The thesis further analyzed the spatial and temporal distribution of PAHs contamination across river basins in the two countries and identified primary sources of PAHs pollution in these rivers. An eco-toxicological risk assessment of PAHs was conducted, along with the calculation of the Incremental Lifetime Cancer Risk (ILCR) for both adults and children along the three rivers. The results were compared with international standards and findings from other studies.

Results from the Danube River indicated that the average concentration of 16 PAHs in water ranged from 224.8 ng/L to 365.8 ng/L, while in sediment, it varied from 316.7 ng/g to 422.9 ng/g. In contrast, both Iraqi rivers exhibited significantly higher levels of PAHs contamination. In

the Tigris River, the average PAHs concentrations ranged from 567.8 to 3750.7 ng/L in water samples and from 5619.2 to 12795.0 ng/g in sediment. For the Euphrates River, average PAHs levels were between 464 and 992 ng/L in water and from 5940 to 9723.9 ng/g in sediment. The correlation between total organic matter (TOM) and PAHs concentrations revealed that both the Danube and Euphrates Rivers exhibited mixed sources of PAHs contamination. In contrast, the Tigris River showed no significant correlation, indicating that PAHs pollution in this river is primarily attributable to oil refinery activities.

These findings underscore the urgent need for the Iraqi government to promptly implement pollution control strategies to protect its water bodies. They also highlight the importance of the Hungarian government establishing stricter guidelines to reduce PAHs levels in the Danube River.

Keywords: Pollution; Diagnostic ratios; Monitoring; Human health risk assessment, Oil refinery; Sediment; Water.

الملخص

يعد الماء أحد أهم الموارد الحيوية والثمينة على كوكب الأرض، حيث لا يقتصر دوره على الحفاظ على حياة الإنسان فحسب، بل يمتد ليشمل استخدامات سكنية وزراعية وصناعية. على مدى العقود الأخيرة، أدت الزيادة السريعة في التصنيع والنمو السكاني إلى تلوث المياه بشكل كبير عبر مجموعة من الملوثات، مما تسبب في انخفاض ملحوظ في جودة المياه وتهديدات خطيرة للنظم البيئية المائية. تشمل هذه الملوثات مجموعة من المركبات العضوية الناشئة التي يتم طرحها عالميًا بمعدلات متزايدة كل عام، من بينها الأدوية، والمبيدات الحشرية، ومنتجات العناية الشخصية، والهيدروكربونات العطرية متعددة الحلقات(PAHs) ، التي تُستخدم بشكل واسع في العمليات الصناعية. وتعد الـ PAHsمركبات خطيرة تتكون فقط من الكربون والهيدروجين، مرتبة في حلقات عطرية متصلة مرتبة بشكل خطي أو زاوي أو في تجمعات. تم تحديد أكثر من 100 نوع من الـPAHs، وتم تصنيف 16 منها كمركبات خطرة من قبل وكالة حماية البيئة الأمريكية .(EPA) وبسبب انتشارها الواسع في البيئة (الهواء، المياه السطحية، التربة، والكائنات الحية)، فرضت العديد من الدول قوانين صارمة للتحكم في تأثيراتها السامة على النظم البيئية وصحة الإنسان. يترافق تعرض الإنسان للـ PAHsمع مجموعة من التأثيرات السامة، بما في ذلك التسرطن، واضطرابات الغدد الصماء، والتسمم الجيني، والتسمم العصبي، وتثبيط المناعة، والتسمم التناسلي.

تمثل هذه الاطروحة أول قياس لمستويات تلوث 16 نوعًا من الـ PAHsفي المياه والرواسب على طول ثلاثة أنهار رئيسية في كل من المجر والعراق: نهر الدانوب في المجر، ونهري دجلة والفرات في العراق. تم أخذ عينات من ستة مواقع على طول نهر الدانوب على مدى 12 شهرًا، بينما تمت مراقبة 13 موقعًا على طول نهر الفرات على مدى خمسة أشهر. كما تم فحص مستويات الـ PAHsفي المياه السطحية والرواسب بالقرب من المصافي النفطية على طول نهر دجلة، حيث تم أخذ عينات من مناطق أعلى وأسفل المصافي. تضمنت الاطروحة أيضًا تحليل التوزيع المكاني والزماني لتلوث الـ PAHsفي أحواض الأنهار في المجر والعراق وتحديد المصادر الرئيسية لهذا التلوث. كما تم إجراء تقييم مخاطر سمّية بيئية للـPAHs، إضافةً إلى حساب مخاطر الإصابة بالسرطان مدى الحياة (ILCR) لكل من البالغين والأطفال على طول الأنهار الثلاثة، ومقارنة النتائج مع المعايير الدولية والدراسات الأخرى.

أظهرت نتائج نهر الدانوب أن متوسط تركيزات الـ PAHsالـ16 في الماء تتراوح بين 224.8 نانوغرام/لتر و365.8 نانوغرام/لتر، بينما تراوحت في الرواسب بين 316.7 نانوغرام/غرام و422.9 نانوغرام/غرام. أما في النهرين العراقيين، فقد كانت مستويات التلوث بالـ PAHsأعلى بشكل ملحوظ؛ حيث تراوحت تركيزات الـ PAHsفي نهر دجلة بين 567.8 و3750.7 نانوغرام/لتر في عينات الماء، وبين 5619.2 و12795.0 نانوغرام/غرام في الرواسب. وفي نهر الفرات، كانت مستويات الـ PAHsتتراوح بين 464 و992 نانوغرام/لتر في الماء، وبين 5940 و9723.9 نانوغرام/غرام في الرواسب. وأظهر التحليل علاقة بين المادة العضوية الكلية (TOM) وتركيزات الـPAHs، حيث وُجدت مصادر مختلطة للتلوث في كل من نهري الدانوب والفرات، في حين لم تظهر علاقة ملحوظة في نهر دجلة، مما يشير إلى أن التلوث بالـ PAHsفي هذا النهر يعود بشكل رئيسي إلى نشاط المصافي النفطية.

تؤكد هذه النتائج على الحاجة الملحة للحكومة العراقية إلى تطبيق استراتيجيات فعالة للسيطرة على التلوث لحماية مواردها المائية. كما تبرز أهمية قيام الحكومة المجرية بفرض إرشادات أكثر صرامة للحد من مستويات الـ PAHsفي نهر الدانوب.

الكلمات المفتاحية: التلوث؛ النسب التشخيصية؛ المراقبة؛ تقييم مخاطر صحة الإنسان؛ مصفاة النفط؛ الرواسب؛ المياه.

Abbreviations

PAHs	Polycyclic Aromatic Hydrocarbons
CPAHs or 7CPAHs	Seven carcinogenic PAHs
DCM	Dichloromethane
EC	European Community
ERL	Effect Range Low
ERM	Effect Range Median
EU	European Union
GC–MS	Gas chromatography-mass spectrometry
HMW PAHs	High molecular weight polycyclic aromatic hydrocarbons
ILCR	Incremental Lifetime Cancer Risk
LMW PAHs	Low molecular weight polycyclic aromatic hydrocarbons
LOD	Limits of detection
MCL	Maximum contamination limit
NIOSH	Occupational Safety and Health
SPE	Solid-phase extraction
SQGs	Sediment quality guidelines
TEF	Toxic Equivalence Factor
TOM	Total organic matter
USEPA	United States Environmental Protection Agency
WFD	Water Framework Directive

Contents

List of Figures

List of Tables

Appendix

ACKNOWLEDGEMENT

I would like to express my heartfelt gratitude to my supervisor, Prof. Dr. Csilla Stenger-Kovács, for her unwavering support, guidance, and encouragement throughout my PhD journey. Her expertise, insightful advice, and constant motivation have been invaluable to my research and personal growth. I am truly fortunate to have had the opportunity to work under her mentorship, and I deeply appreciate all the time and effort she dedicated to my development. Thank you for being a source of inspiration and for making this journey a truly rewarding experience.

I also would like to extend my heartfelt thanks to Dr. Mónika Meiczinger for her invaluable support throughout my PhD journey. Dr. Meiczinger's kindness and willingness to help, both professionally and personally, have had a significant impact on my experience. I am deeply grateful for her assistance, which has been crucial to my success and growth during this challenging period. Her support has truly made a difference in my life.

1. INTRODUCTION

Freshwater is a valuable and scarce resource for both individuals and ecosystems. The protection and preservation of freshwater are increasingly important with the drive to promote food security and sustainable development growth agenda for life below water. The majority of the world's biggest cities were constructed on or near regions of freshwater, mostly rivers [1]. Most research on aquatic systems is primarily concerned with the effects of anthropogenic activities and natural phenomena, such as volcanism and biological processes, on both human health and ecology [2]. The emission levels of several anthropogenic toxins, including Polycyclic Aromatic Hydrocarbons (PAHs), have grown in the environment due to population expansion and associated increases in industrial, agricultural, and urban activities [3]. These chemicals have attracted significant worldwide interest due to their toxicity, persistence, bioaccumulation, and potential adverse health effects on living beings [4]. Thus, the European Union (EU) and the United States Environmental Protection Agency (USEPA) have identified 16 PAHs as priority pollutants among the hundreds of PAHs in the environment [5]. Table 1 shows the main physicochemical properties of the 16 priority PAHs. PAHs could be bounded to soil particles [6] and could also adsorb on suspended particulate matter when entering the water and ultimately settle into the sediment. This is due to their high octanol–water partition coefficient and hydrophobic lipophilicity [7]. Consequently, river sediments are susceptible to PAHs accumulation and release. Moreover, they are commonly used as an indicator for detecting probable emission sources and determining the exposure risk of PAHs to benthic biotas [8]. Therefore, the environmental fate and the possible ecological risk related to PAHs are serious matters of public concern [9].

1.1. PAHs and their sources

They are a class of organic compounds that are ubiquitous hazardous pollutants, present in air, sediments, soil, water, as well as biota, typically as mixes. PAHs comprise solely hydrogen and carbon atoms organized into two or more benzene rings connected in angular, linear, or clustered configurations. They encompass both unsubstituted parent PAHs and their alkyl-substituted derivatives. PAHs are often characterized by low water solubility and low vapor pressure [5]. In the 1970s, USEPA identified 16 PAHs as priority pollutants because of their detrimental effects on human health and the environment, as well as the availability of analytical methods [10]. In 2005,

the European Community (EC) established a list of 15+1 priority PAHs, mostly in reaction to food contamination issues, that encompassed 8 of the PAHs from the USEPA list [11]. The USEPA's priority list is more commonly utilized for examining the environmental impacts of PAHs compared to the EC's list. PAHs are categorized based on their molecular structure and weight into two classes: low molecular weight (LMW) and high molecular weight (HMW). LMW PAHs possess two to three benzene rings, while HMW PAHs have four or more benzene rings [5].

Table 1 Main physicochemical properties of the 16 priority PAHs [5]

	PAHs	Molecular structure [12]	Abb.	CAS number	Solubility at 25 °C (mg/L)	Rings number	Molecular weight (g/mol)	TEF[13]	Log K_{oc}	Log K_{ow}	Vapor pressure (Pa)
LMW	Naphthalene	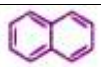	Nap	91-20-3	31	2	128.12	0.001	3.11	3.37	-
	Acenaphthylene		Acy	208-96-8	16.1		152.20	0.001	3.64	4	3.87
	Acenaphthene		Ace	83-32-9	3.8		154.21	0.001	4.02	3.92	$5.96x10^{-1}$
	Fluorene	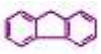	Fl	86-73-7	1.9	3	166.2	0.001	4.35	4.18	$4.27x10^{-2}$
	Phenanthrene		Phe	85-01-8	1.1		178.2	0.001	4.31	4.57	$9.07x10^{-2}$
	Anthracene		Ant	120-12-7	0.045		178.2	0.01	4.39	4.54	$2.27x10^{-3}$
HMW	Fluoranthene		Flu	206-44-0	0.26	4	202.26	0.001	5.04	5.22	$6.67x10^{-4}$
	Pyrene		Pyr	129-00-0	0.132		202.3	0.001	4.86	5.18	$3.33x10^{-4}$
	Benzo[a]anthracene	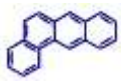	BaA	56-55-3	0.011		228.29	0.1	5.33	5.91	$2.93x10^{-6}$
	Chrysene	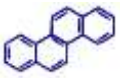	Chr	218-01-9	0.0019		228.3	0.01	5.14	5.86	$8.40x10^{-5}$
	Benzo[b]fluoranthene		BbF	205-99-2	0.0015	5	252.3	0.1	5.72	5.8	0.0012

Benzo[kjfluoranthene	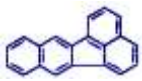	BkF	207-08-9	0.0008		252.3	0.1	5.73	6	$7.6x10^{-4}$
Benzo[a]pyrene		BaP	50-32-8	0.0038		252.3	1	6.24	6.04	$2.3x10^{-3}$
Benzo (g,h,i) perylene		BghiP	191-24-2	0.00026		276.3	1	6.23	6.5	$2.6x10^{-4}$
Indeno(1,2,3-cd)pyrene	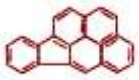	IND	193-39-5	0.00019	6	276.3	0.01	6.20	6.7	0.062
Dibenz(a,h)anthracene	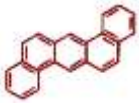	DBA	53-70-3	0.0006	5	278.35	0.1	5.96	6.75	$5.0x10^{-4}$

The origins of PAHs contamination are often categorized into two primary groups. Figure 1 shows natural sources and anthropogenic emissions [14], [15]. Natural events such as volcanic eruptions, forest fires, and moorland fires triggered by thunder as well as lightning are negligible sources of PAHs emissions [16]. Anthropogenic emission sources are the primary contributors to PAHs pollution, categorized into four types: agricultural, automobile, industrial, and domestic waste [17]. Numerous emissions of PAHs result from incomplete combustion processes in the production of steel, iron, cement, dyes, tire rubber, coal-tar pitch, aluminum, insecticides, and fungicides. PAHs are also generated via waste incineration, particulate matter in the asphalt sector, and petroleum refining [18]. Oxygen furnaces, diesel engines, gasoline-powered heavy machinery engines, and coal gasification arc furnaces are other sources of PAHs emissions [16]. The emissions generated from transportation via trains, ships, aircraft, and both light and heavy cars are categorized as PAH-related automotive emissions [17]. Household sources of PAHs encompass wood burning, trash incineration, coal coking byproducts, cooking with oil or gas burners, and kerosene or wood stoves [19]. Agricultural waste and open biomass combustion generate PAHs pollution in rural regions, while automotive industrial, and household, sources predominantly contribute to PAHs contamination in urban areas.

PAHs levels vary seasonally, with peak concentrations occurring in winter, followed by spring, fall, as well as summer, respectively. Reduced fuel combustion, photodegradation efficacy and oxygen diffusion due to low temperatures and quiet winds throughout spring and winter

elevate atmospheric levels of PAHs. Pyrogenic PAHs are generated by some intentional actions, notably the thermal breakdown of petroleum, particularly during incomplete combustion [20]. Consequently, pyrogenic PAHs levels are elevated in urban regions. Petroleum and its derivatives contain Petrogenic PAHs, which are extensively disseminated due to the preservation, transportation, leakage, and utilization of crude oil. HMW PAHs are predominant in pyrogenic sources, while LMW PAHs are prevalent in petrogenic source materials [21].

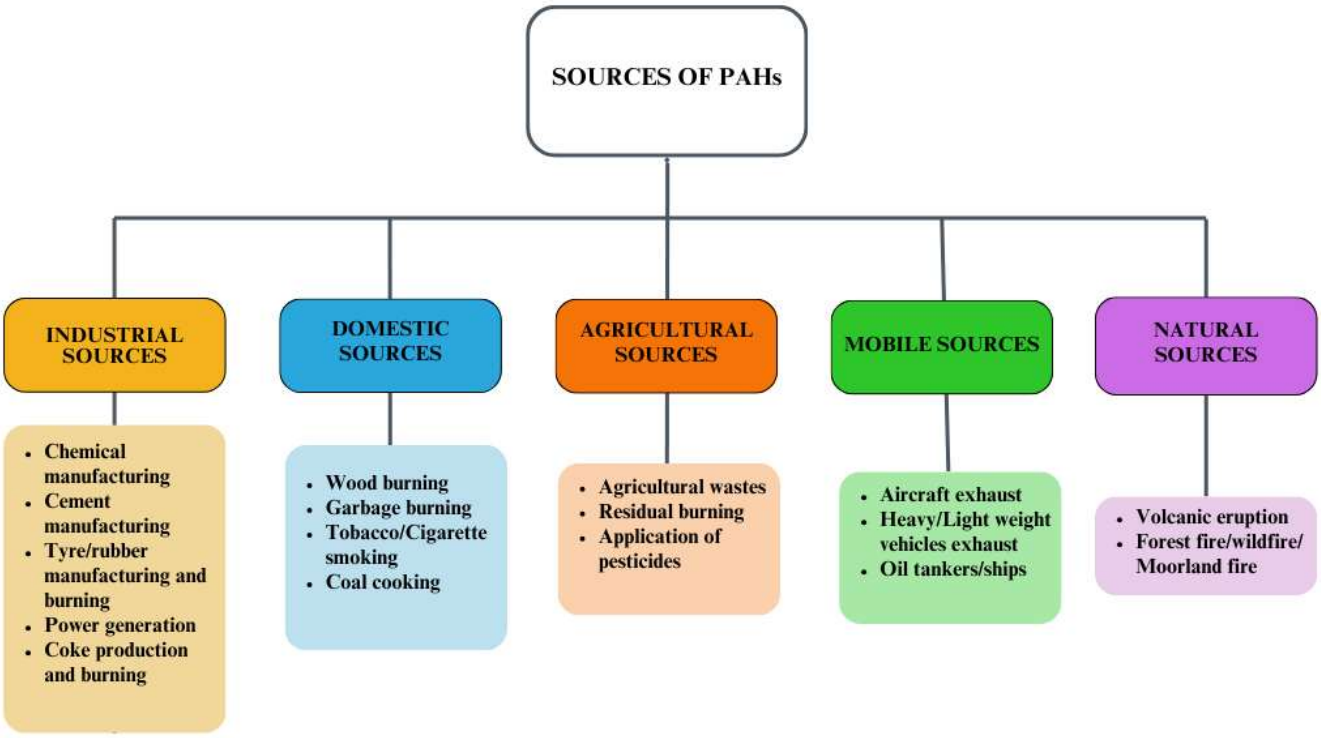

Figure 1 PAHs emission sources.

1.2. PAHs heath effect

The International Agency for Research on Cancer categorizes some PAHs as known, possible, or probable carcinogens to humans (Groups 1, 2A, or 2B). These are naphthalene, benzo[k]fluoranthene, benzo[b]fluoranthene chrysene, and benz[a]anthracene, (Group 2B) as well as benzo[a]pyrene (Group 1) [22]. Certain PAHs are recognized as mutagens, carcinogens, and teratogens, hence presenting a significant risk to human health and well-being.

1.2.1. Short-term health effects

The effects of PAHs on human health mostly depend on the duration and method of exposure, the concentration of PAHs encountered, and the inherent toxicity of the specific PAHs involved [20]. Numerous factors can influence health outcomes, including subjective elements such as pre-existing health conditions and age. The capacity of PAHs to elicit acute health consequences in humans remains ambiguous. Occupational exposure to elevated concentrations of pollutant mixtures containing PAHs has led to symptoms including ocular irritation, nausea, emesis, diarrhea, and disorientation [23]. Nevertheless, the specific components of the mixture responsible for these effects remain unidentified, and other substances typically associated with PAHs may be the source of similar symptoms. Combinations of PAHs are recognized to induce inflammation and skin irritation. Anthracene, naphthalene and benzo(a)pyrene are direct irritants to the skin. Benzo(a)pyrene and anthracene are identified as skin sensitizers, capable of eliciting allergic reactions in the skin of both animals and humans [20].

1.2.2 Long-term health effects

Long-term or chronic exposure to PAHs may result in diminished immunological function, cataracts, renal and hepatic damage, respiratory issues, asthma-like symptoms, and changes in lung function [20]. Repeated contact with the skin may provoke erythema and dermal irritation. Naphthalene, a particular PAH, can induce hemolysis if inhaled or swallowed in substantial quantities. The detrimental effects of PAHs exposure in humans predominantly rely on the mode of exposure [24].

1.3. Carcinogenicity

Evidence suggests that combinations of PAHs are carcinogenic to humans. The data predominantly derives from occupational research involving workers exposed to mixes containing PAHs. Long-term exposure indicated an elevated risk of primarily skin and lung cancers, along with bladder and gastrointestinal cancers. However, these investigations do not clarify whether exposure to PAHs was the primary cause, as workers were concurrently exposed to other carcinogenic agents [25]. Laboratory studies indicate that animals subjected to prolonged exposure to some PAHs have acquired stomach cancer from ingestion via food, lung cancer from inhalation, and skin cancer from dermal contact. Benzo(a)pyrene is distinguished as the inaugural chemical carcinogen

identified. Furthermore, it is the predominant PAHs associated with carcinogenesis in animals. According to the existing information, several PAHs are categorized as carcinogenic to animals [26]. Additionally, several PAH-rich combinations are categorized as carcinogenic to humans [20]. The EPA has designated the following seven PAHs compounds as probable human carcinogens: indeno(1,2,3-cd)pyrene, benz(a)anthracene, benzo(k)fluoranthene, dibenz(ah)anthracene, benzo(a)pyrene, chrysene, and benzo(b)fluoranthene [26].

1.4. Common PAHs measuring methods

Three primary approaches are employed for their identification: chromatographic, spectrometric and immunoassay [27]. Immunoassay approaches, commonly available as kits, are unpopular due to their propensity to create significant biases in the final results [28]. Among spectrometric methods, infrared (IR) and ultraviolet (UV) techniques are the most prevalent; however, UV techniques, which are notably sensitive and selective to aromatic compounds such as PAHs, are more frequently influenced by interference from other compounds like lipids. Furthermore, the IR spectrometric technique, which is swift and cost-effective, necessitates a compulsory cleansing procedure for the sample post-extraction prior to analytical assessment [27].Chromatographic techniques for analyzing PAHs in environmental media have been developed and extensively used during the past few decades, with liquid chromatography (LC) and gas chromatography (GC) being the primary methods employed [29]. The advantages of utilizing GC and LC for the analysis of PAHs include operational simplicity, decreased solvent volume, and the potential for automation [30]. The following are the most commonly employed techniques for the detection of PAHs:

- High Performance Liquid Chromatography (HPLC) and Ultra-high performance liquid chromatography (UHPLC)

HPLC is a common technique for the qualitative and quantitative analysis of PAHs. This approach utilizes a single liquid as the high-speed mobile phase to facilitate separation based on the varying affinities between a solid stationary phase and a liquid mobile phase. The kinetics of solute distribution between the stationary and mobile phases are mostly governed by diffusion [31]. Despite its widespread use in identifying PAHs, HPLC still has several deficiencies that need enhancement and refinement [32]. The efficacy of HPLC is significantly contingent upon the detectors used. A detector characterized by high sensitivity, low detection limits, and universality

is crucial for the detection and analysis of PAHs. Consequently, the development of an appropriate high-efficiency detector may have considerable relevance. Secondly, the high-powered separation device requires additional development. Presently, HPLC coupled with solid phase membrane extraction has many drawbacks that need improvement, including intricate pretreatment processes and costly equipment and reagents [31]. Significantly, the existing hybrid HPLC techniques are limited to revealing information on the composition and concentration of diverse materials. However, the significance and complexity of several elements remain obscured in raw data. A comprehensive exploration of the conversion, transition, and synergy among various components of PAHs will be intriguing and hold possibilities for an in-depth research of PAHs.

UHPLC is an advanced chromatographic technique that builds upon the principles of HPLC while offering enhanced analytical throughput and improved chromatographic peak capacity [32]. Additionally, UHPLC provides greater efficiency in the detection process, with significantly higher speed, sensitivity, and resolution compared to HPLC. However, UHPLC also presents certain limitations. One notable drawback is the high internal pressure generated during sample analysis, which can potentially cause damage to the instrument, thereby reducing its operational lifespan and accelerating equipment degradation. The stationary phases used in UHPLC are largely similar to those in HPLC, with the primary distinction being a smaller particle size [33]. For the analysis of various types of PAHs using UHPLC, fluorescence detection (FLD) or ultraviolet (UV) detection may be employed depending on specific analytical requirements [34]. In some cases, a photodiode array (PDA) detector combined with FLD can also be utilized to enhance detection capabilities.

-Liquid chromatography-mass spectrometry (LC-MS, LC-MS/MS)

Liquid chromatography (LC) can also be integrated with mass spectrometry (MS) for PAH detection; however, liquid chromatography-mass spectrometry (LC-MS) is less commonly utilized than gas chromatography-mass spectrometry (GC-MS) for this purpose [32]. Nevertheless, certain LC-MS techniques, such as LC-atmospheric pressure laser ionization-MS (LC-APLI-MS) and dopant-assisted atmospheric pressure photoionization-high performance liquid chromatography-MS (DA-APPI-HPLC-MS), have been effectively employed for the detection of PAHs in environmental and food samples. Additionally, LC-MS/MS has proven valuable for PAHs analysis. For instance, LC-APPI-MS/MS has been developed for the detection of carcinogenic PAHs in complex environmental matrices, while LC-DA-APPI-MS/MS has been applied to the analysis of

PAHs in edible oils. These approaches address the limitations of GC-MS, such as inadequate separation efficiency, as well as the susceptibility of HPLC with fluorescence detection (HPLC-FLD) to interferences. Moreover, they enhance sample preparation flexibility and improve detection sensitivity [35]. PAHs have also been analyzed using LC-MS/MS in combination with atmospheric pressure chemical ionization (APCI) or electrospray ionization (ESI) with tropylium post-column derivatization. A comparative analysis of these ionization techniques revealed that APCI offers a simpler and faster analytical process but requires higher consumption of nitrogen and mobile phase, whereas ESI provides greater sensitivity but necessitates chemical derivatization [32]. Ultra-high performance liquid chromatography coupled with atmospheric pressure laser ionization mass spectrometry (UHPLC-APLI-MS or UHPLC-APLI-MS/MS) is another effective technique for the analysis of PAHs. Owing to the exceptional efficiency and high sensitivity of UHPLC, PAHs in complex samples can be more effectively separated. Furthermore, the integration of UHPLC with MS significantly enhances analytical performance, leading to improved detection accuracy and resolution [32].

-Gas Chromatography (GC)

It is a flexible and widely used separation technique in laboratory settings. This experimental technique offers great selectivity, high sensitivity, and a straightforward operating system, demonstrating effective resolution of the analyzed compounds[31]. GC, a subset of chromatographic techniques, employs a gaseous mobile phase. It is further categorized into gas-solid chromatography and gas-liquid chromatography based on whether the stationary phase consists of a solid adsorbent or a monomer coated with a fixative. Selecting an appropriate stationary phase is crucial for effectively separating PAHs using GC. Recent advancements in GC separation of PAHs have introduced novel stationary phases, including metal–organic frameworks (MOFs) [36], graphene sheets [37], and graphitic carbon nitride (g-C_3N_4) [38]. Additionally, materials such as polymer-coated fibers [39] and carbon nanotubes [40], which offer high thermal stability and enhanced resolution, have been successfully employed as GC stationary phases for PAH separation. While conventional stationary phases, such as polysiloxanes, poly(ethylene glycol), ionic liquids (ILs), and macrocyclic derivatives, have been widely used, ongoing research has led to significant advancements in these materials. For instance, modified polysiloxanes, including 7,10-diphenylfluoroxane-grafted polysiloxane [41] as well as ultra-high thermal stability perarylated ILs [42], and fluoro-substituted tetraphenyl-phenyl-grafted polysiloxane [43], have

been effectively applied in PAH separation. Furthermore, ionic liquid-bonded polysiloxane stationary phases have demonstrated high selectivity in GC-based PAH analysis. Gas chromatography-mass spectrometry (GC-MS), being a very sensitive analytical technique, is often used to identify volatile and semi-volatile organic contaminants. This technique integrates gas chromatography with mass spectrometry, enabling concurrent qualitative and quantitative investigation; nevertheless, the separation of isomers in PAHs presents challenges [31].

-Gas chromatography-mass spectrometry (GC-MS, GC-MS/MS)

Gas chromatography (GC) is highly effective for the separation and detection of PAHs in samples, while mass spectrometry (MS) provides precise identification of these compounds. By integrating these two techniques, PAHs in complex samples can be separated using GC and subsequently analyzed in an MS system, enabling accurate qualitative and quantitative results [32].

GC-MS offers several advantages for PAHs detection, including high separation efficiency, precise quantification, and the requirement of only a small sample volume. Another advanced approach, GC-MS/MS, also combines GC with MS but operates in a sequential manner. After PAHs are separated by GC, they enter the first MS for initial screening. The ions then pass into a reaction chamber, where they undergo a second screening by another MS before detection. Typically, the second MS in a GC-MS/MS system consists of either two quadrupole mass spectrometers or a combination of a quadrupole MS and a time-of-flight mass spectrometer (TOFMS) [32].

-Capillary Electrophoresis (CE)

Capillary electrophoresis (CE), often referred to as high performance capillary electrophoresis (HPCE), is an innovative liquid-phase separation method that utilizes capillaries as the separation channel and a high-voltage direct current electric field as the driving force [31]. In capillary electrophoresis, electrophoresis, chromatography, and the capillary tube's cross-section facilitate the advancement of analytical chemistry from the microliter to the nanoliter scale. CE has been used for the investigation of diverse samples because of its rapidity, elevated plate number, superior separation efficiency, cost-effectiveness, minimal injection volume, and ease of operation [31]. It is evident that CE has also advanced in the detection of PAHs; moreover, the CE method often serves as a valuable complement to GC for specific high boiling point PAHs. Moreover, there are other derivative capillary electrophoresis methods, including micellar electrokinetic capillary chromatography (MEKC) and parking capillary chromatography (PCC), both of which have been

used in the investigation of PAHs. Nonetheless, in this domain, sensitivity remains much improvable, particularly when integrating UV-Vis spectrometry, mostly due to the minuscule capillary width, which results in an excessively short light path [32]. This may be mitigated by optimizing the light route, for instance, by the use of multi-pass techniques. The primary limitation of CE is its inadequate repeatability, which is affected by variations in electroosmotic flow resulting from the sample's composition. From this perspective, it still requires considerable work.

-Mass spectrometry (MS)

Mass spectrometry (MS) is an analytical technique that utilizes electric and magnetic fields to separate ions based on their charge-to-mass ratio, enabling their detection. By analyzing these ions, MS provides critical information regarding the relative molecular weight and chemical structure of compounds, facilitating both qualitative and quantitative analysis of PAHs [32]. Two-step laser mass spectrometry (L2MS) is a high time-resolution technique for detecting PAHs in various samples [44]. Additionally, when coupled with time-of-flight mass spectrometry (TOFMS), it enhances detection efficiency. Single-particle laser desorption/ionization time-of-flight mass spectrometry (SP-LDI-TOFMS) has been applied to identify PAHs present in soot particles generated from industrial combustion processes [45]. Furthermore, thermal desorption resonance-enhanced multiphoton ionization single-particle time-of-flight mass spectrometry (TD-REMPI-SP-TOFMS) has been employed for the detection of particle-bound PAHs.

-Surface Enhanced Raman Spectroscopy (SERS) and fluorescence resonance energy transfer (FRET)

The Raman spectrum corresponds to the molecular vibration spectrum, which reveals the distinctive structural characteristics of molecules. However, the Raman scattering phenomenon is inherently weak, with the intensity of the scattered light being approximately 10^{-10} of the incident light intensity [31]. Consequently, Raman spectroscopy is particularly effective when applied to surface-adsorbed species that induce an enhancement effect, a phenomenon known as surface-enhanced Raman spectroscopy (SERS). SERS not only retains the fundamental advantages of conventional Raman spectroscopy but also substantially amplifies molecular signal intensity. Over the past four decades, SERS has been extensively utilized across various disciplines due to its notable benefits, including ease of application, a low detection limit, and high sensitivity. The

adsorption of PAHs onto rough noble metal substrates can significantly enhance Raman signals, making SERS an effective technique for PAH detection.

Fluorescence resonance energy transfer (FRET) is a process in which energy is transferred between two fluorescent molecules in close proximity. This principle has been applied in the detection of PAHs using a CdTe quantum dot-modified TiO_2 nanotube array. In this system, CdTe quantum dots (QDs) serve as energy donors, while PAHs act as acceptors, facilitating the occurrence of FRET [32].

Compared to conventional fluorescence spectroscopy, this approach significantly improves the sensitivity of benzopyrene (BaP) detection, enhancing it by approximately two orders of magnitude. Additionally, the fluorescence intensity of BaP increases by a factor of 15. Furthermore, this method exhibits minimal interference from other substances, ensuring higher specificity in PAH detection [31].

-Optical Spectrometry

Optical spectrometry represents a broad category of widely utilized instrumental techniques that span nearly all analytical and testing domains, offering advantages such as non-destructive analysis and ease of operation. This method has long been employed for the detection of PAHs, primarily through fluorescence spectrometry, phosphorescence spectrometry, and spectrophotometry. From a methodological perspective, the first two techniques fall under emission spectrometry, similar to SERS, and are characterized by higher sensitivity, whereas spectrophotometry is classified as an absorption-based technique [31].

1.4.1. Comparison of common PAHs detections techniques

When selecting an analytical technique for detecting PAHs, various factors such as advantages, limitations, time requirements, sample matrix compatibility, operating conditions, and selectivity for size play crucial roles. Each technique offers distinct advantages that make it suitable for specific applications. For instance, GC-MS excels at identifying and quantifying multiple PAHs simultaneously, providing comprehensive analysis. Similarly, SERS is known for its high sensitivity, specificity, and rapid detection, requiring minimal sample preparation [46]. HPLC is particularly effective for separating higher molecular weight PAHs, while also being relatively less demanding in terms of sample preparation [47]. These strengths make each method highly valuable, depending on the analytical goals, whether it's speed, sensitivity, or separation efficiency

[48].However, each technique has its limitations that should be considered. GC-MS, while highly effective, comes with high equipment and maintenance costs and requires extensive sample preparation, making it time-consuming [49]. Techniques such as Fluorescence Spectrophotometry can only detect PAHs that naturally fluoresce, limiting its application. CE, although offering high separation efficiency, suffers from lower sensitivity compared to chromatographic methods [50]. Additionally, some methods require very specific operating conditions, such as high temperatures or precise pH control, which could restrict their use in certain environments. The time required for each technique varies, with some offering rapid analysis while others take longer. For example, GC-MS typically involves hours of sample preparation, followed by 30–60 minutes of analysis. On the other hand, SERS and Fluorescence Spectrophotometry are much faster, providing results in minutes [48]. Depending on the urgency of the analysis, these time factors are crucial when choosing the right technique. Techniques that require less time are ideal for scenarios where quick results are essential, while those requiring more time are better suited for in-depth analysis.

The sample matrix, or the type of material being analyzed, is another important consideration. Techniques like GC-MS and LC-MS are versatile and can be applied to a wide range of sample types, including water, soil, sediments, and air. In contrast, methods like SERS are primarily used for water and soil samples [46]. Knowing the sample matrix is essential to ensure compatibility with the chosen method, as some techniques may not be suitable for certain sample types. Operating conditions also impact the practicality of each technique. GC-MS, for example, requires high-purity gases and operates at high temperatures (200–300°C), which may limit its use in some settings. HPLC, in contrast, operates at more moderate temperatures, typically between 20–40°C, making it more adaptable [47], [48]. Techniques like CE require precise control over voltage and pH, adding complexity to their use. The operating conditions must align with the capabilities of the equipment and the specific analysis being performed [48].Finally, selectivity for size refers to how well a technique can distinguish PAHs based on their molecular size or other properties. GC-MS is highly selective for PAHs due to its ability to separate compounds based on volatility and molecular size [48]. HPLC offers customizable selectivity using different column phases, which can enhance its ability to separate larger PAHs. CE, however, relies on the charge-to-size ratio for separation, influencing its selectivity [48] [50]. Understanding the size selectivity of each technique ensures that the most suitable method is chosen based on the characteristics of the PAHs being analyzed.

1.5. Regulations

PAHs chemicals are generally components of intricate combinations. Certain PAHs are highly effective carcinogens that may interact with several chemical substances. U.S. government agencies have created guidelines pertinent to PAHs exposures in occupational and environmental settings. A standard exists for PAHs in both the workplace and drinking water. The National Institute for Occupational Safety and Health (NIOSH) has advised that the permissible exposure limit for PAHs be established at the lowest detectable concentration, specifically a recommended exposure limit (REL) of 0.1 mg/m^3 for volatile agents in coal tar pitch, applicable over a 40-hour workweek or 10-hour workday [51]. The EPA water quality requirements for PAHs exposure, including a maximum contamination limit (MCL), were established for benzo(a)pyrene, the most carcinogenic PAH, at 0.0001 mg /L^3 [29]. MCL for dibenz(a,h)anthracene is 0.0003 mg/ L^3 and 0.0004 mg /L^3 for indenol(1,2,3-c,d)pyrene. In addition, the MCL for benzo(k) fluoranthene, benzo(a)pyrene, chrysene benzo(b)fluoranthene set to be 0.0002 mg/ L^3. Moreover, the MCL for benzo(a)pyrene, benzo(b)fluoranthene, chrysene and benzo(k) fluoranthene is 0.0002 mg/L^3 [52]. The WHO stated that maximum permissible limit of PAHs in water is 10 mg/L [53]. The European Water Framework Directive (WFD) intends to attain and maintain "good status", which should be the combination of "good chemical" and "good ecological" status [54], [55]. It mandates that EU Member States assess, monitor, and manage a variety of Priority Substances (PS) in all inland and coastal waterways. To protect human life and the environment, Environmental Quality Standards (EQS) were developed for every PS level that must not be exceeded. The vast majority of the PS consists of polar chemical compounds, including eight PAHs: naphthalene, anthracene, fluoranthene, indeno[1,2,3-cd]pyrene, benzo[a]pyrene, benzo[b]-fluoranthene, benzo[k]-fluoranthene, and benzo[ghi]perylene. Within the European Union, specifically under the Drinking Water Directive, the permissible concentration of PAHs in water is defined at a maximum total level of 100 ng/L [56], [57]. Unfortunately, Iraqi standards were more generic and only specify limits for hydrocarbons as (10 µg/L) [58]. Sediment pollution assessed by total PAHs concentrations may be categorized as follows: (A) low polluted (less than 100 ng/g), (B) moderately polluted (between 101 and 1000 ng/g), (C) highly polluted (between 1001 and 5000 ng/g), and (D) very polluted (more than 5000 ng/g) [59]. Additionally, Canadian Council of Ministers of the Environment reported that the total potency equivalents for soil contaminated with creosote or coal tar mixtures is 0.6 mg/m^3[60].

1.6. SCOPE OF THE WORK

The effluents from industrial operations and wastewater treatment plants significantly impact river ecosystems. These discharges pose a serious threat to aquatic life by degrading water and sediment quality through various pollutants. In Europe, the WFD mandates European Union member states to achieve satisfactory quantitative and qualitative assessments of all water bodies [61],[62]. In Asia, specifically in Iraq, increasing pollution sources, including oil refineries, automobiles, routine gas and fuel combustion activities, and gasoline- and diesel-powered generators, have contributed to the degradation of water and sediment quality in two major and historically significant rivers, the Tigris and Euphrates. Thus, the study aims to:

1- Monitoring the presence of 16 PAHs contaminants in water and sediment across all investigated rivers.
2- Determining the primary sources of 16 PAHs contamination across all investigated rivers.
3- Examining the compositional profiles of 16 PAHs in all rivers.
4- Evaluating the ecological risks associated with 16 PAHs in all rivers.
5- Identifying and quantifying the Incremental Lifetime Cancer Risk (ILCR) for both adults and children across all rivers.

In Hungary, the specific aims in the Danube River are as follows:

- Conduct a spatial and temporal assessment of 16 PAHs contaminants in the water and sediment of the Danube River in Hungary.

- Identify the primary sources of 16 PAHs contaminants in the Danube River.

- Evaluate the eco-toxicological risks associated with PAHs in the Danube River.

- Assess and quantify the Incremental Lifetime Cancer Risk (ILCR) for both adults and children exposed to PAHs in the Danube River.

- Compare the pollution levels with international guidelines and other reported global pollutions.

In Iraq, given the limited number of studies on PAHs pollution in the Tigris and Euphrates Rivers basins, the aims are:

- Investigate the 16 PAHs pollutants in areas near oil refineries along the Tigris River by measuring contamination levels before and after major refineries, including Baiji, Kirkuk, Al-Siniyah, Qayyarah, Al-Kasak, Daura, South Refineries Company, and Maysan.

- Conduct a spatial assessment of PAHs contamination in the water and sediment of the Tigris River.

- Investigate 16 PAHs in both water and sediment samples along the Euphrates River.

- Assess the ecological risk of 16 PAHs in both the Tigris and Euphrates Rivers.

- Analyze the composition profiles of 16 PAHs in the Tigris and Euphrates Rivers.

- Determine the contribution rates of various pollution sources in the Tigris and Euphrates Rivers.

- Assess the potential health and environmental risks of PAHs pollution in the Tigris and Euphrates Rivers.

- Compare the pollution levels with international guidelines and reported global pollution.

2. MATERIAL AND METHODS

2.1. Study area

2.1.1. Danube River

With a length of 2,780 km, the Danube is the second-longest river in Europe, with a catchment area of 801,500 km² [63]. The waters of the Danube River Basin serve multiple purposes, including the production of drinking water, industrial and agricultural activities, recreation, hydroelectric power generation, and transportation. The Hungarian segment of the Danube spans 417 km (river kilometers 1850–1433). Six locations along this segment were investigated. Figure 2 shows the sampling sites along the river. Sites S1 and S2 represent northern areas in our study, both affected by agricultural and industrial activities. Site 3 is located in the center of Budapest, downstream from the city's second-largest wastewater treatment plant, which processes 180,000-200,000 m³/day. Site 4 is downstream from a polystyrene factory producing impact-resistant and expandable polystyrene. Site 5 is downstream from various industries, including paper mills and electricity suppliers. Site 6, the southernmost site, was chosen to reflect the cumulative impact of upstream human activities. (Appendix 1 List the GPS coordinates of the Danube sampling locations).

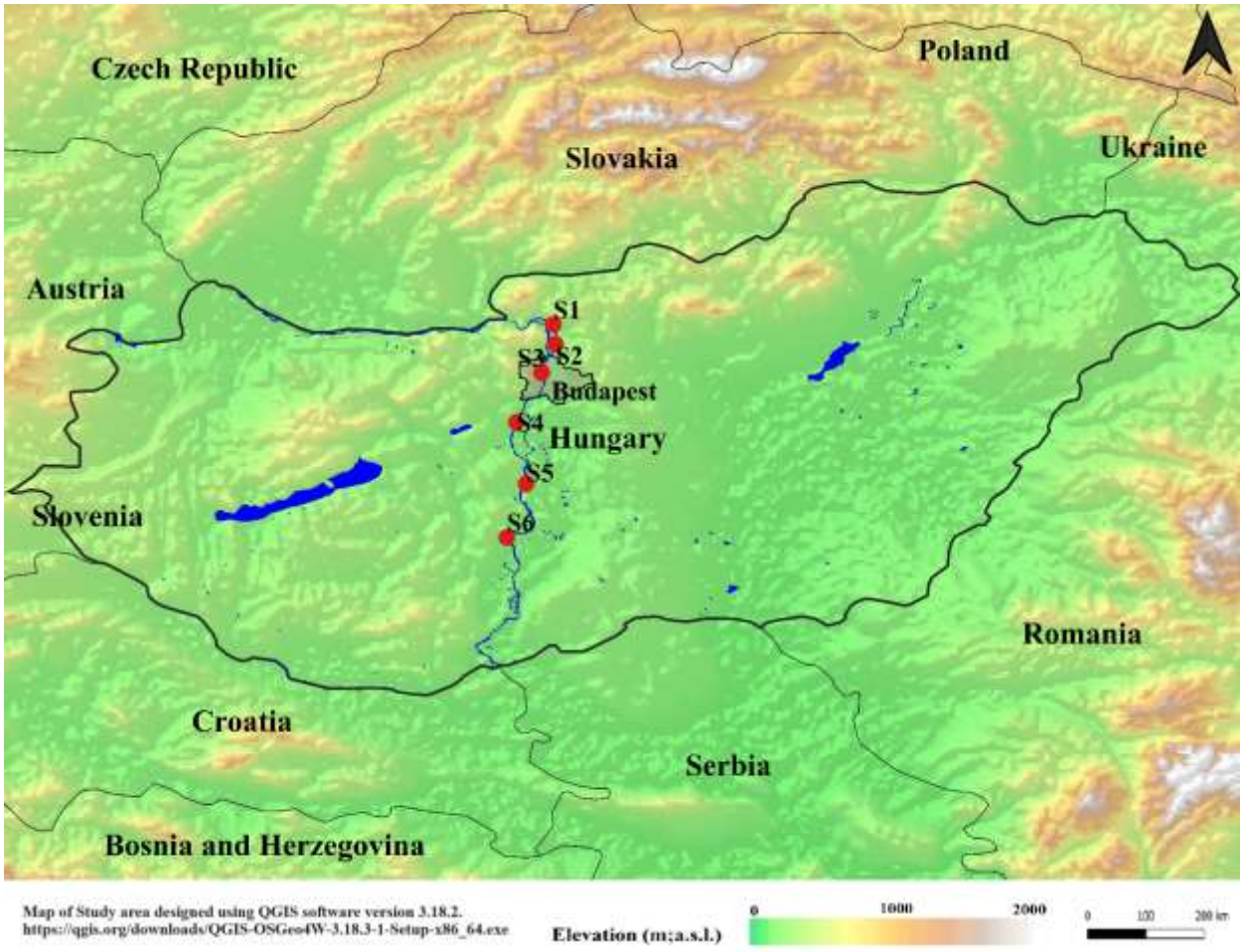

Figure 2 Sampling points in the Danube River within the Hungarian region.

2.1.2. Tigris River

The Tigris River is the second-largest river in Western Asia. It converges with the Euphrates River in southern Iraq to form the Shatt al-Arab, which empties into the Persian Gulf. The Tigris basin spans four riparian countries: Iran, Iraq, Syria, and Turkey. Covering an area of approximately 221,000 km^2, the basin is distributed as follows: 24.5% in Turkey, 0.4% in Syria, 56.1% in Iraq, and 19% in Iran[64]. The river stretches 1,800 km in length, with its waters primarily utilized for agriculture. Irrigation projects are present in all the riparian countries. After flowing for nearly 400 km within Turkey, the Tigris serves as the Syrian Turkish border for approximately 47 km before continuing into Iraq, where it flows more than 1,350 km. The Tigris Basin comprises a total population of approximately 23.4 million inhabitants[64]. Among them, over 18 million reside in

Iraq, 1.5 million in Iran, and 3.5 million in Turkey. The Syrian section of the basin is sparsely populated, with only about 50,000 inhabitants[64].

In term of oil refineries, Iraq rank fifth worldwide in proven crude oil reserves and seventh in oil production volume, compared with the US, Russia, and China [65]. As of February 2021, Iraq's total nameplate refinery capacity was approximately 1.2 million barrels per day, though the effective capacity is around 900,000 barrels per day. The discrepancy between planned and actual capacity at the northern refineries is primarily due to the damage from ISIS attacks in 2014 and 2015, during which facilities were destroyed or severely damaged. Since 2015, part of this capacity has been restored, including a section of the Baiji refinery. Iraqi refineries produce excess heavy fuel oil but insufficient gasoline and diesel to meet local demand, necessitating imports of refined oil products. In 2021, the South Refineries Company expanded its Basra refinery by 70,000 barrels per day. In this study, twelve sites near oil refineries along the Tigris River and its estuaries in Iraq were selected for sampling, including locations at the Al-Kasak oil refinery (S1), Qayyarah before (S2) and after (S3) the oil refinery, Kirkuk oil refinery (S4), Al-Siniyah (S5), Baiji before (S6) and after (S7) the oil refinery, Daura before (S8) and after (S9) the oil refinery, Maysan oil refinery (S10), South Refineries Company before (S11) and after (S12) the Shatt Al-Basra Electricity gas station. The term "South Refineries Company" may also refer to "South Refineries". Monthly samples of surface water and sediment were collected from these sites from July to December 2022. Figure 3 illustrates the coordinates of the sampling sites, which are also listed in the supplemental materials (Appendix 2). The 2021 capacities (in thousands of barrels per day) of the studied oil refineries are as follows: Baiji (310, 140), Kirkuk (56, 56), Al-Siniyah (30, 20), Qayyarah (20, 14), Al-Kasak (10, 10), Daura (210, 140), South Refineries Company (210, 210), and Maysan (40, 40) [66]. Given these refineries and the continuous waste disposal into nearby water bodies with limited treatment processes, there is a concerning potential for increased accumulation of various toxic pollutants in the environment.

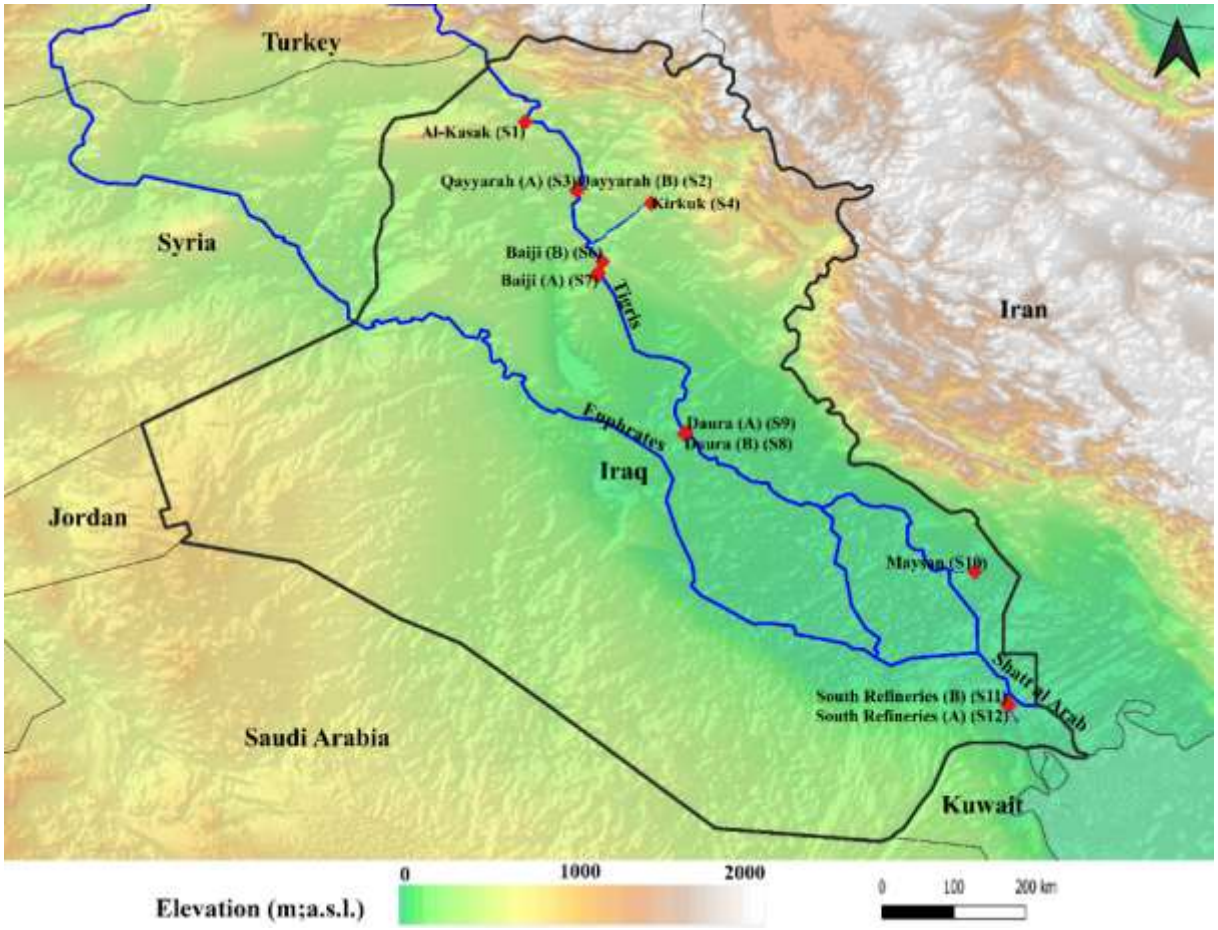

Figure 3 Sampling site locations near the Iraqi oil refineries in the Tigris River and its estuaries.

2.1.3 Euphrates River sampling sites

The Euphrates River, with a catchment area of 440,000 km² and a length of 2,786 km, is the longest river in Western Asia. Originating in Turkey, the Euphrates flows through Syria and joins the Tigris River in Iraq to form the Shatt al-Arab, which ultimately empties into the Persian Gulf. The Euphrates Basin has an estimated population of around 23 million, with 44% residing in Iraq, 31% in Turkey, and 25% in Syria. Within the river's catchment area, water is primarily used for irrigation, hydropower, and drinking supplies, with agriculture consuming over 70% of the water. This underscores the river's crucial role in the agricultural and energy sectors of the countries it traverses, especially Iraq, which has the largest population dependent on it. Return flows from agricultural drainage have led to secondary salinization along the river's course, particularly in Iraq. Additionally, the discharge of untreated sewage further degrades water quality [67]. To assess water quality, thirteen sampling sites along the Euphrates in Iraq were examined: Haditha (S1), Hit

(S2), Ramadi (S3), Al-Fallujah (S4), Jorf Al-Sakhar (S5), Musayyib (S6), Hindiyah (S7), Kefel (S8), Najaf (S9), Al-Qadisiyyah (S10), Samawah (S11), Nasiriyah (S12), and Basrah (S13) (Figure 4). (GPS Coordinates for these sites are shown in Appendix 3).

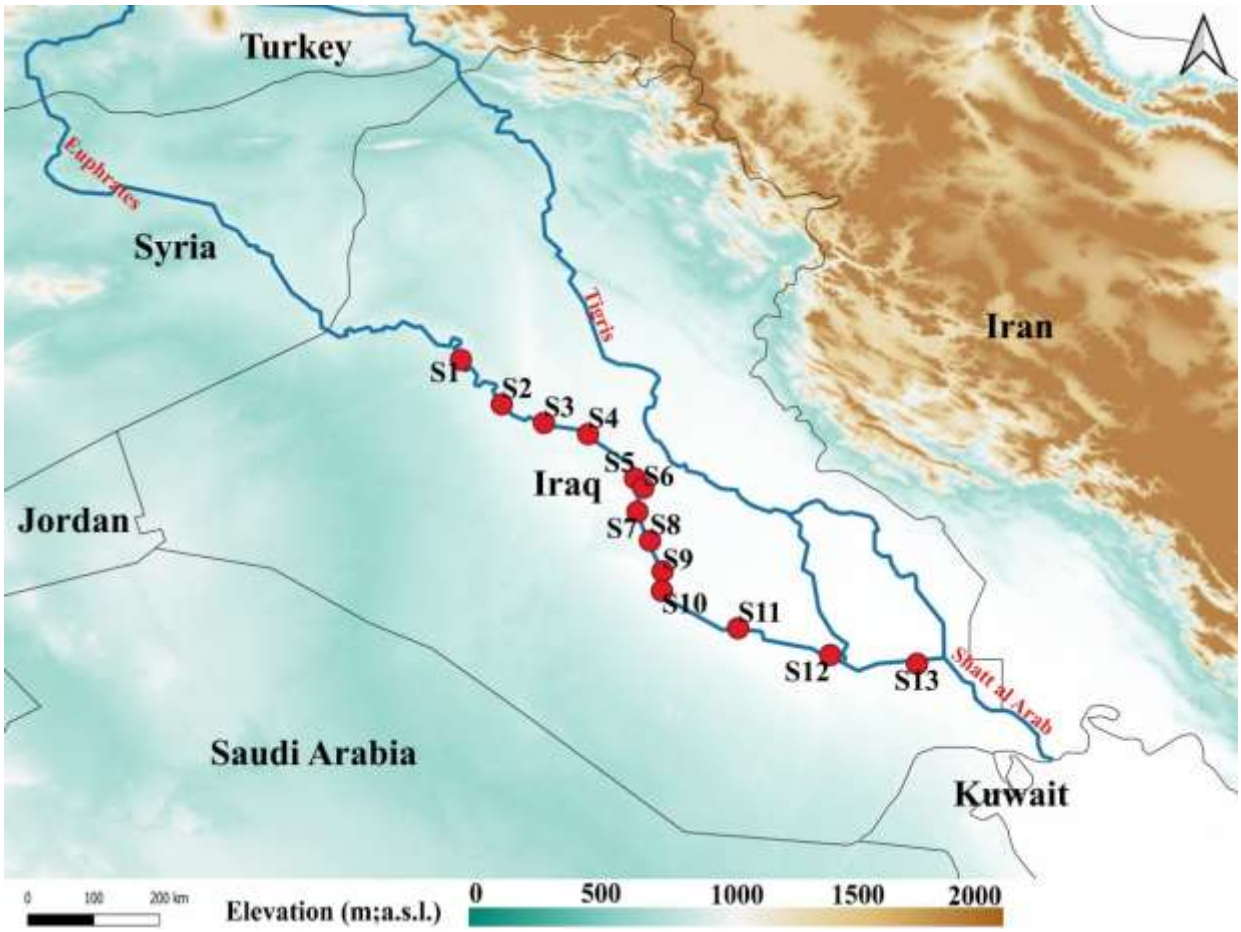

Figure 4 Sampling locations along the Euphrates River in Iraq

2.2. Chemicals

All solvents, including methanol, methylene chloride, hexane, ethyl acetate, and acetone, were HPLC-grade with a minimum purity of 99% and were obtained from Fisher Chemical Co. (United States). Supelco (Bellefonte, PA, USA) provided the reference standards (QTM PAH-Mix, 2000 µg/mL) for the 16 priority PAHs, including naphthalene (Nap), acenaphthylene (Acy), acenaphthene (Ace), fluorene (Fl), phenanthrene (Phe), anthracene (Ant), fluoranthene (Flu), pyrene (Pyr), benzo(a)anthracene (BaA), chrysene (Chr), benzo(b)fluoranthene (BbF), benzo(k)fluoranthene (BkF), benzo(a)pyrene (BaP), dibenz(a,h)anthracene (DBA), benzo(ghi)perylene (BghiP), and indeno(1,2,3-cd)pyrene (IND). Surrogates such as naphthalene-

d_8, anthracene-d_{10}, fluoranthene-d_{10} and perylene-d_{12} were obtained from Supelco (Bellefonte, PA, USA). Solid-phase extraction membranes (ENVI™-18 DSK SPE Disk, diameter 47 mm), anhydrous sodium sulfate, silica gel (desiccant, 2-5 mm), and PAHs recovery standards were supplied by Sigma-Aldrich (USA). The sodium sulfate and silica gel were heated in a furnace (FI 600-60, Borel) at 500 °C for 4 hours to remove moisture and organics, then stored in a desiccator until use. Milli-Q water, with a resistivity of 18.2 MΩ·cm at room temperature and a total organic carbon value of less than 5 ppb, was used in the experiments. Before each measurement, glassware was cleaned with ultrasonic cleaners (Heidolph™, Fisher Scientific), washed sequentially with acetone, n-hexane, methanol, and dichloromethane to eliminate background contamination, and dried at 105 °C before use.

2.3. Samples collection and pretreatment in Danube River

The Danube has a mean discharge of 2,350 m³/s at Budapest and 5,600 m³/s at Belgrade [68], [69]. The average depth of the middle Danube region ranges from 6 m to 10 m [70]. Throughout the study, water and sediment samples were collected monthly (two samples per month) from February 2022 to February 2023, spanning a 12-calendar-month period. Sediments were typically collected after water sampling to prevent disturbance and resuspension of the sediment into the water. Water samples were obtained from depths of 5 to 30 cm using 1 L brown glass containers that had been previously cleaned by acetone and methanol then heated to 100 °C. The samples were temporarily stored in refrigerated containers with crushed ice until they were transported to the laboratory and kept at -20 ºC. Upon arrival at the laboratory, the water samples were filtered using a 0.45 μm glass fiber membrane [71]. Sediment samples were collected from the riverbed at depths of 0–10 cm using a stainless-steel grab sampler and placed in clean polyethylene bags. These samples were sieved through a 100-mesh sieve to remove roots, debris, and large particles [72], [73]. The sieved sediments were dried at 25 °C and then ground. Finally, the dried sediments were stored in a freezer at –20 °C for further analysis.

2.3.1. PAHs Extraction procedures for Danube River

2.3.1.1 Water sample extraction procedure for Danube River

Solid-phase extraction (SPE) was used to extract one liter of filtered water samples for analysis. The extraction process followed previously reported procedures [71], [74], [75]. An SPE membrane was pre-washed with six milliliters of dichloromethane (DCM) before conditioning (activation) with six milliliters of methanol, six milliliters of ultrapure water, and an additional ten milliliters of methanol. A ten-microliter surrogate standard mixture solution (naphthalene-d_8, anthracene-d_{10}, fluoranthene-d_{10}, perylene-d_{12}) was added to one liter of the water sample to enrich it. The sample was then passed through the SPE membrane at a flow rate of 3 mL/min. Once extraction was complete, a vacuum pump was used to dry the column. Six milliliters of dichloromethane was added to soak the column for 5 minutes before eluting the sample into a clean glass test tube. The eluate was then concentrated to 0.5 mL using nitrogen gas, after which ten microliters of a standard mixture solution was added. Finally, the samples were analyzed using gas chromatography-mass spectrometry (GC–MS).

2.3.1.2. Sediment sample extraction procedure for Danube River

The freeze-dried sediment samples were pulverized using a mortar and pestle and sieved through a 100-mesh sieve to remove large particles. The dried and homogenized sediment samples were placed in brown glass vials for further laboratory analysis. Sediment sample extraction followed previously reported procedures [73], [74], [75]. A 2-gram sample was precisely weighed, and five milliliters of an acetone/n-hexane (1:1, v/v) solution along with a standard surrogate solution were added to the test tube. The sample was vortexed for 60 seconds, followed by ultrasonic extraction in a water bath for 15 minutes. Afterward, the test tubes were centrifuged for 20 minutes at 2000 rpm to separate the solid and liquid phases. The supernatant was then transferred to a clean test tube using a Pasteur pipette. Next, five milliliters of a 1:1 mixture of acetone and n-hexane was added to each sample. The extracts were combined in a single test tube, and activated copper was added for desulfurization. Anhydrous sodium sulfate was then added to remove residual water, followed by concentration to 0.5 milliliters using a nitrogen-blowing concentrator. Finally, an internal standard solution was added for GC–MS analysis.

2.4. Samples collection and analysis for Tigris River

The methodology used in this work followed techniques described by Dong et al. [76], Grmasha et al. [71], and Lin et al. [72]. During the sampling campaign from July to December 2022, each location was sampled six times. Water samples were collected between 20 and 40 cm below the surface using a pre-cleaned stainless-steel container. Samples were spiked with surrogates (naphthalene-d_8, anthracene-d_{10}, fluoranthene-d_{10}, and perylene-d_{12}) as the PAHs recovery standard, sealed in five-liter glass containers, transported to the laboratory within 24 hours, and refrigerated at 4°C until further analysis. Five liters of surface water were filtered through a 0.45 μm glass fiber membrane and a methanol-activated solid-phase extraction (SPE) membrane to isolate PAHs for analysis. According to procedures outlined by Lin et al. [72], the PAH-containing SPEs were wrapped in aluminum foil and refrigerated until further measurements.

Sediment samples were collected using a grab sampler, with three samples taken at each site (0–10 cm depth) and then combined in dark glass bottles for transport. The PAHs were extracted from the SPEs using a previously described method [72], [77]. SPE membranes were eluted twice with dichloromethane-ethyl acetate and ethyl acetate solutions. The extracts were pooled, dried over anhydrous sodium sulfate, concentrated with a rotary evaporator, and redissolved in one milliliter of n-hexane.

For sediment extraction, four grams of freeze-dried sediment were weighed, sieved with a 100-mesh stainless steel sieve, spiked with surrogates, and placed in an extraction tube containing 50 mL of a 1:1 acetone-hexane mixture. Extraction was performed using a microwave digestion system, with the temperature rising from 25 to 120°C at 8°C per minute and held for 20 minutes. Samples were then centrifuged for 20 minutes at 1000 rpm. The supernatant was passed through anhydrous sodium sulfate, then subjected to extraction and purification in a glass chromatography column. The final extract was concentrated to approximately 2 mL, after which 1 mL of n-hexane was added for analysis.

2.5. Samples collection and analysis for Euphrates River

Surface water and sediment samples were collected monthly from March 2022 to July 2022, with five measurements taken at each site during this period. Surface water samples were taken from a depth of 10–30 cm below the water's surface using a pre-cleaned stainless-steel container. Each sample was spiked with 1 μg of fluoranthene-d_{10} (the PAHs recovery standard), sealed in 6 L glass

containers, and transported to the laboratory within a day, where they were stored at 4 °C until analysis. For PAHs separation, 6 L of surface water was filtered through a 0.45 μm glass fiber membrane, followed by a methanol-activated solid-phase extraction (SPE) membrane to isolate PAHs. Following the procedure reported by Lin et al. [72], the SPE membrane containing PAHs was wrapped in foil and cooled for further analysis.

Sediment samples were collected using a pre-cleaned grab sampler and stored in sealed bags. At each site, sediment samples (0–10 cm) were taken three times, combined, and stored in dark glass bottles. After collection, samples were promptly transported to the laboratory for further analyses.

The PAHs extraction from the SPE membrane followed the method detailed by Lin et al. [72] and Ternon and Tolosa [77], in which dichloromethane-ethyl acetate and ethyl acetate solutions were used to elute the SPE membrane twice. The combined extracts were then dried over anhydrous sodium sulfate, concentrated with a rotary evaporator, and redissolved in 1 mL of n-hexane.

For sediment extraction, approximately 2 g of freeze-dried sample, sieved through a 100-mesh stainless steel screen and spiked with 1 μg of fluoranthene-d_{10}, was transferred to an extraction tube containing 25 mL of acetone-hexane (1:1) and extracted using a microwave digestion system. The temperature was raised from 25 °C to 120 °C at a rate of 8 °C/min and held for 20 min. Samples were then centrifuged at 2000 rpm for 20 min, and the supernatants were dried over anhydrous sodium sulfate, purified through a glass chromatography column, and evaporated to approximately 2 mL. Finally, 1 mL of n-hexane was added for measurement. PAHs measurements were performed using GC–MS.

2.6 .Gas chromatography-mass spectrometry (GC–MS) and Total organic matter (TOM)

PAHs were measured using GC–MS (Agilent 6890 N with a 5975C mass selective detector, Agilent Technologies, USA). Helium served as the carrier gas at a flow rate of 1.5 mL/min through an HP-5MS column (30 m × 0.32 mm × 0.25 μm) [6]. Selective ion monitoring (SIM) mode was used for quantitative analysis. The injector temperature was set to 300 °C. The oven temperature program was as follows: initial temperature of 100 °C held for 1 minute, then increasing to 300 °C at a rate of 8 °C per minute, where it was held for 39 minutes. Triplicate measurements were taken for each sample, yielding a relative standard deviation of less than 10.2% (for Danube River and

<6% for Tigris and Euphrates Rivers). Total organic matter (TOM) was quantified by determining the weight reduction in sediment samples that had been oven-dried at 105 °C for 48 hours, followed by combustion at 550 °C for 2 hours[78].

2.7. Quality Control (QC) and Quality Assurance (QA)

2.7.1. Danube River

Quality control measures included triplicate samples, matrix spike standards, calibration standards, procedural blanks, and detection limits. Prior to each measurement, the glassware was cleaned using ultrasonic cleaners, followed by washing with acetone, n-hexane, methanol, and dichloromethane to eliminate background contamination, and then dried at 105 °C before use. The concentrations of 16 PAHs in sediment samples were determined using the dry weight approach. The limits of detection (LOD) were established based on analyte concentration and a 3-fold signal-to-noise ratio [79], [80]. LODs ranged from 0.02 to 0.59 ng/L for water and from 0.37 to 0.96 ng/g (dry weight) for sediment. PAHs recoveries were assessed by spiking water and sediment samples with standard solutions. Each sample analysis included a procedure blank (solvent), a spiked blank (standards added to solvent), and triplicate samples. Analysis of method blanks confirmed the absence of detectable PAHs contamination. Recovery ranges for the 16 PAHs were 91.5% ± 4.3% to 104.1% ± 7.6% for water samples and 86.8% ± 5.5% to 99.2% ± 6.2% for sediment samples. For spiking standards, recovery ranges were 92.8% ± 4.5% to 109.7% ± 6.9% for water samples and 90.5% ± 8.3% to 97.4% ± 4.4% for sediment samples. Concentrations of the 16 PAHs were adjusted based on these recovery rates. Reference and blank samples were measured to confirm analysis accuracy. Each sample was measured in triplicate, yielding a relative standard deviation between 1.7% and 10.4%, well within the acceptable limit (< 25%). Mean values are presented for all measurements. The data in this study were tested for normality using the Kolmogorov-Smirnov test at a significance level of 0.05.

2.7.2. Tigris River

Glassware was heated to 100 °C and cleaned with acetone, methanol, and dichloromethane before each measurement to eliminate background contamination. Quantitative standards for 16 PAHs in water samples were established using external standard techniques. Linearity correlation values

for the 16 PAHs monomers ranged from 0.997 to 0.998. PAHs levels in sediment samples were determined using the dry weight method. Limits of detection (LOD) were calculated based on analyte concentration, using a 3:1 signal-to-noise ratio [79]. The LOD ranged from 0.06 to 0.35 ng/L for water and from 0.13 to 0.75 ng/g dry weight (dw) for sediment. For recovery analysis, the 16 PAHs standard solutions were spiked into water and sediment samples [79], [80]. Each sample analysis included a method blank (solvent), a spiked blank (standards added to solvent), and sample triplicates. Method blank analysis confirmed the absence of detectable PAHs contamination. Recovery ranges for water and sediment samples were 93.2% to 100% and 85.3% to 98.8%, respectively, while spiking standard recoveries ranged from 94.5% to 110.4% in water and 89.3% to 96.6% in sediment. Concentrations of 16 PAHs were adjusted to account for recovery. Blank and reference samples were also measured to verify accuracy, and each sample was analyzed in triplicate, resulting in a relative standard deviation of less than 4%. Mean values are reported in this study. The Kolmogorov-Smirnov normality test was applied to all data at a significance level of 0.05.

2.7.3. Euphrates River

Prior to each experiment, glassware was heated to 150 °C and rinsed with methanol, acetone, and dichloromethane to minimize background contamination. Quantitative standards for PAHs in the water samples were determined using external standard methods. For the 16 PAHs monomers, the linear correlation coefficients ranged between 0.998 and 0.999. PAHs concentrations in sediment samples were measured as dry weight. Limits of detection (LOD) were calculated based on analyte concentration using a three-fold signal-to-noise ratio [79]. LOD values for water samples ranged from 0.04 to 0.28 ng/L, while those for sediment samples ranged from 0.09 to 0.65 ng/g (dry weight, dw). For recovery experiments, 16 PAHs standard solutions were spiked into water and sediment samples following the procedures of Dong et al. [76], Lin et al. [72], and Zhu et al. [79]. Recovery rates for the 16 PAHs standards ranged from 90.4% to 100% for water samples and from 81.4% to 97.6% for sediment samples. Recovery rates for the spiking standards (surrogates) were 92.6%–106.8% for water samples and 85.4%–95.3% for sediment samples (Appendix 4). PAHs concentrations were corrected for recovery. Both water and sediment samples were analyzed in triplicate, and results are presented as mean values. All data in this study were subjected to a normality test using the Kolmogorov-Smirnov method with a significance level of 0.05.

2.8. Eco-toxicological concerns and Incremental Lifetime Cancer Risk (ILCR) for River's sediment

The sediment sample assessment for ecological risk followed the methodology outlined by [81]. PAHs levels in sediments were evaluated according to sediment quality guidelines (SQGs) [82]. By comparing the concentration of each PAHs to the Effect Range Low (ERL) and Effect Range Median (ERM) values, the ecological risk posed to aquatic species from exposure to sediment-bound PAHs was determined. The SQGs classify chemical concentrations into three ranges based on potential biological effects: 1) minimal effects range, where biological effects are rare (<ERL), 2) possible effects range, where biological effects occur occasionally (≥ERL and <ERM), and 3) probable effects range, where biological effects are frequent (≥ERM).

To compare the carcinogenicity of PAHs with that of benzo[a]pyrene (BaP), the toxic equivalency factor (TEF) approach was used to calculate the BaP equivalency (BaPeq) of each PAHs [13]. BaP was selected as a reference due to its high carcinogenicity and was assigned a TEF value of one, allowing the carcinogenicity of other PAHs to be estimated relative to BaP. The TEF values used are shown in Table 1. Based on their relative carcinogenicity to BaP, each PAHs has a unique TEF value. The formulas below were used to calculate the toxic equivalent quotient (TEQ) for each sampling location in this study:

$$\mathrm{BaPeq_i} = (\mathrm{PAH_i} \times \mathrm{TEF_i}) \quad \textbf{(1)}$$

$$\mathrm{TEQ} = \sum_1^n (\mathrm{PAH_i} \times \mathrm{TEF_i}) \quad \textbf{(2)}$$

where PAH_i is the PAH concentration and TEF_i is the toxic equivalency factor.

Using the USEPA's ILCR model, which examined the three main routes of exposure to contaminants (ingestion, dermal contact, and inhalation), a risk assessment to PAHs in river sediments was performed. This assessment was required because of people's daily reliance on the region's aquatic resources [83]. ILCR is used to estimate the human cancer risk posed by exposure to environmental PAHs. The overall carcinogenic risk was determined by summing up the hazards associated with the three routes of exposure. Table 2 and equations (3, 4, 5, and 6) respectively explain the ILCR assessment parameters and model formulations [83], [84], [85].

$$\mathrm{ILCR_{ingestion}} = \mathrm{CS} \times \mathrm{IR_{ingestion}} \times \mathrm{EF} \times \mathrm{ED} \times \left(\mathrm{CSF_{ingestion}} \times \sqrt[3]{\frac{\mathrm{BW}}{70}}\right) \times (\mathrm{BW} \times \mathrm{AT} \times 10^6)^{-1} \quad \textbf{(3)}$$

$$\mathrm{ILCR_{inhalation}} = \mathrm{CS} \times \mathrm{IR_{inhalation}} \times \mathrm{EF} \times \mathrm{ED} \times \left(\mathrm{CSF_{inhalation}} \times \sqrt[3]{\frac{\mathrm{BW}}{70}}\right) \times (\mathrm{BW} \times \mathrm{AT} \times \mathrm{PEF})^{-1} \quad \textbf{(4)}$$

$$\mathrm{ILCR}_{\text{dermal contact}} = \mathrm{CS} \times \mathrm{SA} \times \mathrm{AF} \times \mathrm{ABS} \times \mathrm{EF} \times \mathrm{ED} \times \left(\mathrm{CSF}_{\text{dermal contact}} \times \sqrt[3]{\frac{\mathrm{BW}}{70}} \right) \times (\mathrm{BW} \times \mathrm{AT} \times 10^{6})^{-1} \quad \textbf{(5)}$$

$$\text{Carcinogenic risk} = \mathrm{ILCR}_{\text{ingestion}} + \mathrm{ILCR}_{\text{dermal contact}} + \mathrm{ILCR}_{\text{inhalation}} \quad \textbf{(6)}$$

CSF is the carcinogenic slope factor, which is represented in units of (mg $kg^{-1}day^{-1})^{-1}$. According to the USEPA, the CSF concentrations of BaP for the three exposure pathways are 25, 7, 3 and 3.85 $mg/kg/day^{-1}$ [86]. CS is the total PAHs concentrations that transformed to hazardous equivalents of BaP using the Toxic Equivalence Factor (TEF) (in ng/g). Calculation of the ILCR relies heavily on the detection of PAHs as BaP-equivalent concentrations using the TEF of each PAHs relative to BaP. The total ILCR is equal to the sum of three routes: skin contact, oral consumption, and inhalation. If the ILCR is less than $1/10^6$, it is deemed inconsequential; if it is more than $1/10^4$, there is a reason for serious worry [87].

Table 2 Parameters descriptions used for ILCR model

Parameter	Description	Unit	Adults	Children	References
ABS	Dermal-Absorption-Factor	unitless	0.13	0.13	[87]
AF	Dermal-Adherence-Factor	mg/cm^2	0.07	0.2	[87]
AT	Average-Time(70years_365 days/year)	Days	25,550	25,550	[88]
BW	Body-Weight	Kg	70	15	
ED	Exposure-Duration	Years	20	6	[89]
EF	Exposure-Frequency	days/year	350	350	[89]
IR ingestion	Ingestion-Rate	mg/day	100	200	[87]
IR inhalation	Inhalation-Rate	m^3/day	20	10	[88]
PEF	Particular-Emission-Factor	m^3/kg	1.36×10^9	1.36×10^9	[89]
SA	Dermal-Surface-Area-Exposure	cm^2	5700	2800	[89]

2.9. Visualization

The data was visualized using the following R packages: "ggpubr" [90] and "corrplot"[91]. The maps were created using Quantum Geographic Information System (QGIS) software, version 3.18.

3. RESULTS AND DISCUSSION

3.1. PAHs spatial distribution and seasonal variation in water and sediment for Daube River

3.1.1. PAHs in Daube River water

Figure 5 presents the concentrations of 16 identified PAHs in the water of the Danube River. The total PAHs content in water across all seasons ranged from 224.8 ng/L in summer to 365.8 ng/L in winter. The seasonal variation in PAHs concentrations was as follows: 283.1-541.9 ng/L in winter, 198.6-404.3 ng/L in spring, 160.0-324.6 ng/L in summer, and 228.2-378.1 ng/L in autumn. In water samples from the Danube River, the concentrations of LMWPAHs (with 2-3 rings, such as Nap, Acy, Ace, Fl, Phe, and Ant) were generally higher than those of HMWPAHs (with 4-6 rings, including Flu, Pyr, BaA, Chr, BaP, DBA, BkF, BbF, IND, and BghiP) across all four seasons. HMWPAHs recorded their highest values in summer (Figure 5). In Figure 6, the PAHs profiles in both water and sediment are shown. Ace was found to be the most predominant component, with levels between 16 and 47.8 ng/L, followed by Nap, Acy, FI, Ant, and Phe, which ranged between 11.9 and 45.0 ng/L, 15.5 and 44.0 ng/L, 7.1 and 40.9 ng/L, 10.5 and 40.2 ng/L, and 11.0 and 36.0 ng/L, respectively. The highest HMWPAHs concentrations in water were found for BghiP (11.4-28.3 ng/L), IND (8.2-17.9 ng/L), DBA (9.6-17.8 ng/L), BaP (9.1-17.5 ng/L), BkF (7.2-17.2 ng/L), BbF (9.5-17.1 ng/L), Pyr (7.8-14.9 ng/L), Chr (10.1-14.7 ng/L), Flu (5.9-11.0 ng/L), and BaA (8.2-10.1 ng/L).

Overall, ∑ PAHs concentrations in the Danube River water were higher in winter, spring, and autumn than in summer, likely due to lower temperatures during those seasons. The seasonal patterns of PAHs in water (Figure 5) are likely influenced by PAHs molecular weight and degradation rates, which are more pronounced in warmer seasons [92]. While HMWPAHs (4-6 rings) exhibit low water solubility and dissolution rates and are more resistant to decomposition, LMWPAHs (2-3 rings) are more degradable and soluble in warmer conditions [93]. Consequently, LMWPAHs are more concentrated in colder seasons, while HMWPAHs increase in warmer seasons (Figure 5), as LMWPAHs content in water decreases.

The data also indicates that PAHs concentrations vary across sampling sites. The highest concentrations in water were found at site S3 (center of Budapest) during colder seasons (Figure

6), associated with increased LMWPAHs, suggesting recent local sources of atmospheric deposition, likely from vehicle and industrial emissions. Additionally, significant PAHs concentrations were observed in sediments at site S5 during winter and autumn. Visca et al. [94] also examined PAHs in water samples, identifying high concentrations, particularly in April, attributed to sources such as home heating, vehicle emissions, air transport, and a nearby wastewater treatment facility.

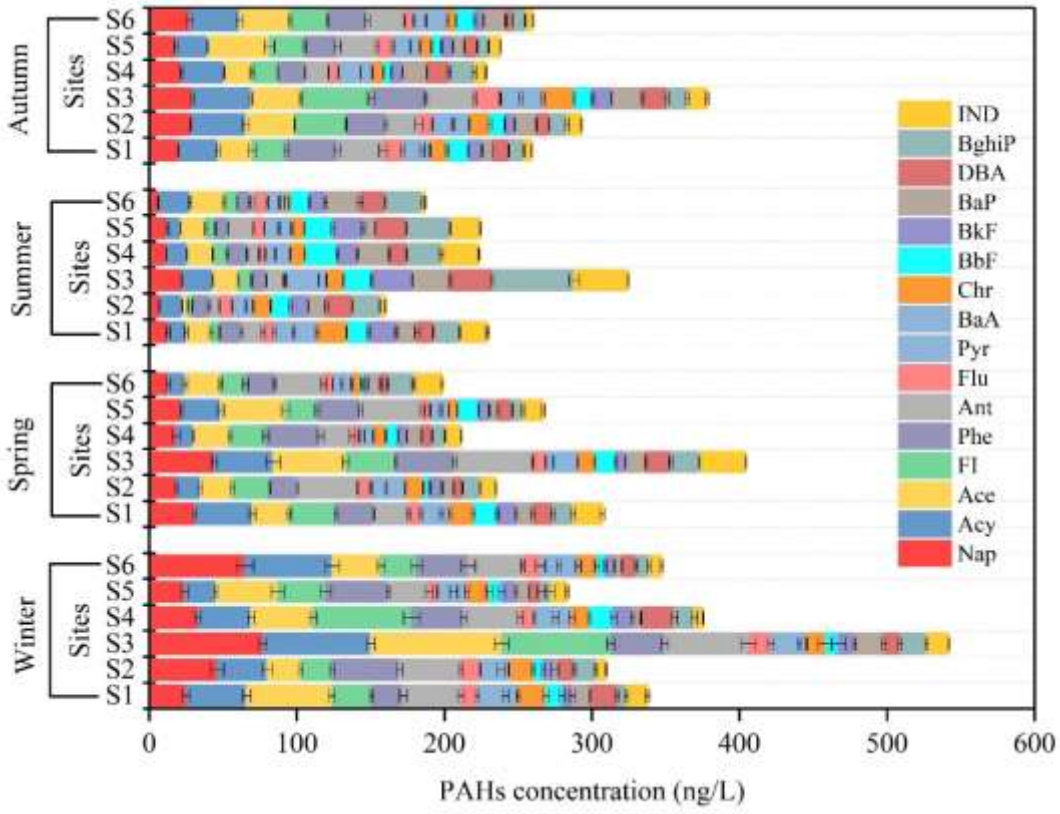

Figure 5 PAHs concentration in water in the six locations with respect to seasons.

The ∑PAHs concentrations in water samples across all seasons (ranging from a low of 224.8 ng/L in summer to a high of 365.8 ng/L in winter) were higher than those reported in the Danube River and its tributaries within Hungary, where concentrations ranged from 67.0 to 96.0 ng/L[95], [96]. They also exceeded other recorded values along the Danube River (16.0–133.0 ng/L) [97] and additional Danube River measurements (15.9 to 53.2 ng/L) [98]. According to the European Union's Drinking Water Directive, the maximum permissible concentration of PAHs in water is set at 100 ng/L[56], [57]. Seasonal ∑ PAHs levels in this study exceeded this standard by 124.8%

in summer and 265.8% in winter. In contrast, ∑ PAHs concentrations in the study area were lower than those observed in the Raba River, the largest Danube tributary in Hungary, where concentrations ranged from 41.0 to 437.0 ng/L [99]. These variations likely result from differences in sampling site selection, as this study targeted sites where contamination sources were anticipated. In general, the PAHs concentrations observed in this study were also lower than those reported in other countries, such as the Tiber River in Italy and the Humen, Bai Chao, and Chaobai Rivers in China, with PAHs ranges of 10.3–951.6 ng/L, 311.1–1012.8 ng/L, and 55.0–882.0 ng/L, respectively [100], [101], [102]. Additionally, the levels were similar to those reported in the Yinma River in China, where Chen and co-workers observed concentrations between 23.2 and 386.9 ng/L [103].

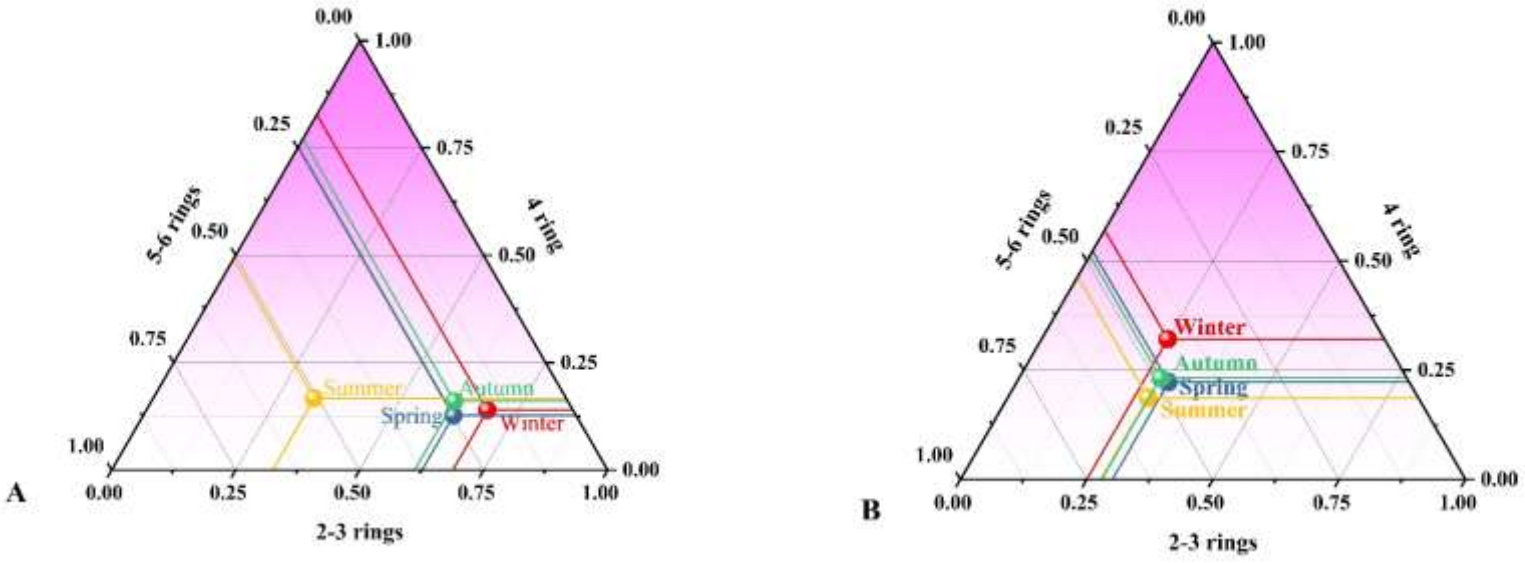

Figure 6 PAHs rings percentages in (A) water and (B) sediment among different sampling seasons: winter, spring, summer, and autumn.

3.1.2. PAHs in Daube River sediment

The concentrations of PAHs in sediments are shown in Figure 7. Across the four seasons, PAHs concentrations in sediment samples ranged from 316.7 ng/g dw in summer to 422.9 ng/g dw in winter. Seasonal variation in PAHs concentrations was observed as follows: 313.7–622.7 ng/g in

winter, 312.7–595.4 ng/g in spring, 215.1–465.4 ng/g in summer, and 311.3–491.7 ng/g in autumn. The variation in PAHs levels within Danube River sediments indicates that concentrations differ by sampling site, suggesting localized anthropogenic sources along the river. The variation by season, due to differences in sampling times and locations, also suggests influences from seasonal changes.

In contrast to PAHs concentrations in water, HMWPAHs were more prevalent than LMWPAHs in Danube River sediments (Figure 5), consistent with other studies [104], [105]. Due to their higher water solubility and volatility (attributable to lower octanol-water coefficients), LMWPAHs typically recorded lower concentrations in sediments [106]. On the other hand, HMWPAHs have low water solubility, higher partitioning coefficients, and strong hydrophobicity in water, leading to greater sediment accumulation [107]. The most predominant PAHs in sediment samples were BaP, Chr, BbF, and BkF, with concentrations ranging between 28.7–52.4 ng/g, 16.1–50.8 ng/g, 22.9–42.6 ng/g, and 14.9–42.4 ng/g, respectively. These were followed by BkF, Pyr, BghiP, and BaA, with concentrations of 26.3–36.8 ng/g, 11.4–36.0 ng/g, 13.3–33.8 ng/g, and 10.1–32.8 ng/g, respectively. As with water samples, site S3 recorded the highest PAHs concentrations (Figure 4). The lowest concentrations were found for IND and Flu, ranging from 17.0–29.3 ng/g and 9.0–21.4 ng/g, respectively. The highest concentrations of LMWPAHs were recorded for Ant (13.2–24.8 ng/g), Fl (11.9–23.3 ng/g), and Phe (14.5–23.2 ng/g), while Acy, Nap, and Ace recorded the lowest concentrations, with ranges of 11.6–18.4 ng/g, 14.0–19.2 ng/g, and 11.2–22.0 ng/g, respectively. No distinct seasonal patterns were identified in PAHs concentrations in sediments, indicating that they are relatively unaffected by seasonal changes.

Sediment pollution levels, based on total PAHs concentrations, can be categorized as follows: (A) low pollution (<100 ng/g), (B) moderate pollution (101–1000 ng/g), (C) high pollution (1001–5000 ng/g), and (D) very high pollution (>5000 ng/g) [59]. Therefore, sediment pollution levels in the Danube River can be classified as low.

The seven carcinogenic PAHs (CPAHs) accounted for most of the total PAHs, with concentrations ranging from 181.09 ng/g in summer to 240.0 ng/g in winter. CPAHs exhibited the same spatial distribution as ∑ PAHs, with site S3 showing the highest levels (Figure 8). Variations in PAHs concentrations in sediments across sites are likely influenced by several factors [104], [108], [109], including (1) untreated municipal wastewater discharges, traffic emissions, industrial activities, and fuel consumption; (2) hydrodynamic variations influenced by meteorological

conditions, which can cause sediment resuspension and redeposition; (3) spatial differences in sediment texture based on sampling site characteristics; and (4) redox conditions in sediments and PAHs biodegradation. The maximum PAHs concentration observed at site S3 may be attributed to its location within Budapest and its proximity downstream to a wastewater treatment plant. PAHs concentrations in wastewater are a significant concern for industry, as PAHs are highly toxic and persistent, posing long-term environmental risks. Their carcinogenic, genotoxic, and mutagenic properties present serious health hazards [110], [111]. PAHs pollution can persist in wastewater effluents if not adequately removed, ultimately contaminating river water through these sources [112], [113], [114].

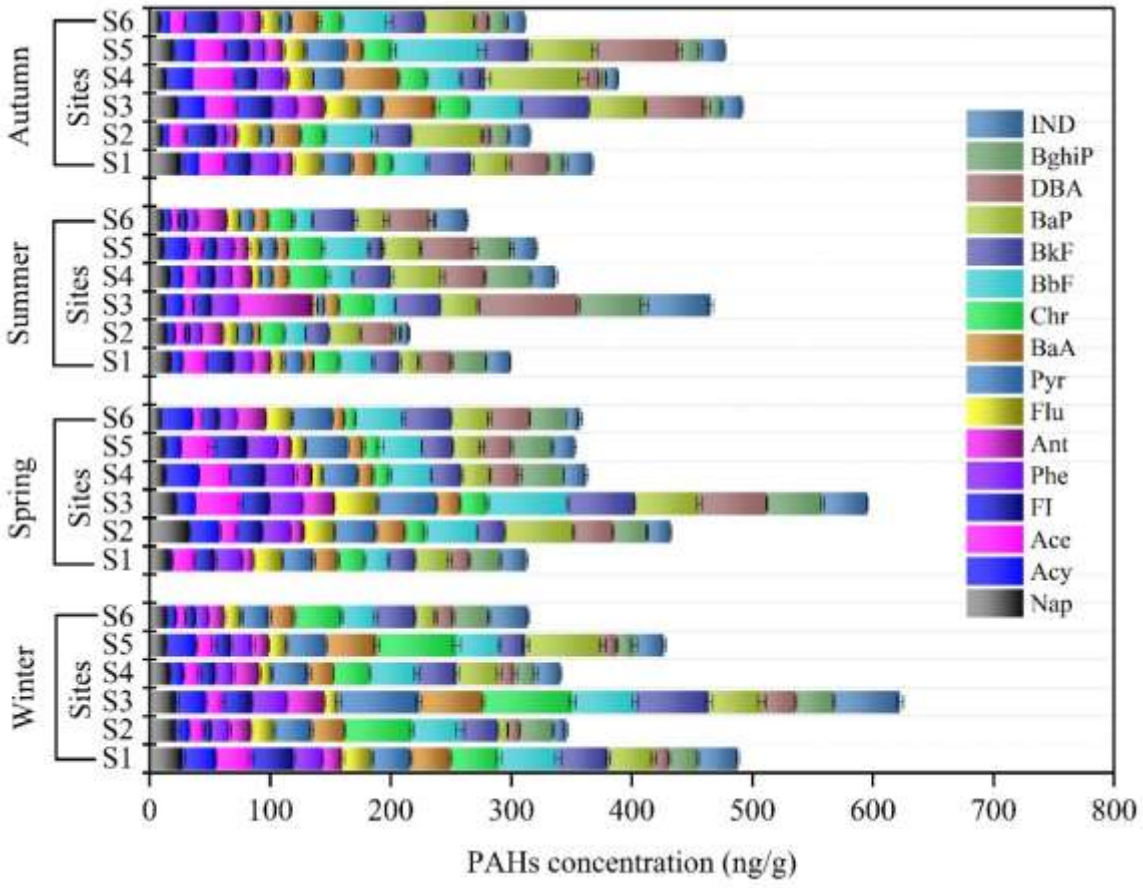

Figure 7 PAHs concentration in sediment samples among various sampling sites and seasons campaigns.

The concentrations of PAHs in sediment samples from the Danube River ranged from 316.7 ng/g dw in summer to 422.9 ng/g dw in winter. These levels were higher than those detected in the

upper section of the Danube River and its tributaries in Hungary (35.2 to 288.3 ng/g) [96] and in the Danube River and the Moson Danube Arm (118.0 to 283.0 ng/g) [97], but lower than those reported in the upper section of the Danube River and the Mosoni-Danube branch (8.3 to 1202.5 ng/g) [99]. Overall, the PAHs concentrations measured in the present study were consistent with those reported from other countries, such as the Soltan Abad River in Iran (180.3 to 504.0 ng/g) [115]and the Ovia River in Nigeria (5.2 to 573.3 ng/g) [116]. These concentrations were lower compared to those reported by Liu et al. in rivers in Shanghai, China (248.8 to 36,198.2 ng/g) [117].

In the Seine River basin, France, PAHs concentrations in soils ranged from 450 to 5650 µg/kg [118]. Otte and co-workers found that the 16 PAHs in the sediments of the Elbe River Estuary in Germany were moderately contaminated, with concentrations ranging from 0.02 to 0.906 mg/g dw [119]. PAHs levels in the Tiber River and its estuary in Italy ranged from 10.3 to 951.6 ng/L in water and from 36.2 to 545.6 ng/g in sediment samples, respectively [101]. In the Sele River in southern Italy, total PAHs concentrations ranged from 632.4 to 844.9 ng/g dw. Furthermore, PAHs in the sediments of the Sarno and Volturno Rivers were found to range from 5.2 to 678.6 ng/g and from 434.8 to 872.1 ng/g, respectively [120].

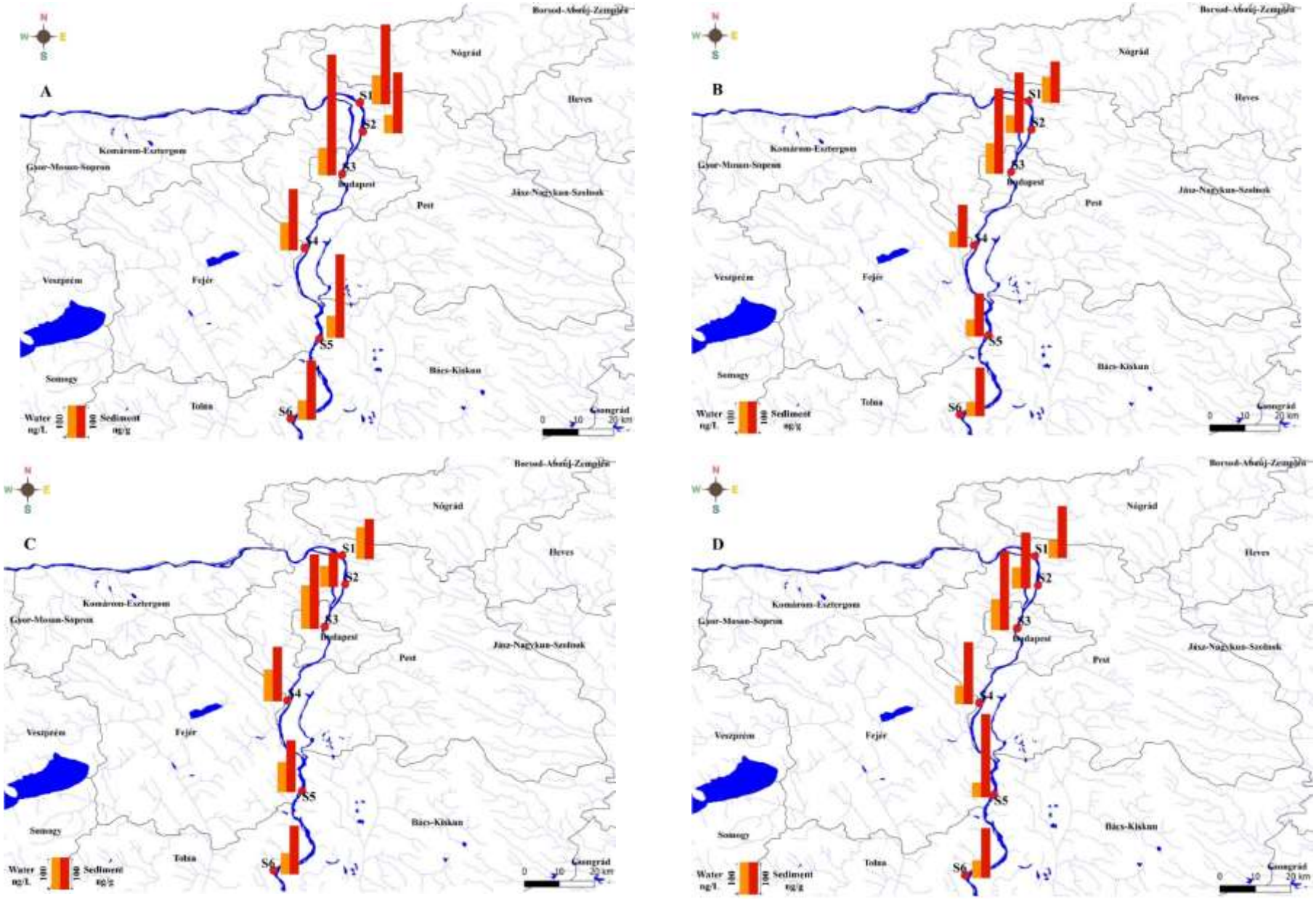

Figure 8 7CPAHs for each site for winter (A), spring (B), summer (C), and autumn (D). Map of Study area designed using QGIS software version 3.18.2. https://qgis.org/downloads/QGIS-OSGeo4W-3.18.3-1-Setup-x86_64.exe

3.2. Sources identification ratios of PAHs in water and sediment samples for Danube River

Based on the average concentrations of individual PAHs in water and sediments for each sampling season (winter, spring, summer, and autumn), the following diagnostic ratios were determined to identify the dominant sources and related emission routes. The specific meanings of each ratio—Flu/(Flu+Pyr), LMW/HMW, Flu/Pyr, BaA/(BaA+Chr), IND/(IND+BghiP), IND/BghiP, and BaA/(BaA+Chr)—along with the determined ratios, are provided in Appendix 5 and 6 for water and sediments, respectively. According to the literature, a ratio of BaA/(BaA+Chr) less than 0.2 suggests that PAHs are primarily generated from petrogenic inputs (liquid fuel discharges). A ratio between 0.2 and 0.35 indicates that PAHs originate from mixed sources (petrogenic/pyrogenic), while a ratio greater than 0.35 implies that PAHs are predominantly formed from pyrogenic sources, such as the combustion of solid fuels, biomass, and coal. Similarly, a ratio of Flu/(Flu+Pyr) less than 0.4 indicates that PAHs originate from petrogenic inputs, a ratio between 0.4 and 0.5 suggests pyrolytic sources (such as burning liquid fossil fuels and crude oil), and a ratio greater than 0.5 indicates pyrogenic sources from the combustion of solid fuels. Additionally, a ratio of IND/(IND+BghiP) lower than 0.2 suggests petrogenic origins, a ratio between 0.2 and 0.5 indicates pyrolytic sources, and a ratio greater than 0.5 points to pyrogenic sources. The ratios plotted as BaA/(BaA+Chr) against Flu/(Flu+Pyr) and as BaA/(BaA+Chr) against IND/(IND+BghiP) are presented in Figure 9. Generally, LMWPAHs originate from oil or fuel spills and have a short lifetime in the ecosystem, whereas HMWPAHs arise from combustion products, pyrolysis, or petrogenic origins [3]. As shown in Figure 9, Flu/(Flu+Pyr) ratios range from 0.4 to 0.5 in all seasons except summer for water samples. In sediment samples, the opposite was observed, indicating pyrolytic sources in both cases. Furthermore, these ratios were less than 0.4 in the summer season for water samples and in both the winter and spring seasons for sediment samples, indicating petrogenic inputs. The only instance of ratios exceeding 0.5 occurred in autumn for sediment samples, suggesting that wood, coal, and grass combustion are the primary sources of PAHs. The BaA/(BaA+Chr) ratios for both water and sediment samples were greater than 0.35, indicating pyrogenic sources, except in the summer season for sediments, where values were scattered and clustered between 0.2 and 0.35, indicating mixed sources (petrogenic/pyrogenic). The ratios of IND/(IND+BghiP) for water samples were greater than 0.5 only in the spring season, while for sediment samples, ratios were greater than 0.5 in all seasons

except spring, suggesting the contribution of solid fossil fuel combustion, such as biomass and coal, in agricultural regions. For water samples, the ratios of IND/(IND+BghiP) ranged between 0.2 and 0.5 in the winter, summer, and autumn seasons, while sediment samples showed this range only in spring, indicating pyrolytic sources. The BaP/BghiP ratio in both water and sediment samples was greater than 0.6 in all sampling seasons, indicating PAHs of petrogenic origin. Overall, the results indicate that the putative anthropogenic sources of PAHs are both pyrolytic (incomplete combustion of liquid fossil fuels and vehicle exhaust emissions) and pyrogenic (incomplete combustion of biomass and coal), with pyrogenic sources predominating over pyrolytic sources.

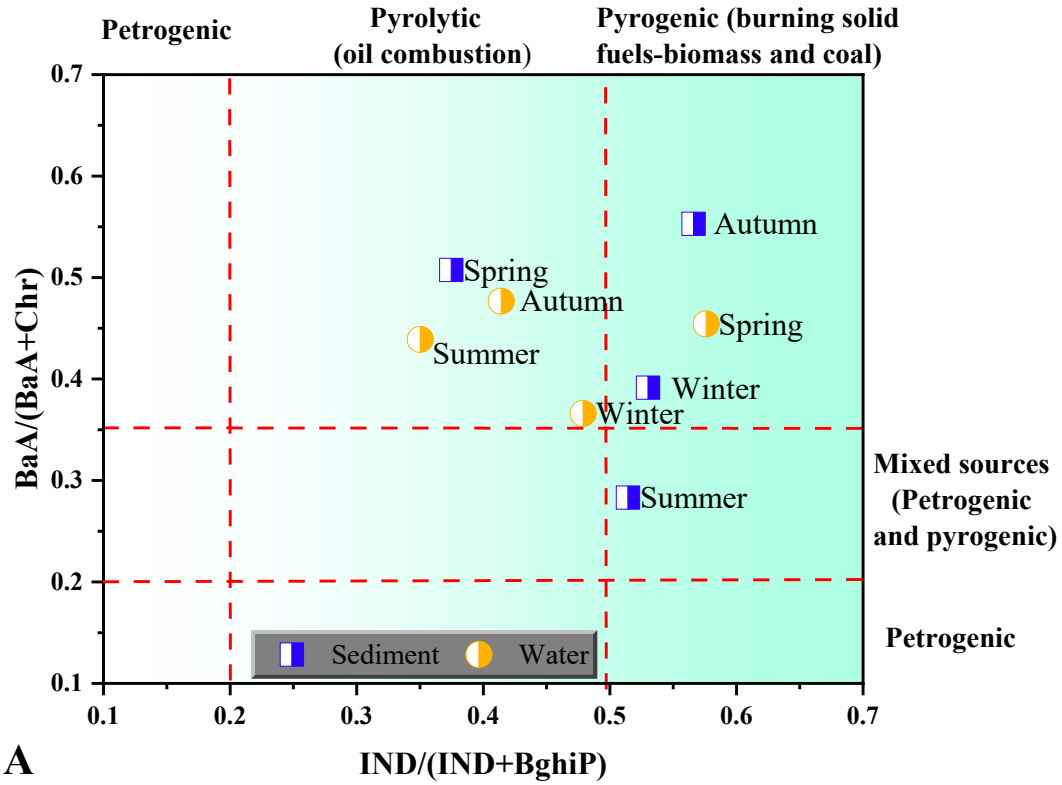

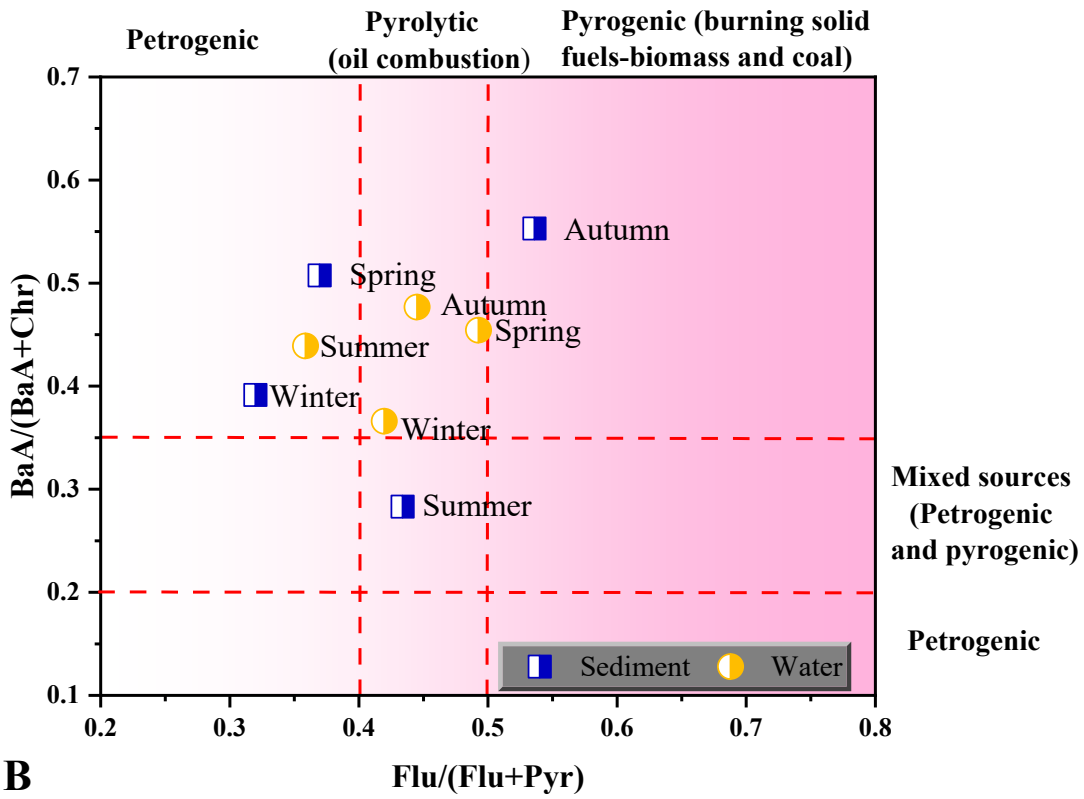

Figure 9 Cross plots of the diagnostic ratios of (A) BaA/(BaA+Chr) to IND/ (IND+BghiP) and (B) ratios BaA/(BaA+Chr) to Flu/(Flu+Pyr) for water and sediment samples in all seasons from the Danube River

3.3. Principal Component Analysis (PCA) based on PAHs in water and sediment for Danube River

PCA was used to describe the individual loading of 16 PAHs variables in water and sediment samples from all six sites in the Danube River (Figure 10). Bartlett's test revealed that the variables are substantially correlated and appropriate for PCA analysis. The first two principal components account for 88.6% of the overall variation in the findings related to water samples and 84.5% of the variance in the sediment samples. Generally, PCA1 was positively dominated by high loadings of all examined PAHs in both water (Figure 10, A) and sediments (Figure 10, B).The PCA analysis results corroborated the previously observed distinction between sampling seasons, particularly regarding the concentrations of LMWPAHs (Nap, Acy, Ace, Fl, Phe, and Ant) in water samples, which were notably higher in the cold seasons compared to the warm season. Specifically, Figure 10 shows that, according to the PCA results, all LMWPAHs were characterized by cold seasons—

winter, autumn, and spring. In contrast, most HMWPAHs predominantly occurred in the summertime. This observation can be attributed to the poor water solubility and dissolution rate of HMWPAHs, which render them more resistant to decomposition, while LMWPAHs are more soluble and degradable during the warm season. Figure 10 also indicates that the PCA results for sediment samples revealed no distinct trends for PAHs across seasonal sediment samples, demonstrating that sediments are independent of seasonal variations.

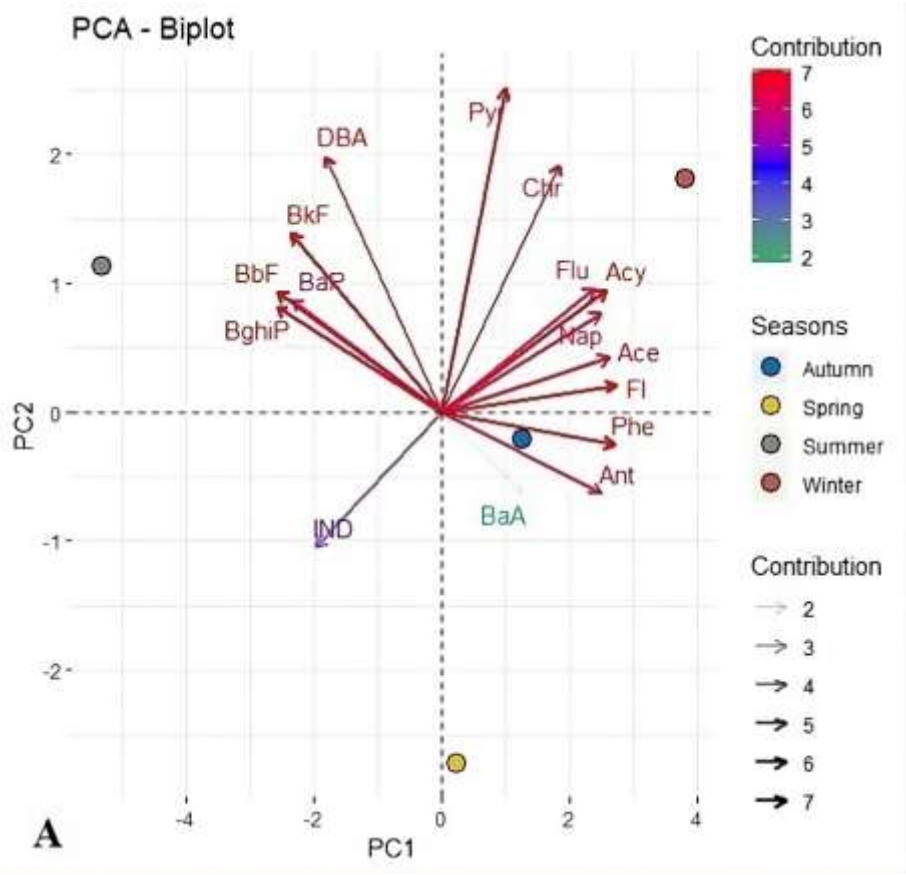

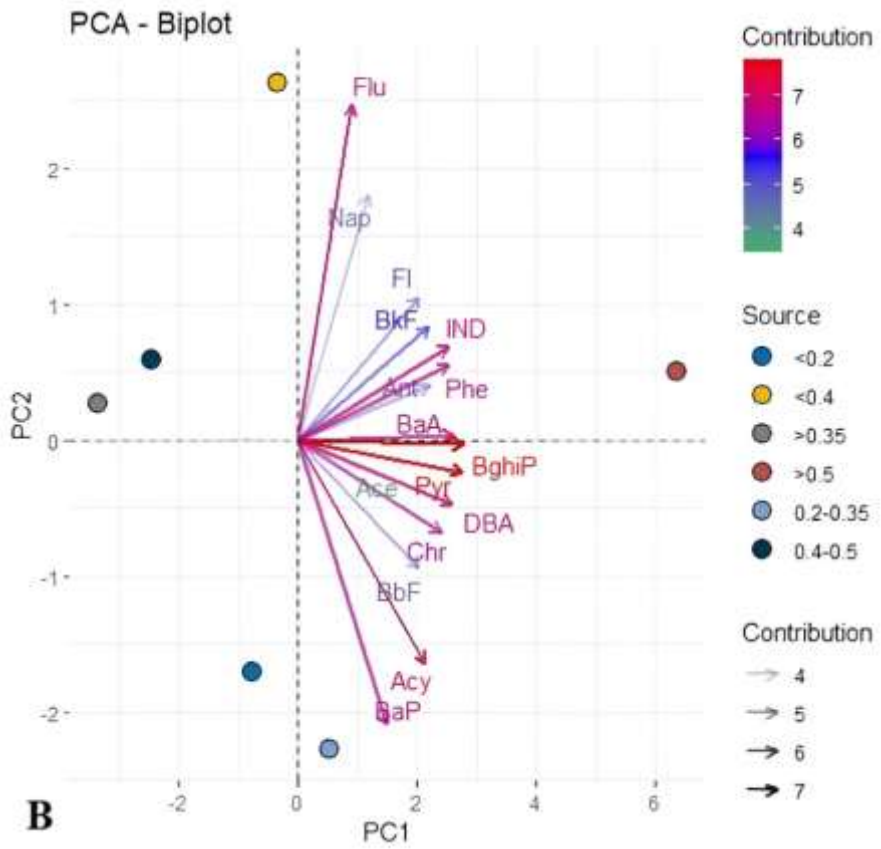

Figure 10 PCA analysis for water (A) and sediment (B)

Table 3 displays the concentration ranges and toxicity recommendations for 16 individual PAHs. The concentrations of all PAHs in sediments were below the Effects Range Low (ERL) except for Acy and FI, indicating the possibility of rare biological effects. However, the concentrations of Acy in winter and spring, and FI in autumn and spring, were above the ERL but lower than the Effects Range Median (ERM), suggesting occasional biological effects. Generally, aside from the two mentioned PAHs, ecotoxicological concerns for the aquatic environment of the Danube River do not pose a significant hazard. The combined impact of the 16 PAHs pollutants in sediments suggests a low likelihood of negative biological impacts and a low ecological threat. To ensure that the residual levels of PAHs in the sediments of the Danube River do not exceed ecological quality criteria, routine monitoring of PAHs in sediments is required. Additionally, pollution control initiatives must be undertaken to prevent the spread of PAHs in the Danube River.

Table 3 Concentration range of 16 individual PAHs (ng/g dw) and toxicity guidelines

PAHs	ERL-ERM	Range (ng/g dw)		<ERL	≥ERL and ≥ERM <ERM
		Min	Max		
Nap	160–2100	14.01	19.23	✓	
Acy	16–500	11.67	18.45	Rest Seasons	Winter, Spring
Ace	44–640	11.20	21.99	✓	
FI	19–540	11.89	23.30	Rest Seasons	Spring autumn
Phe	240–1500	14.58	23.21	✓	
Ant	600–5100	13.21	24.85	✓	
Flu	85.3–1100	8.99	21.44	✓	
Pyr	665–2500	11.40	36.00	✓	
BaA	261–1600	10.17	32.88	✓	
Chr	384–2800	16.16	50.82	✓	
BbF	320–1880	22.93	42.62	✓	
BkF	280–1620	26.31	36.85	✓	
BaP	430–1600	28.79	52.47	✓	
DBA	63.4–260	14.97	42.42	✓	
BghiP	430–1600	13.33	33.81	✓	
IND	240-	17.00	29.38	✓	

The Toxic Equivalency Quotient (TEQ) for sediment samples ranged from 29.88 ng/g in the winter season to 140.39 ng/g in the autumn season. According to Canadian soil quality guidelines for the preservation of ecosystems and human health, a threshold value of 600 ng/g is considered safe for humans [121]. The ILCR values for adults and children detected in sediment samples from the Danube River are shown in Figure 11. The total ILCR for both children and adults are more than 1 in 10,000 in all seasons, with the highest values recorded at site 3, which is

a serious concern. Furthermore, these values are substantially higher than those reported in the Brisbane River in Australia [122]. When high amounts are found through long-term surveillance, residents within the river basin area must be warned, and precautions must be taken to prevent human contact with the sediments.

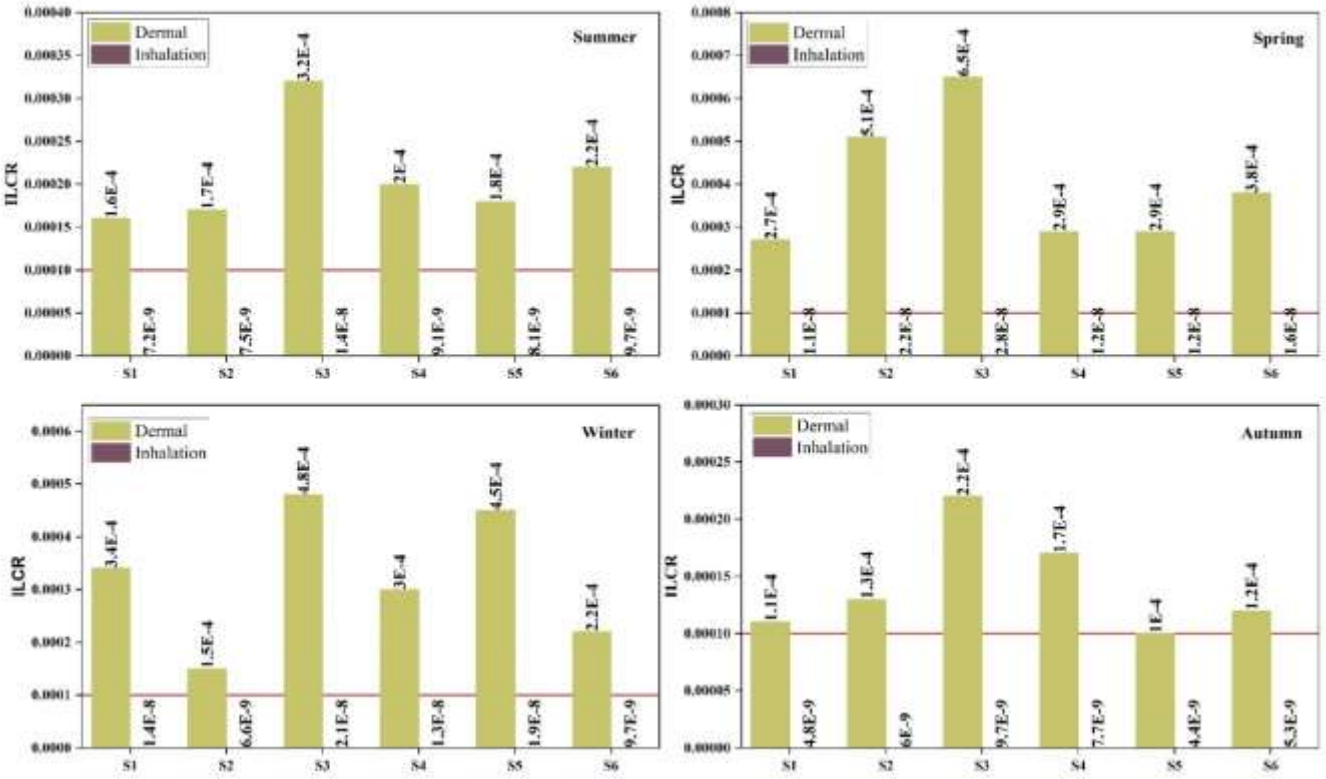

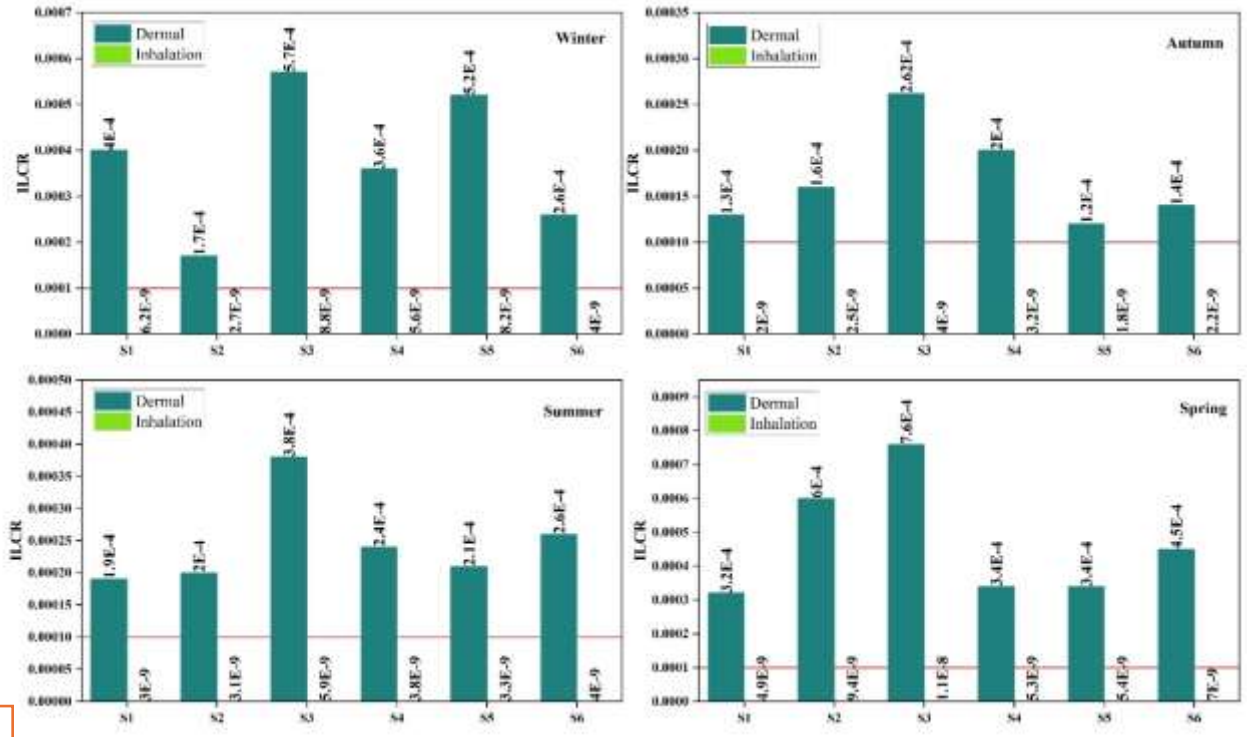

ii

Figure 11 ILCR levels in the Danube River sediments for adults (i) and children (ii). The red line is the ILCR ($1/10^4$).

4.1. Surface water and sediment PAHs range in each location of Tigris River

Figure 12 shows the changes in 16 PAHs concentrations in water samples over six months (July–December 2022). The ∑ 16 PAHs at examined sites ranged from 678.2 to 718.5 ng/L for Al-Kasak (S1); 1080.2 to 1354.6 ng/L for Qayyarah (S2) (before the oil refinery); 3033.0 to 3263.9 ng/L for Qayyarah (S3) (after the oil refinery); 501.7 to 606.7 ng/L for Kirkuk (S4); 571.7 to 694.2 ng/L for Al-Siniyah (S5); 1739.0 to 2101.2 ng/L for Baiji (S6) (before); 3110.0 to 3290.0 ng/L for Baiji (S7) (after); 1141.9 to 1577.5 ng/L for Daura (S8) (before); 2690.2 to 2984.5 ng/L for Daura (S9) (after); 897.7 to 1040.5 ng/L for Maysan (S10); 1128.7 to 1502.3 ng/L for South Refineries Company (S11) (before); and 3614.6 to 3861.9 ng/L for South Refineries Company (S12) (after). Overall, field observations and PAHs measurements indicate significant pollution in the surface water along the Tigris River and its estuaries, with especially high contamination levels near oil refineries. The closer the refinery is to the water, the higher the pollution, suggesting inadequate waste management strategies.The variation in PAHs concentration in sediment samples is illustrated in Figure 13. The ∑ 16 PAHs at examined sites ranged from 8224.8 to 9455.8 ng/g for Al-Kasak (S1); 5313.8 to 5942.0 ng/g for Qayyarah (S2) (before the oil refinery); 12037.2 to

13920.4 ng/g for Qayyarah (S3) (after the oil refinery); 6053.8 to 7241.2 ng/g for Kirkuk (S4); 7545.1 to 9575.8 ng/g for Al-Siniyah (S5); 6916.4 to 7466.6 ng/g for Baiji (S6) (before); 11321.2 to 13156.8 ng/g for Baiji (S7) (after); 5285.9 to 6260.8 ng/g for Daura (S8) (before); 11675.0 to 14089.9 ng/g for Daura (S9) (after); 7642.1 to 9718.8 ng/g for Maysan (S10); 5337.8 to 6025.5 ng/g for South Refineries Company (S11) (before); and 11318.2 to 13254.3 ng/g for South Refineries Company (S12) (after). The distribution of 16 PAHs in sediments mirrored that in surface water, with elevated levels observed after each refinery site, indicating consistent contamination trends across both water and sediment samples.

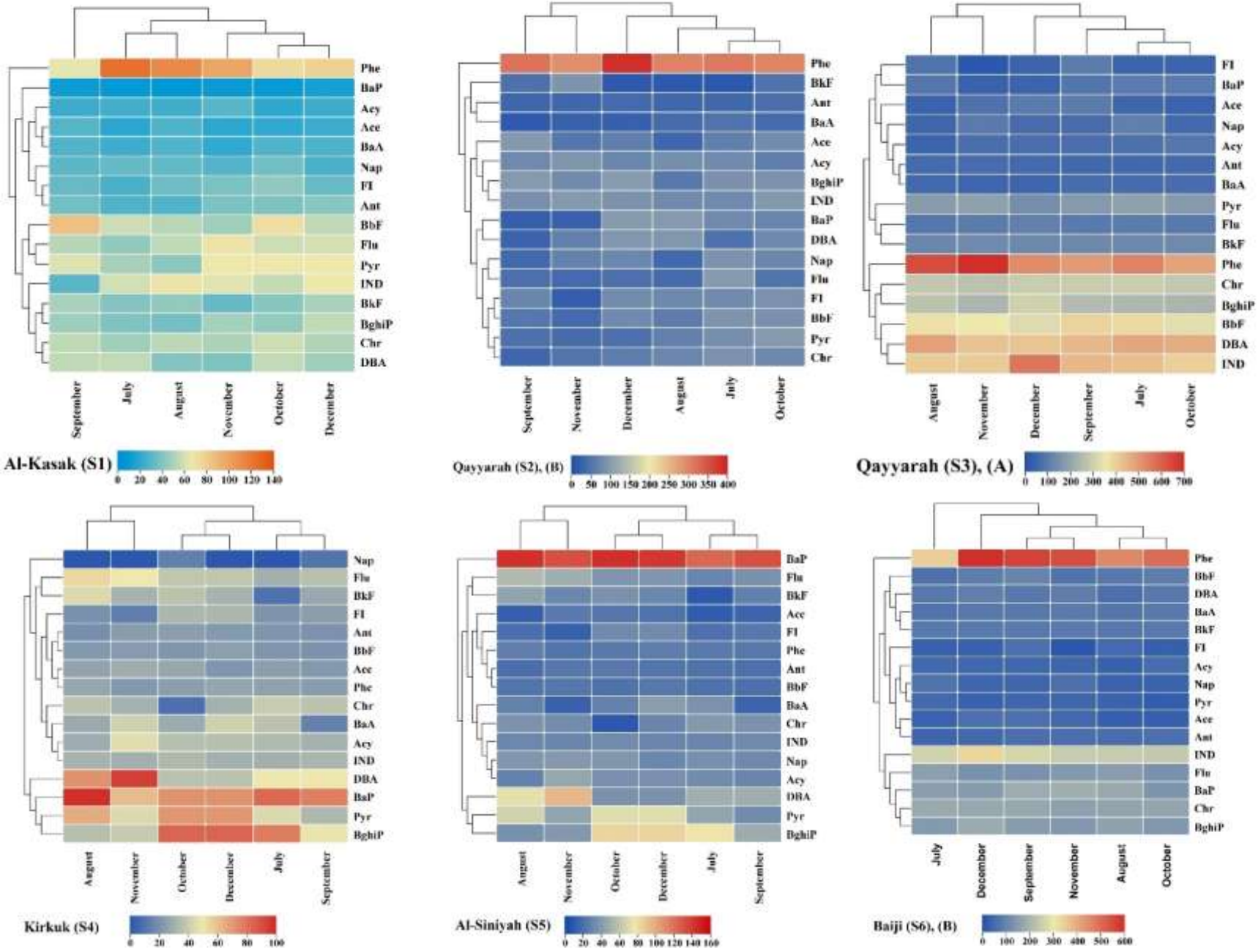
Phe
BaP
Acy
Ace
BaA
Nap
Fl
Ant
BbF
Flu
Pyr
IND
BkF
BghiP
Chr
DBA
September
July
August
November
October
December
Al-Kasak (S1)
0 20 40 60 80 100 120 140
Phe
BkF
Ant
BaA
Ace
Acy
BghiP
IND
BaP
DBA
Nap
Flu
Fl
BbF
Pyr
Chr
September
November
December
August
July
October
Qayyarah (S2), (B)
0 50 100 150 200 250 300 350 400
Fl
BaP
Ace
Nap
Acy
Ant
BaA
Pyr
Flu
BkF
Phe
Chr
BghiP
BbF
DBA
IND
August
November
December
September
July
October
Qayyarah (S3), (A)
0 100 200 300 400 500 600 700
Nap
Flu
BkF
Fl
Ant
BbF
Ace
Phe
Chr
BaA
Acy
IND
DBA
BaP
Pyr
BghiP
August
November
October
December
July
September
Kirkuk (S4)
0 20 40 60 80 100
BaP
Flu
BkF
Ace
Fl
Phe
Ant
BbF
BaA
Chr
IND
Nap
Acy
DBA
Pyr
BghiP
August
November
October
December
July
September
Al-Siniyah (S5)
0 20 40 60 80 100 120 140 160
Phe
BbF
DBA
BaA
BkF
Fl
Acy
Nap
Pyr
Ace
Ant
IND
Flu
BaP
Chr
BghiP
July
December
September
November
August
October
Baiji (S6), (B)
0 100 200 300 400 500 600

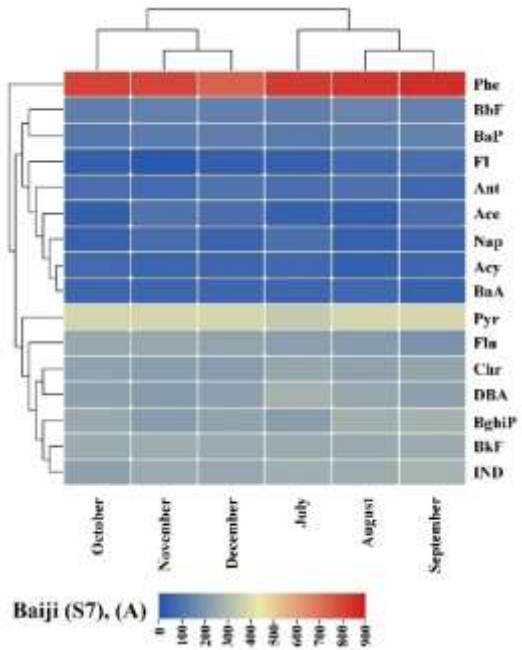
Phe
BbF
BaP
Fl
Ant
Ace
Nap
Acy
BaA
Pyr
Flu
Chr
DBA
BghiP
BkF
IND
October
November
December
July
August
September
Baiji (S7), (A)
0 100 200 300 400 500 600 700 800 900

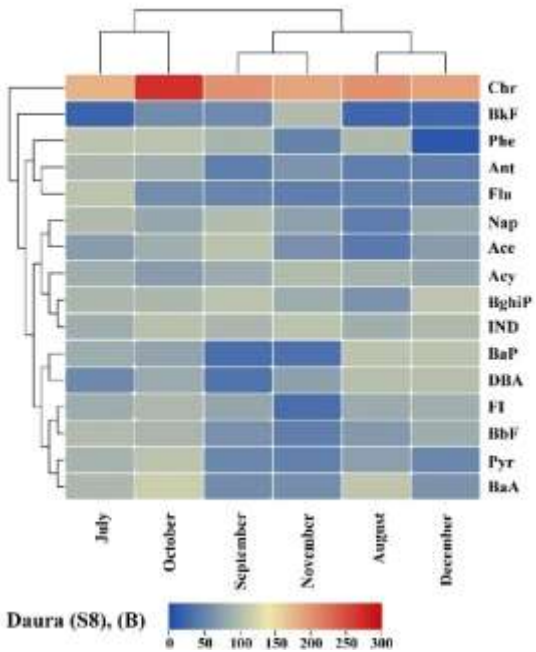
Chr
BkF
Phe
Ant
Flu
Nap
Ace
Acy
BghiP
IND
BaP
DBA
Fl
BbF
Pyr
BaA
July
October
September
November
August
December
Daura (S8), (B)
0 50 100 150 200 250 300

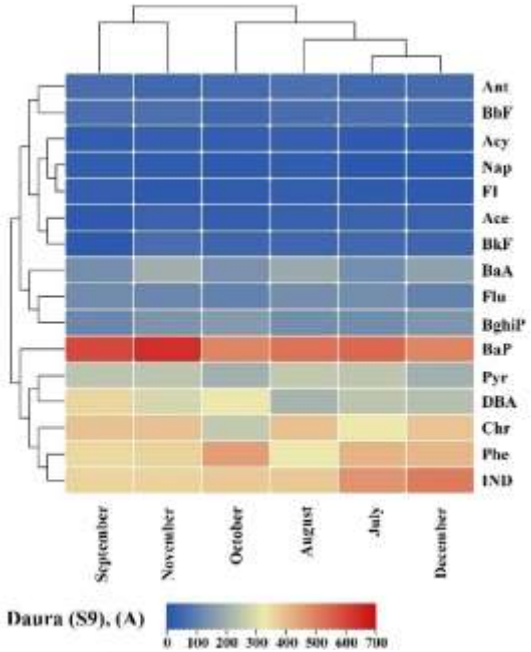
Ant
BbF
Acy
Nap
Fl
Ace
BkF
BaA
Flu
BghiP
BaP
Pyr
DBA
Chr
Phe
IND
September
November
October
August
July
December
Daura (S9), (A)
0 100 200 300 400 500 600 700

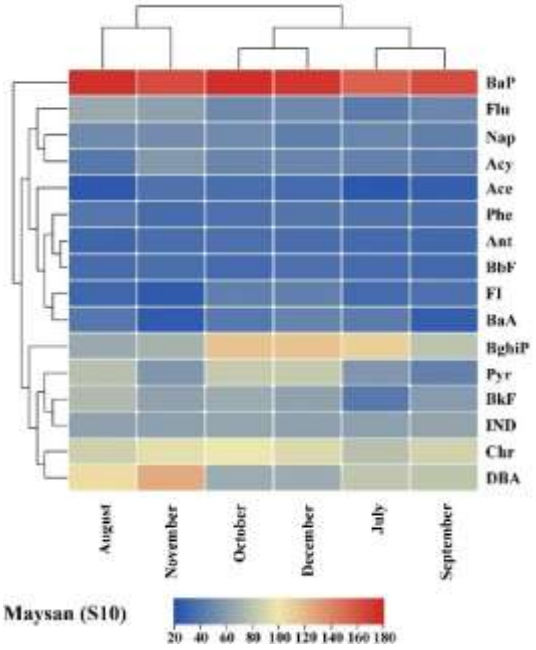
BaP
Flu
Nap
Acy
Ace
Phe
Ant
BbF
Fl
BaA
BghiP
Pyr
BkF
IND
Chr
DBA
August
November
October
December
July
September
Maysan (S10)
20 40 60 80 100 120 140 160 180

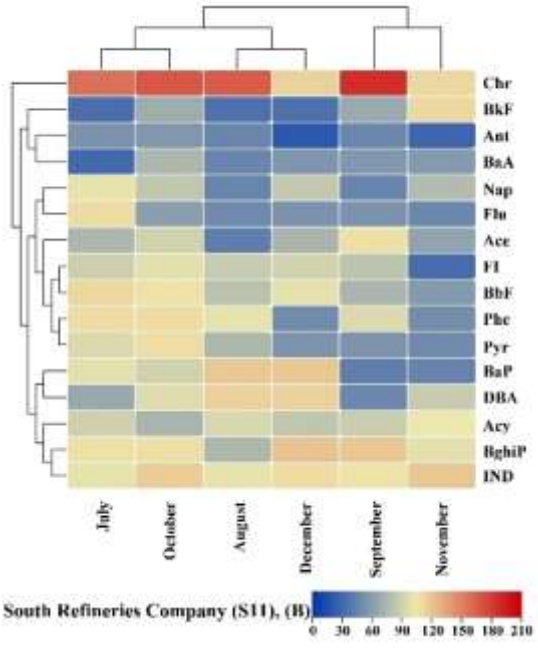
Chr
BkF
Ant
BaA
Nap
Flu
Ace
Fl
BbF
Phe
Pyr
BaP
DBA
Acy
BghiP
IND
July
October
August
December
September
November
South Refineries Company (S11), (B)
0 30 60 90 120 150 180 210

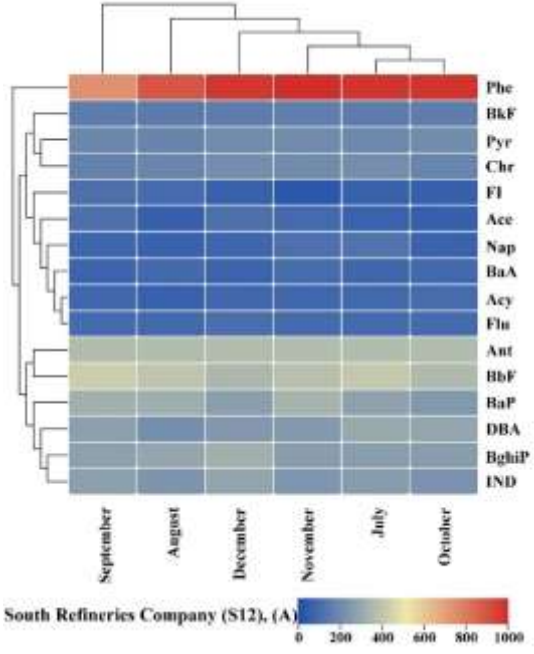
Phe
BkF
Pyr
Chr
Fl
Ace
Nap
BaA
Acy
Flu
Ant
BbF
BaP
DBA
BghiP
IND
September
August
December
November
July
October
South Refineries Company (S12), (A)
0 200 400 600 800 1000

Figure 12 Change in 16 PAHs concentrations for the water samples (ng/L) near the oil refineries in Tigris and its estuaries. The standard deviation is less than 6%. (A) The location after the oil refineries and (B) the location before the oil refineries.

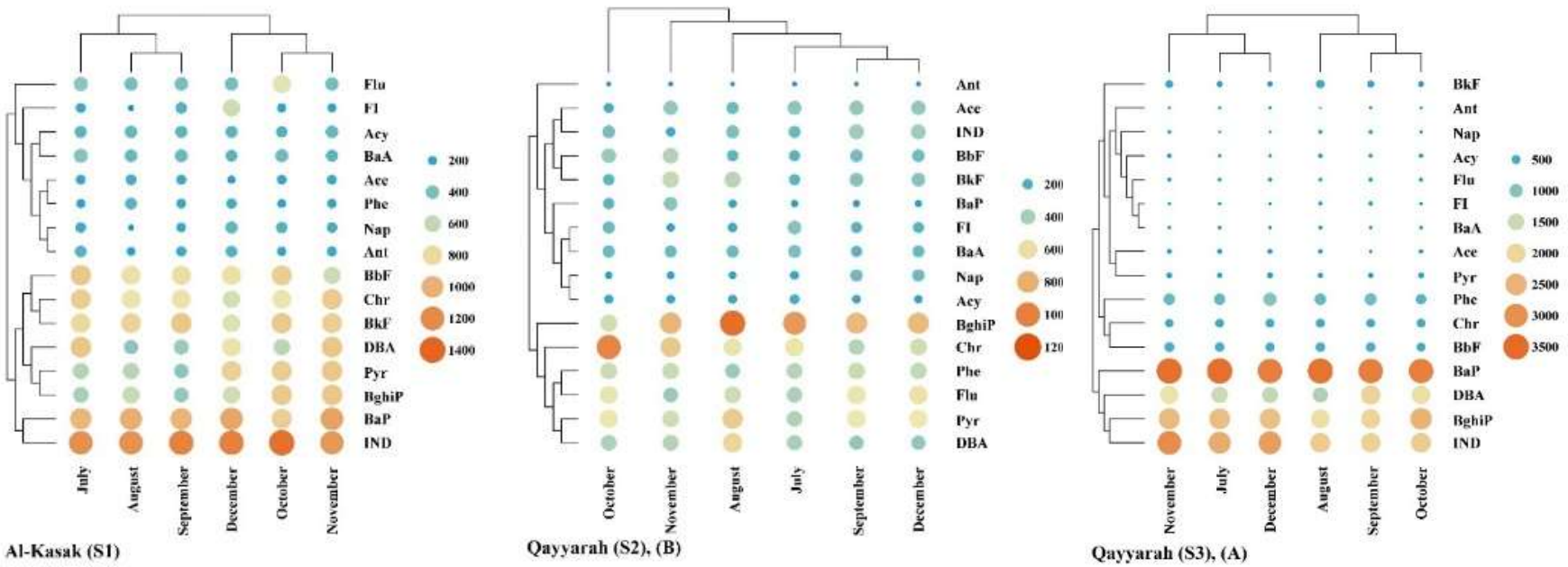

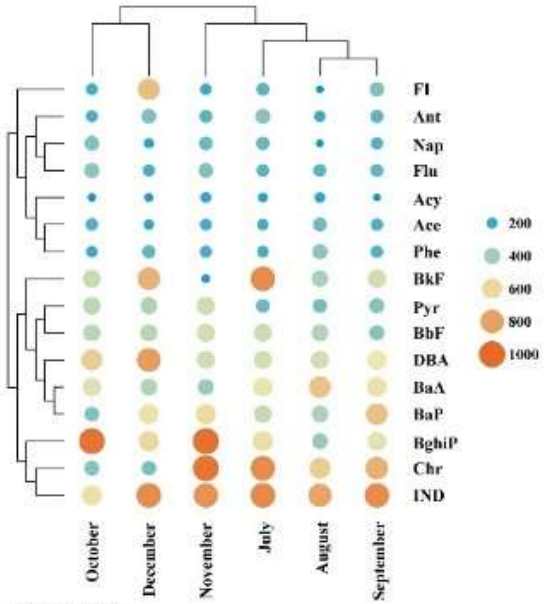

Kirkuk (S4)

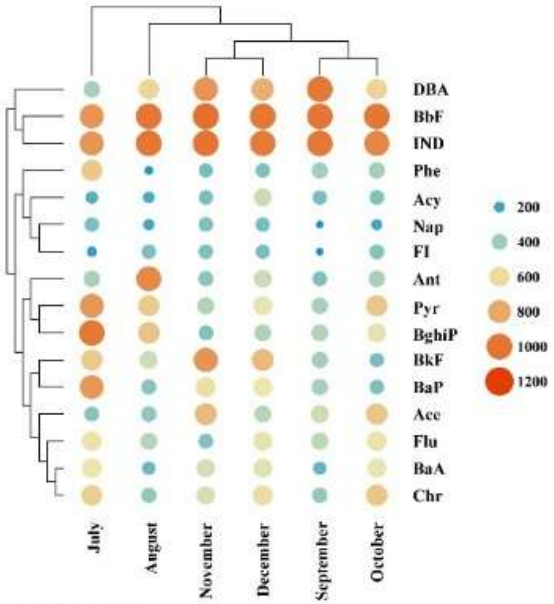

Al-Siniyah (S5)

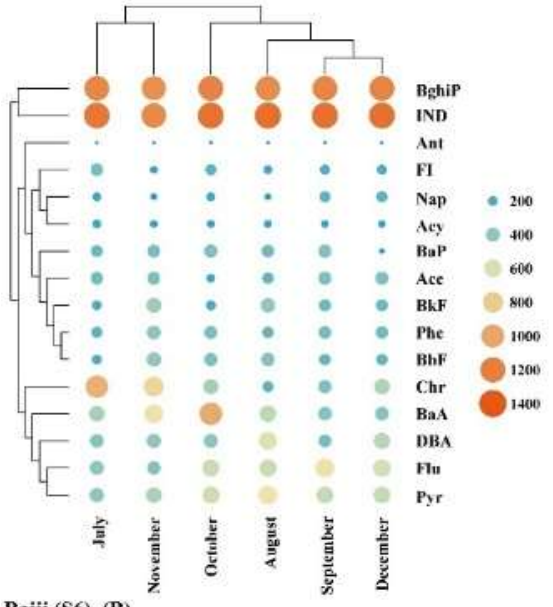

Baiji (S6), (B)

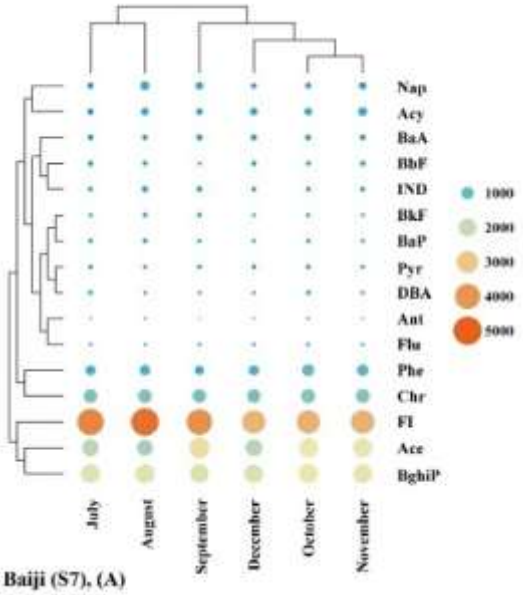

Baiji (S7), (A)

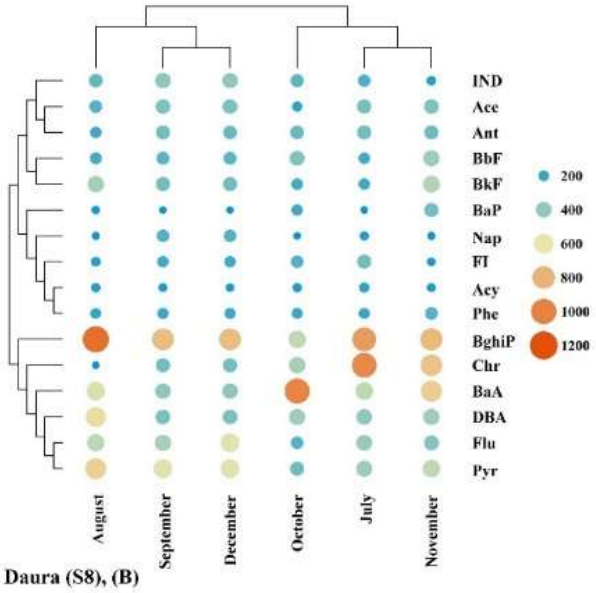

Daura (S8), (B)

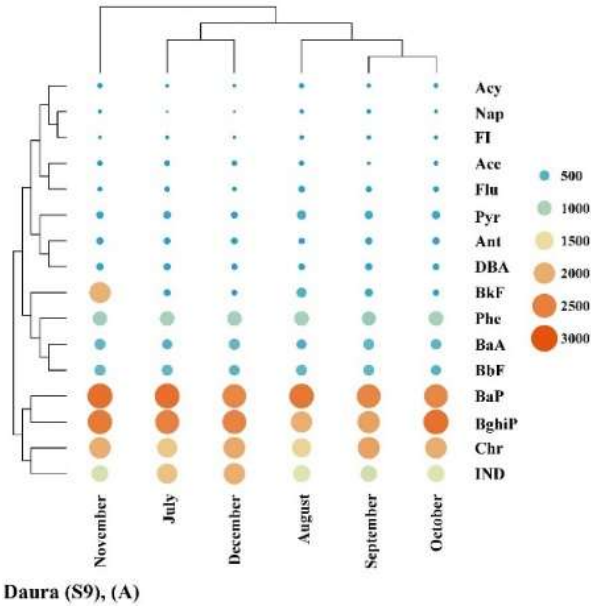

Daura (S9), (A)

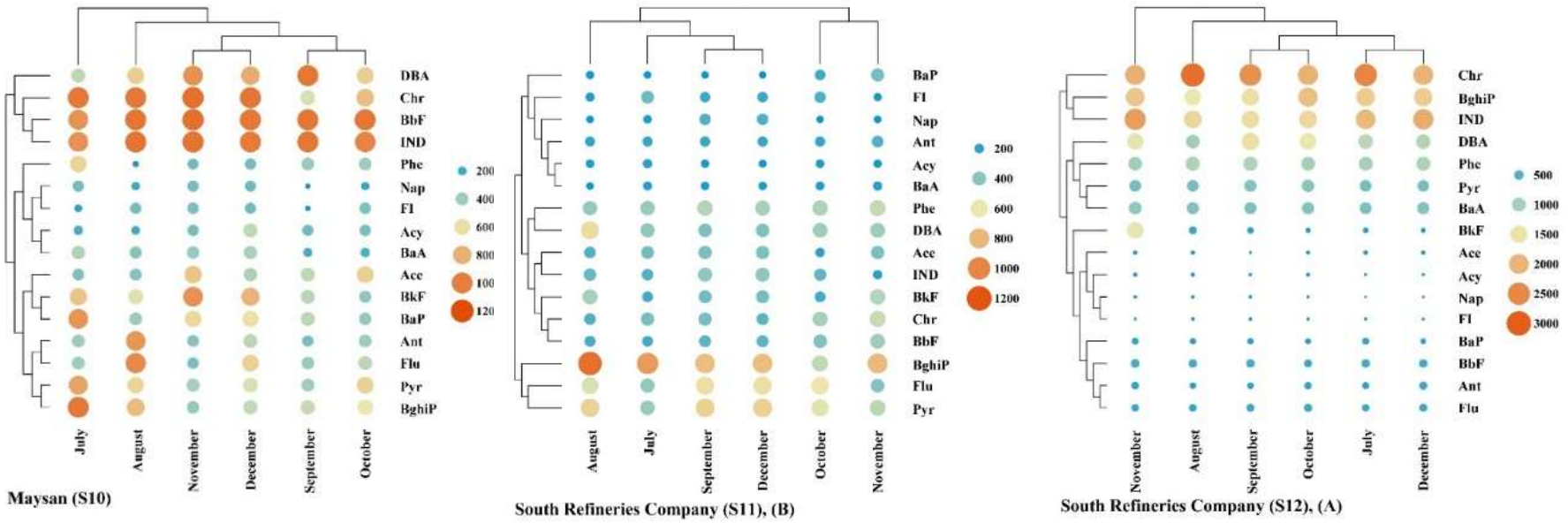

Figure 13 The 16 PAHs concentrations in sediments samples (ng/g) near oil refineries in Tigris and its estuaries. Bubble bar represents the concentration of PAH. The standard deviation is less than 8%. (A) The location after the oil refineries and (B) the location before the oil refineries.

4.2 Spatial and temporal variation of PAHs concentrations in water and sediment of Tigris River

The overall findings for 16 PAHs in water (A) and sediment (B) samples are shown in Figure 14, which presents mean PAHs concentrations for each site. Sixteen PAHs were detected at all riverine sites, with concentrations ranging from 567.8 to 3750.7 ng/L in water and from 5619.2 to 12795.0 ng/g in sediment.In Figure 14 (A), all sites near refineries exhibit high ∑ 16 PAHs levels in water samples. Concentrations doubled after refinery locations, with Qayyarah, Baiji, and South Refineries showing the highest ∑ 16 PAHs after the refinery sites, at 3203.0, 3192.5, and 3750.7 ng/L, respectively. Figure 14(A) highlights that the most contaminated sites are S12, S3, S7, and S9. Phe, IND, BaP, and BghiP were the PAHs with the highest concentrations at these locations. Since sampling was conducted from July to December, a relatively warm period in Iraq, HMW PAHs were higher than LMW PAHs throughout, likely due to higher degradation rates for LMW PAHs in warmer conditions [92]. HMW PAHs, with lower water solubility, tend to resist decomposition, whereas LMW PAHs are more soluble and degrade faster in warmer seasons.

Similarly, sediment samples in the same locations showed high ∑ 16 PAHs levels, with concentrations of 12795.0, 12484.8, and 12449.1 ng/g for Qayyarah, Baiji, and South Refineries, respectively. Variations in PAHs concentrations in Tigris River sediments suggest that levels fluctuate with sampling sites, indicating the influence of anthropogenic activities along the river, as well as seasonal changes, as samples were taken at different times and locations. However, no significant seasonal differences were noted, suggesting that spatial variation has a greater influence than temporal variation on PAHs accumulation in sediments. These observations may point to petroleum discharge contributions to the Tigris River. IND, BghiP, and BaP consistently showed the highest levels among PAHs measured. Figure 14 (B) indicates that the most contaminated sites are S3, S7, S9, and S12. Predominant PAHs in river samples included Phe, IND, BaP, DBA, and BghiP, while for sediment samples, S1, S3, S7, S9, and S12 were the most contaminated, likely due to nearby pollution sources. IND, BghiP, BaP, and Chr were consistently present in the highest levels in sediment samples.

PAHs contamination in water and sediments has been studied globally across numerous river systems. Sun et al. reported PAHs levels in water between 144.3 to 2361.0 ng/L and in sediment from 16.4 to 1358.0 ng/g along the Henan beach of the Yellow River in central China [123]. Zheng et al. found PAHs levels in the Daliao River estuary ranging from 71.1 to 4255.4

ng/L in water and from 374.8 to 11588.8 ng/g in sediment [124]. Similar studies on the Cauca River in Colombia, the Prai River in Malaysia, and the Brisbane River in Australia reported 16 PAHs concentrations of 15–3739 ng/g (dry weight), 1102–7938 ng/g (dry weight), and 148–3079 ng/g, respectively [106], [122], [125]. Higher PAHs levels in these rivers were often linked to petrogenic and pyrogenic sources, including petroleum products and their combustion. In Egypt, 11 PAHs in Nile River sediments ranged from 4065 to 10033 ng/g, indicating a high contamination level [126]. Studies in northern China's Duliujian and Beiyun Rivers found 16 PAHs in surface sediments ranging from 356 to 4652 ng/g dry weight, with moderate to high contamination [127].

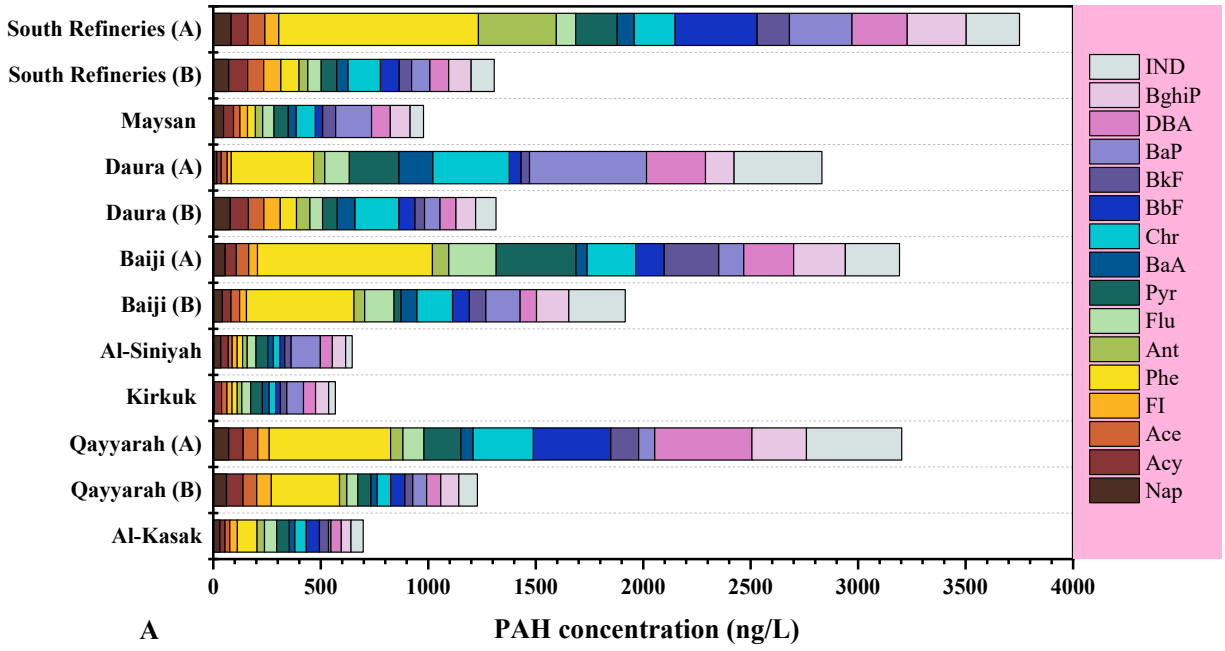

A

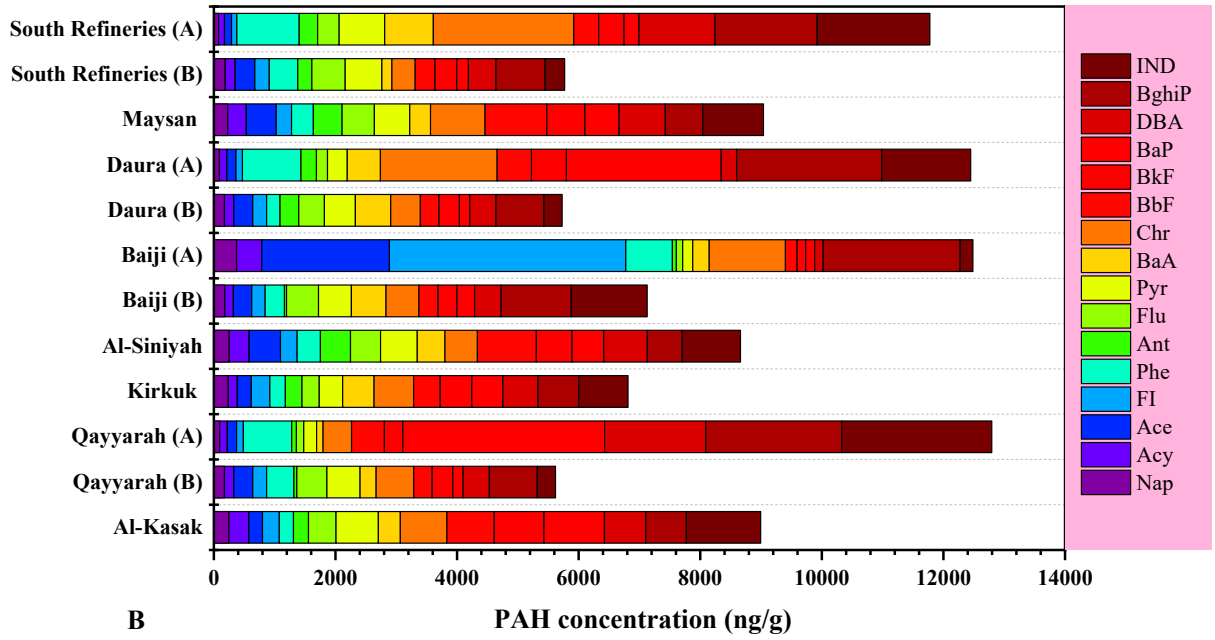

Figure 14 Mean of the 16 PAHs concentration in water (A) and sediment (B) along the Tigris River. The letter (A) near the refinery name refers to the word after and the letter (B) represents the word before (before the refinery location).

The U.S. Environmental Protection Agency (USEPA) classifies seven PAHs—Chr, BaA, BaP, BbF, BkF, IND, and DBA—as carcinogenic [128]. Figure 15 presents the distribution of these 7CPAHs across the twelve sites in both water and sediment samples. These hazardous compounds accounted for approximately 33.5% (S2) to 64.5% (S9) of PAHs in the water samples, which is significantly higher than the 3.5%–28% range observed in seven major Chinese rivers [129]. BaP, recognized as one of the most carcinogenic PAHs, showed concentrations in the Tigris River ranging from 10.5 ng/L at S1 to 544.0 ng/L at S9 (mean = 149.8 ng/L), indicating relatively high levels. Baumard et al. [59]categorized sediment PAHs concentrations as follows: low (<100 ng/g), moderate (100–1000 ng/g), high (1001–5000 ng/g), and very polluted (>5000 ng/g). Based on this classification, the sediments of the Tigris River are considered "very polluted" and require immediate attention from the Iraqi government to mitigate these elevated concentrations.

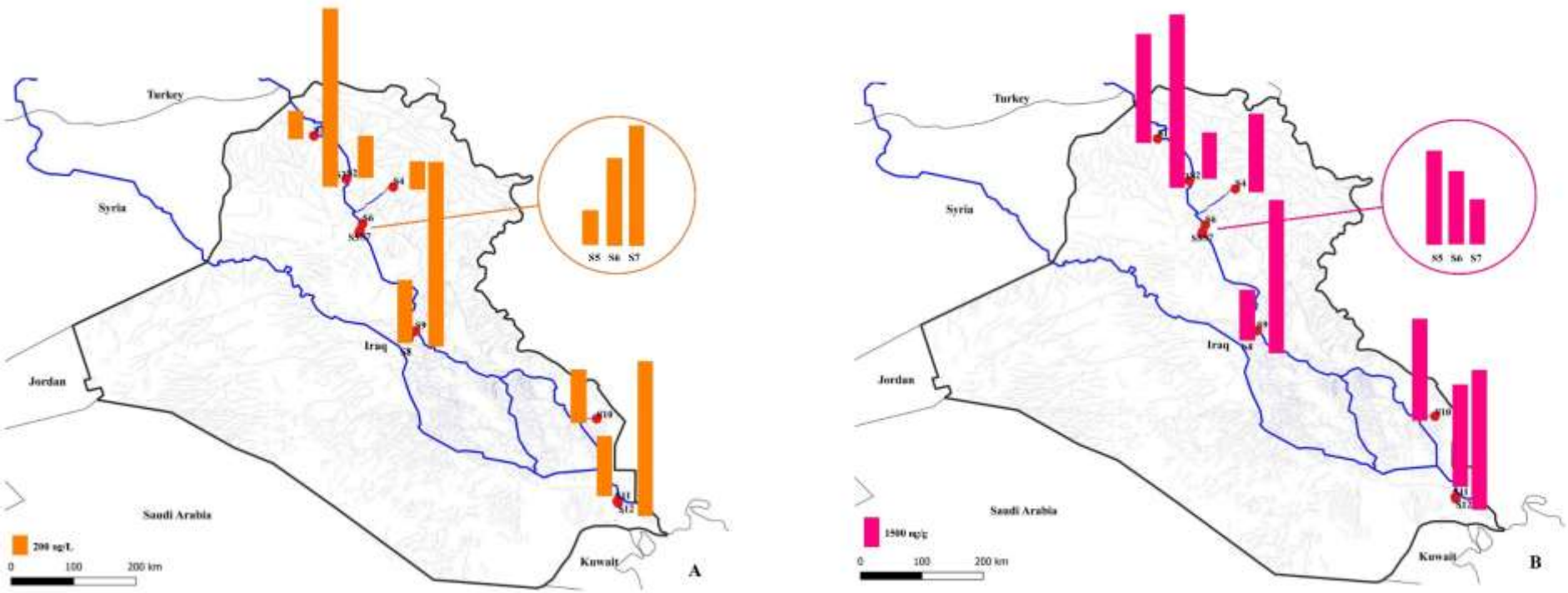

Figure 15 7CPAHs along the twelve sites for water (A) and sediment (B)

4.3. Composition of PAHs in Tigris River

4.3.1 PAHs composition in water

Figure 16 presents a compositional diagram displaying the percentage of each PAHs group in water (A) and sediment (B) samples from the Tigris River. In the water samples, HMWPAHs are more prevalent, ranging from 49.41% at S2 to 81.67% at S9, compared to 4-ring PAHs, which range from 18.33% at S9 to 50.59% at S2. The variation in PAHs percentages across sampling sites may be explained by the greater volatility and biodegradability of LMWPAHs as opposed to the more environmentally persistent HMWPAHs [130]. The dominance of HMWPAHs could be attributed to their low bioavailability and water solubility [131]. Han et al. also found that high HMWPAHs concentrations relative to total PAHs often indicate sources related to petroleum combustion [131].

4.3.2. PAHs composition in sediment

Figure 16 (B) shows the composition patterns of 2–6 ring PAHs detected in sediments. The majority of PAHs in the Tigris sediment samples were 5-6 ring PAHs, comprising 39.06% (S7) to 89.39% (S3) of Σ PAHs. The 2-3 ring PAHs made up 10.61% (S3) to 27.94% (S11) of Σ PAHs, except for S7, which contained 60.94% LMWPAHs. HMWPAHs are more resistant to degradation, allowing for efficient transport and deposition in sediments. While LMWPAHs exhibit observable acute toxicity, HMWPAHs are associated with chronic toxicity [132], indicating high hazard levels in samples with elevated HMWPAHs concentrations. Overall, PAHs composition in both water and sediment from the Tigris River followed a similar trend to our findings from the Euphrates River, where 5-6 ring PAHs also dominated, averaging 42% in water and 50% in sediment samples [71].

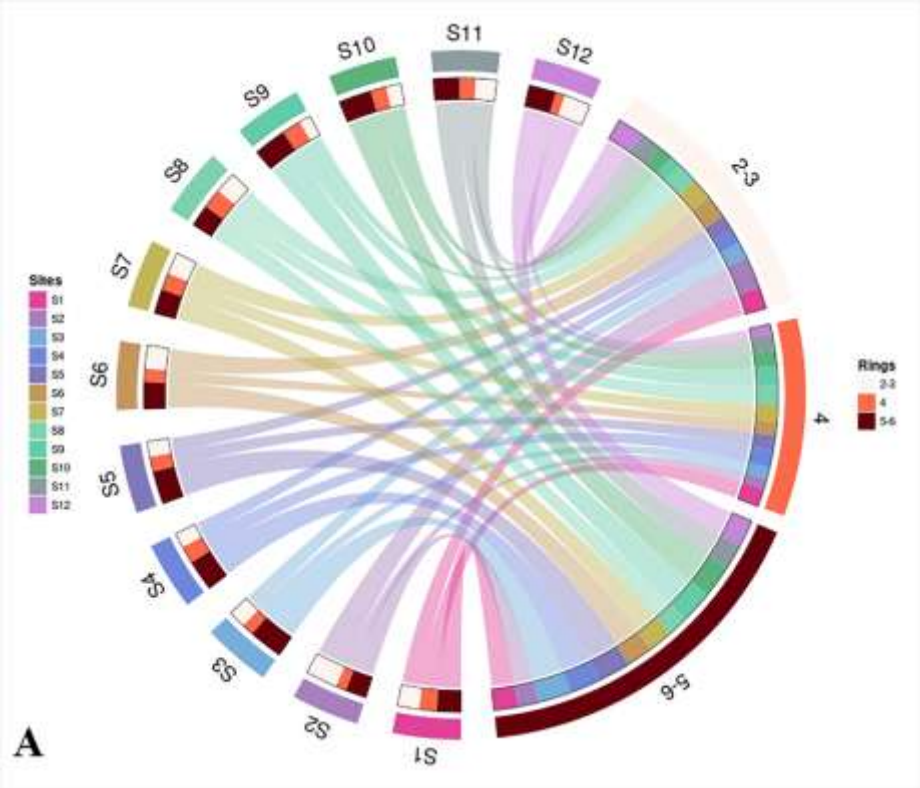

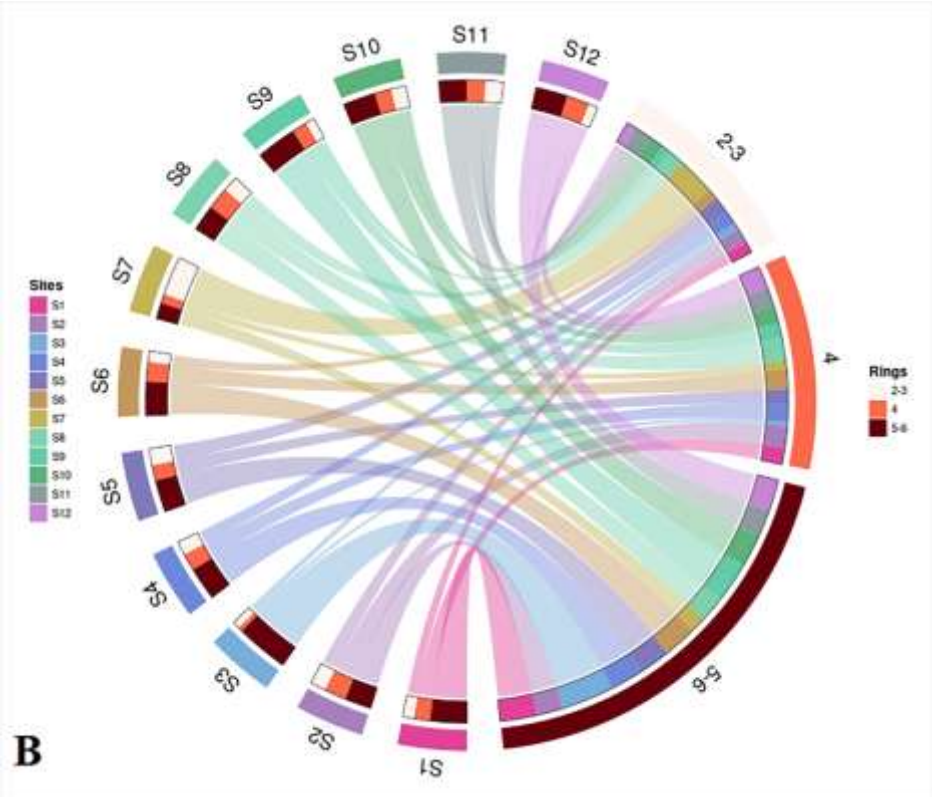

Figure 16 PAHs rings distribution for (A) water as well as (B) sediment.

4.4. Principal Components Analysis (PCA) and Source Identification of Tigris River sites

4.4.1.PCA in Water

The PCA findings for water samples identified three principal components that explained 84.89% of the total variation. Most of this variation is attributed to PCA1, PCA2, and PCA3, as shown in Figure 17 (A), with respective variances of 49.21%, 24.94%, and 10.75%. PCA1 is loaded with PAHs originating from sources such as oil combustion in gasoline and diesel engines and vehicle emissions [133]. In contrast, PCA2 and PCA3 are associated with LMWPAHs and 4-6 ring PAHs compounds, indicating multiple contamination sources. The negative loadings in PCA2 and PCA3 suggest an inverse association between certain PAHs compounds, signifying that specific PAHs are negatively correlated with others. Additionally, direct wastewater discharge and municipal waste disposal along the Tigris may contribute to elevated PAHs levels. Street dust deposition, carrying PAHs from surrounding areas, may further increase PAHs concentrations in the river [6]. Fossil fuel combustion, especially from refineries, could also enhance the levels of toxic chemicals in the local environment.

4.4.2. PCA in Sediment

Figure 17 (B) illustrates the PCA analysis of sediment samples, showing the PAHs distribution across PCA1, PCA2, and PCA3, with a combined variance of 75.16%. PCA1 accounted for 30.97% of the variance and is indicative of primarily 4-6 ring PAHs. PCA2, similar in variance to PCA1, accounted for 29.89% and also represents 4-6 ring PAHs. PCA3, explaining 13.31% of the variance, includes LMWPAHs and 5-6 ring PAHs. As observed in water samples, various negative correlations between PAHs assigned to each component were identified in sediment samples as well.

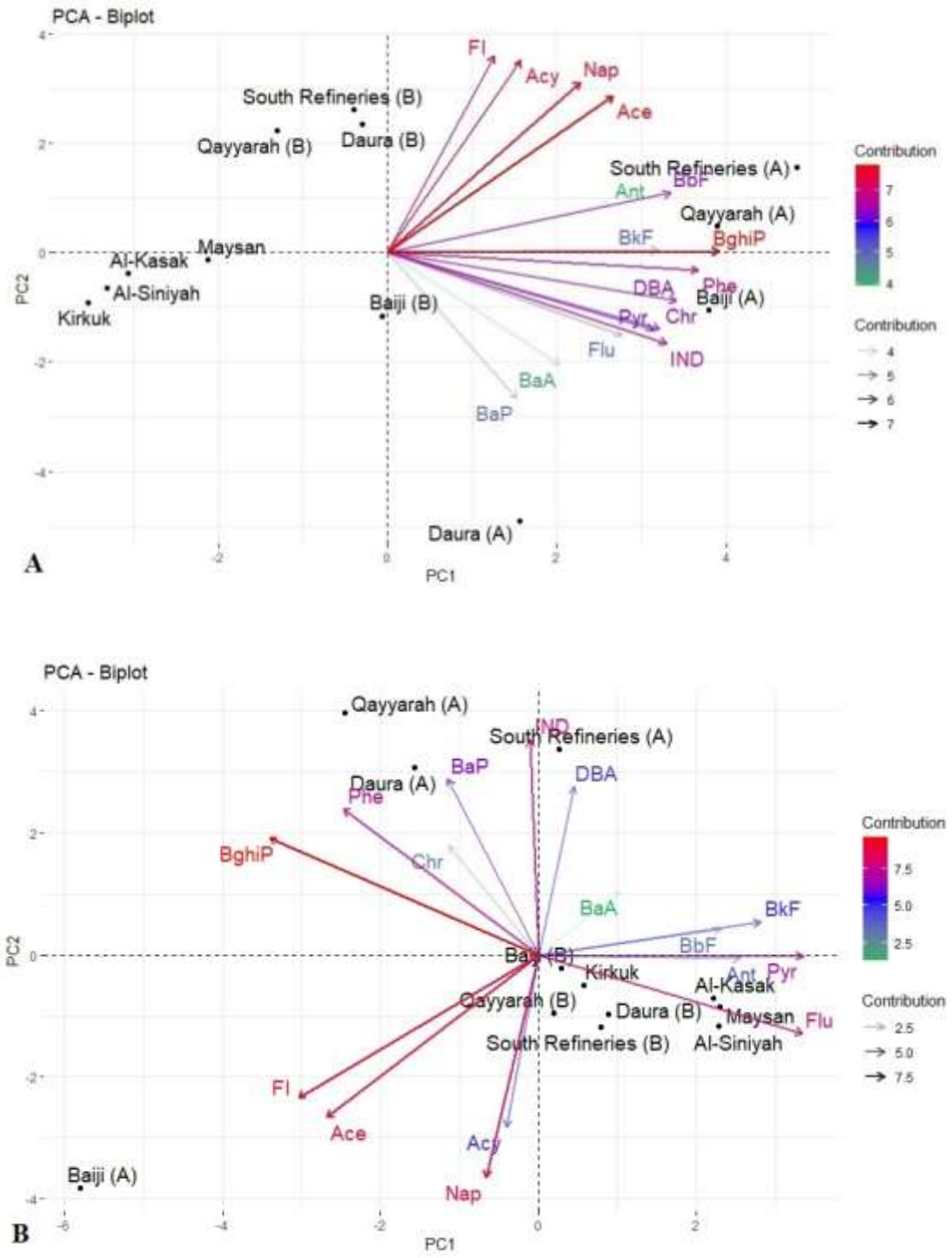

Figure 17 Water (A) and sediment (B) results by PCA

4.5. Source Identification of PAHs in Tigris River water

Geologic, petrologic, pyrolytic, and biological processes are the primary sources of PAHs [134]. Several ratios are taking into account to identify the PAHs sources. The HMW ratios like

BaA/(BaA + Chr) and Flu/(Flu + Pyr) are widely adopted as they are more stable than LMWPAHs ratios. A ratio of BaA/(BaA+ Chr) less than 0.2 indicates that oil emissions are the primary source of PAHs contamination. If the ratio exceeds 0.35, combustion is the predominant cause. A ratio between these two values indicates the presence of both oil and combustion pollutants [135]. If Ant/(Ant+Phe) less than 0.1 indicates pollution from petroleum sources, while Ant/(Ant+Phe) with more than 0.1 suggests pyrogenic sources [136]. In addition, a ratio of Flu/(Flu+Pyr) less than 0.4 is indicative of contamination from petroleum or oil spills. Flu/(Flu+Pyr) more than 0.5 is suggestive of biomass combustion sources. A ratio between 0.4 and 0.5 ($0.4 < Flu/(Flu+Pyr) < 0.5$) is indicative of petroleum combustion sources [137]. The ratio of LMW to HMW and the number of isomers with similar physicochemical properties may be used to qualitatively define contamination sources. A ratio of LMW/HMW of more than 1 implies petroleum sources, whereas a ratio of less than one indicates combustion sources [138]. The ratio of BaP to BghiP may also be used to confirm PAHs source assessments. A ratio of BaP/BghiP less than 0.6 suggests that PAHs come from non-traffic emission, while a ratio more than 0.6 indicates that traffic emission is the main source [139].

Figure 18 illustrates the ratios of Flu/(Flu + Pyr) against Ant/(Ant + Phe) and BaA/(BaA + Chr) to predict the likely sources of PAH. In most sites, the BaA/(BaA + Chr) ratio in water ranged from 0.2 to 0.35, suggesting a mixture of oil and combustion pollution. Similarly, both S3 and S7 exhibited ratios of less than 0.2, indicating that oil-related activities were the predominant cause of PAHs pollution. Sites S4 and S5 had BaA/(BaA + Chr) ratios greater than 0.35, indicating that combustion is the primary source of PAHs contamination. Using the Flu/(Flu + Pyr) ratio, it can be deduced that S3, S7, S9, and S12 had values of less than 0.4, indicating oil contamination. Other locations (excluding S6) revealed sources of PAHs from petroleum burning. The LMW/HMW ratios of less than one were found for all river water sample locations except S2, suggesting that combustion was the predominant source of PAHs constituents. PAHs in water samples S1, S3, and S7 are likely sourced from non-traffic origins based on the BaP/BghiP ratio criteria, whereas PAHs in other sites are likely released from traffic emissions.

4.6. Source Identification of PAHs in Tigris River sediment

In samples from sites S4-S6 and S8, the BaA/(BaA + Chr) ratio was greater than 0.35, indicating that combustion is the primary source. Only sites S3 and S7 revealed oil as a source of PAHs

emissions, while the other sites suggested a mixture of oil and combustion sources. PAHs in S1, S3, S7, S9, and S12 had ratios of Flu/(Flu + Pyr) less than 0.4, indicating pollution from petroleum or oil spills. Other locations exhibited PAHs levels between 0.4 and 0.5, indicating sources from petroleum combustion. In all areas along the Tigris River, except S7, the LMW/HMW ratio was less than 1, suggesting that combustion was the primary origin of PAH. Applying the BaP/BghiP ratio, S1, S3-S5, and S9-S10 indicated traffic pollution sources. PAHs in other sediment areas were sourced from non-traffic-related origins.

PAHs in water and sediment are often derived from pyrogenic sources, as seen in Figure 18. Pyrogenic PAHs are combustion byproducts primarily discharged into the environment through the burning of fossil fuels and biomass [140]. Overall, the ratios suggest that pyrogenic sources account for the majority of PAHs found in the Tigris River. This may be linked to several observed sources near the Tigris River, such as oil refinery emissions, oil sector wastewater discharges, and oil combustion. In certain instances, such as at the refineries in the south (S11 and S12), electrical generators for surrounding enterprises may be the primary PAHs producers in the environment.

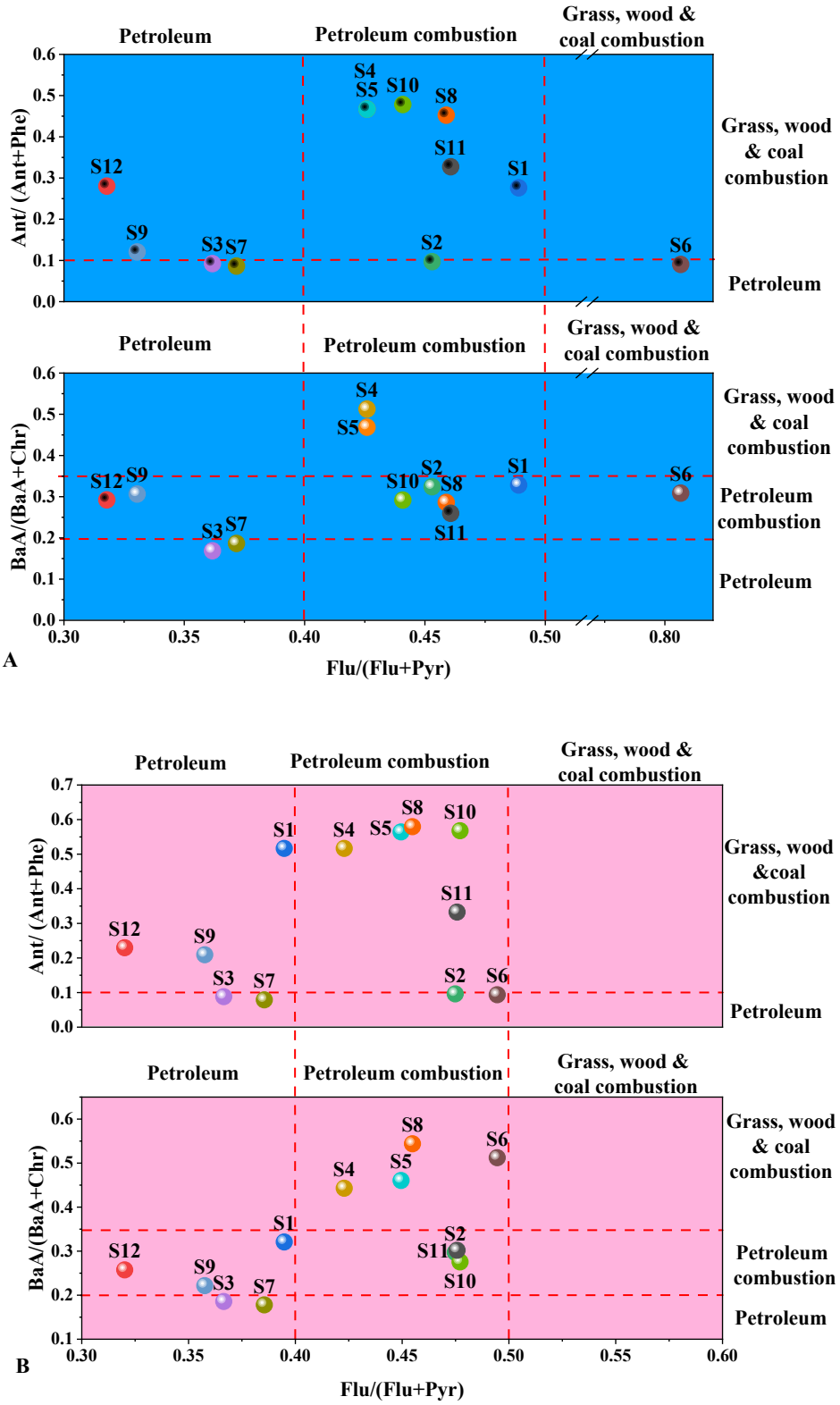

Figure 18 Source identification of PAHs in water (A) and sediment (B).

4.7. Ecological and Health Risks in Tigris River

The ecological risk assessment of sediment samples followed the methodology outlined by Ambade et al. [81]. The concentrations of 16 PAHs were evaluated according to sediment quality criteria (SQGs). The levels of Flu and Acy in sediments at all locations were higher than the ERL but lower than the ERM, placing them within the range of possible effects based on comparison with SQGs (Table 4). At all locations, Ant concentrations were below the ERL, indicating minimal effects with rare biological impacts. PAHs such as Ace, FI, DBA, and BghiP fell within the range of possible effects with occasional biological impacts and the probable effects range with frequent biological effects. Other PAHs, including Nap, Phe, Pyr, BaA, Chr, BbF, and BkF, exhibited either rare biological impacts in certain areas or occasional biological effects in others. However, for BaP, all SQG scenarios were presented. The findings reveal that the majority of PAHs concentrations in all sediment samples fall within the possible effects range, indicating occasional biological effects.

The ecological risks posed by PAHs to the water of the Tigris River were evaluated according to USEPA criteria for surface water quality, while Iraqi regulations were more general and merely prescribed hydrocarbon limits (10 µg) [58]. According to USEPA regulations (standard limit ≤31 ng/L for the total of Acy, BaA, BaP, BbF, BghiP, BkF, Chr, DBA, IND, and Phe), the PAHs concentrations in the samples were significantly higher than the specified limit. This indicates that aquatic life in the Tigris River faces a serious ecological threat. The TEQ findings in water ranged from 79.6 ng/L for S1 and 890.4 ng/L for S9. The minimum TEQ value in the sediment sample was 414.0 ng/g for S7 and 5353.1 ng/g for S3. TEQ results were mostly higher than those observed in other areas, for instance, India, and Pakistan [141]. These worryingly high levels strongly indicate that immediate action by environmental authorities is necessary.

Using the USEPA's ILCR model, a risk assessment of human exposure to PAHs in river sediments was performed. This was necessary because of the individuals' daily dependence on the region's aquatic resources [83]. ILCR is usually employed to quantify the human carcinogenic risk posed by environmental PAHs exposure [83], [142], [143]. The ILCR values found in sediment samples from the Tigris River (Figure 19) are much greater than those reported in Australia's Brisbane River [122]. Since these concentrations were detected by long-term monitoring, the individuals nearby the examined locations must be notified and precautions must be taken to limit human contact with the sediments. The inhalation of PAHs mostly comes from air breathing,

whereas the inhalation of aquatic contamination should probably occur during an incident involving water choking. Due to a low likelihood of accidental water choking, inhaling PAHs in sediments in this investigation was omitted from health risk assessments. Thus, the only PAHs exposure routes considered in this investigation are dermal contact and ingestion [144]. This was also considered in other works when ILCR was computed [145]. The determined ILCR values for water depicted in Figure 19 indicated that all examined sites posed a high risk of carcinogenicity.

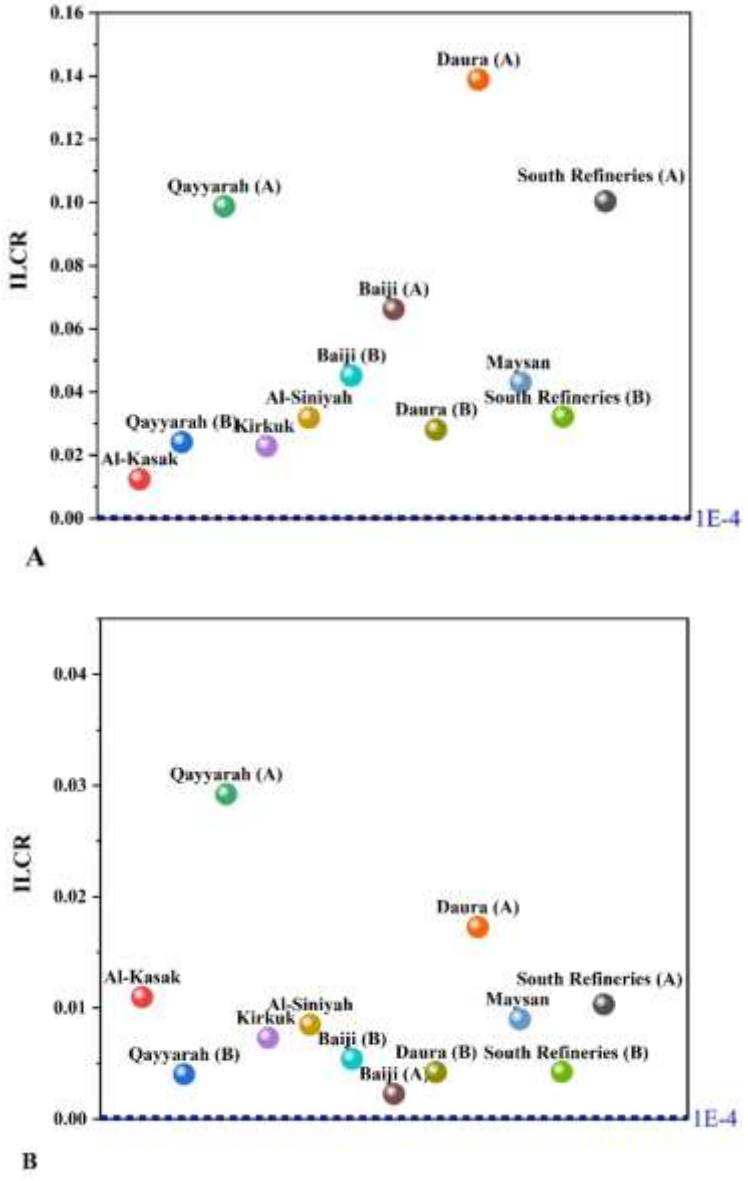

Figure 19 Incremental Lifetime Cancer Risk values in Tigris River sediments (A) water and (B) sediment. The blue line is the ILCR (1/104) limit. The letter (A) in the refineries' names means after, and the letter (B) in the refineries' names means before.

Table 4 Toxicity guidelines with respect to 16 PAHs range

PAH	ERL-ERM	Concentration range (ng/g)	<ERL	≥ERL and <ERM	≥ERM
Nap	160–2100	76.5 -372.4	S3,S9,S12	Rest	Nil
Acy	16–500	97.1-414.3	Nil	All sites	Nil
Ace	44–640	117.9-2099.5	Nil	Rest	S7
FI	19–540	86.2-3889.9	Nil	Rest	S7
Phe	240–1500	222.2-1024.6	S1,S8	Rest	Nil
Ant	600–5100	33.0-494.8	All sites	Nil	Nil
Flu	85.3–1100	103.5-547.6	Nil	All sites	Nil
Pyr	665–2500	164.9-748.8	Rest	S1, S12	Nil
BaA	261–1600	106.6-800.6	S3, S11	Rest	Nil
Chr	384–2800	382.6-2309.7	S11	Rest	Nil
BbF	320–1880	192.7-1013.8	S2, S6-S8	Rest	Nil
BkF	280–1620	139.0-820.4	S7	Rest	Nil
BaP	430–1600	147.9-3320.4	S2, S6-S8, S11, S12	Rest	S3, S9
DBA	63.4–260	141.2-1661.5	Nil	S3, S7, S9	Rest
BghiP	430–1600	572.0-2384.6	Nil	Rest	S3, S7, S9, S12
IND	240-	210.3-2468.5	S7	Rest	

5.1. PAHs concentrations in Euphrates River water

The spatial and temporal variation of PAHs concentrations in water samples is shown in Figure 20. In March, water samples from sites S11 and S13 recorded the highest concentrations of the 16 PAHs. In April, S11 continued to show the highest concentration, followed by S12 and S13. In May and July, however, S12 exhibited the highest levels, followed by S13. In June, measurements indicated that S11, S13, and S12 had the highest concentrations of the 16 PAHs. The downstream

locations—S11, S12, and S13—consistently showed the highest PAHs concentrations compared to other sites along the river's main body. The data indicates a clear spatial pattern, with PAHs concentrations increasing progressively from upstream to downstream. However, Figure 20 does not show a consistent temporal trend in PAHs concentrations across the sampling period. Several factors complicate the interpretation of PAHs variation in the Euphrates River, including the irregular discharge of wastewater, diverse industrial activities (e.g., oil and agriculture), the impact of climate change on seasonal shifts in Iraq, the river's complex geology, and various industrial and agricultural activities surrounding the river.

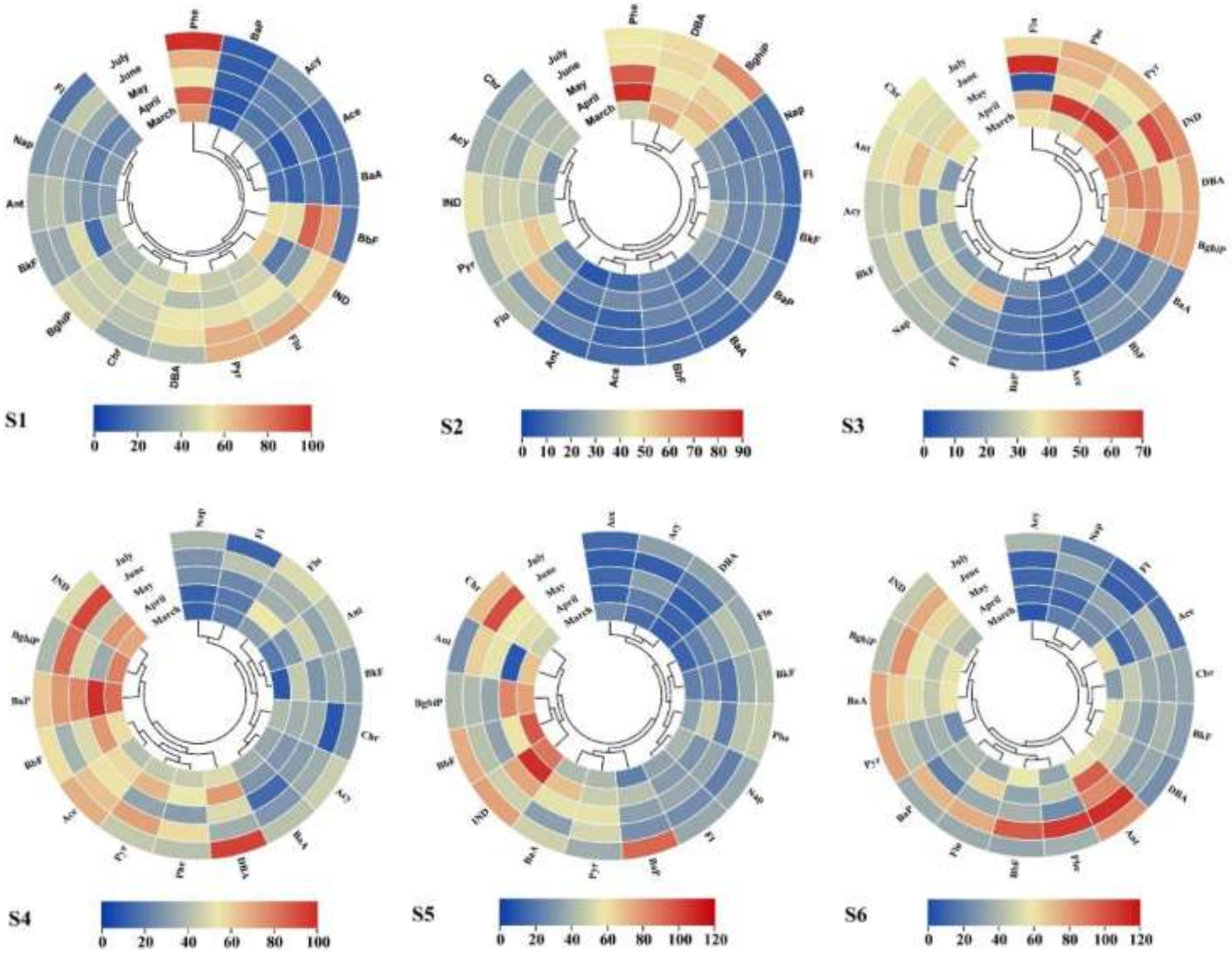

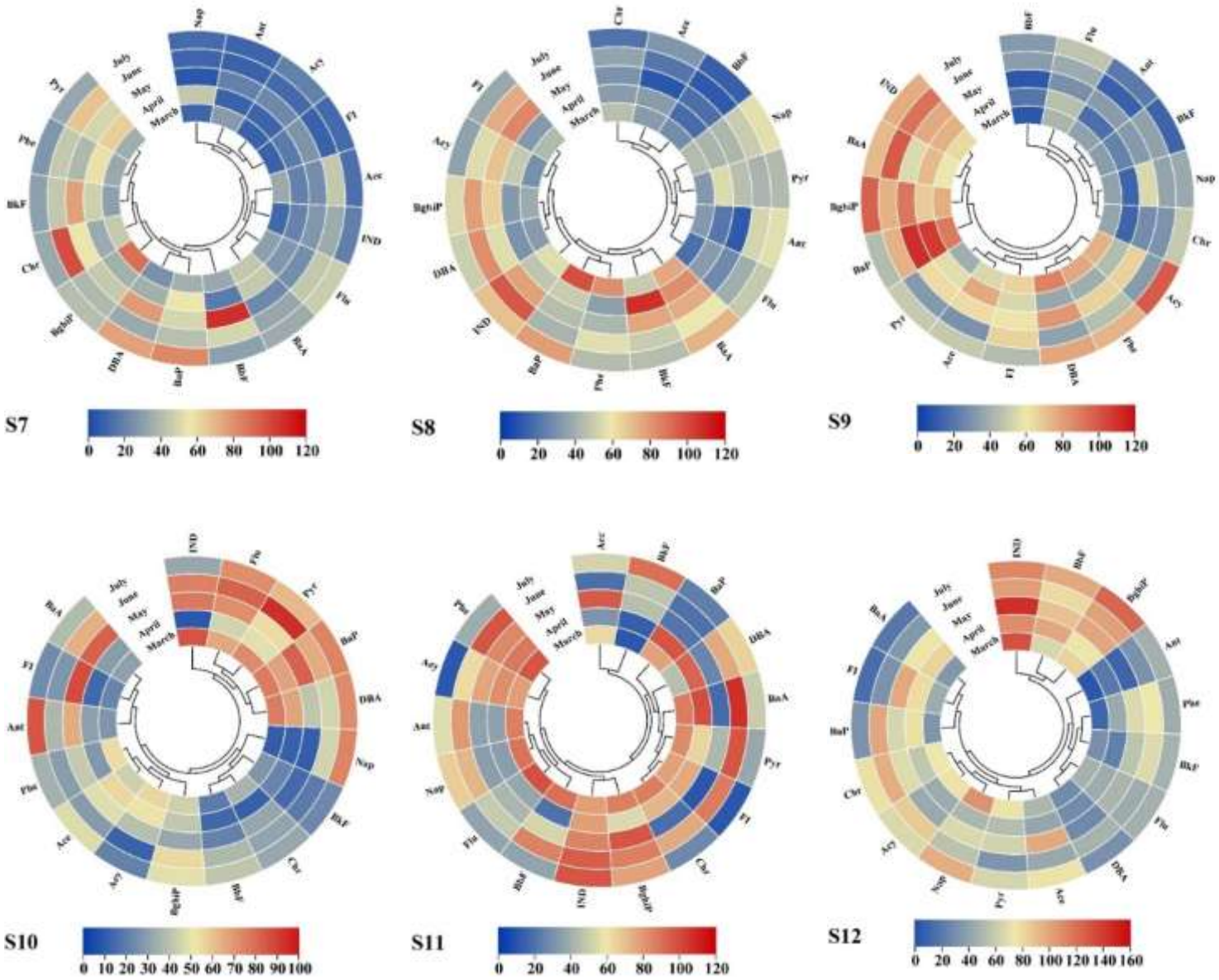
S7
0 20 40 60 80 100 120
S8
0 20 40 60 80 100 120
S9
0 20 40 60 80 100 120
S10
0 10 20 30 40 50 60 70 80 90 100
S11
0 20 40 60 80 100 120
S12
0 20 40 60 80 100 120 140 160

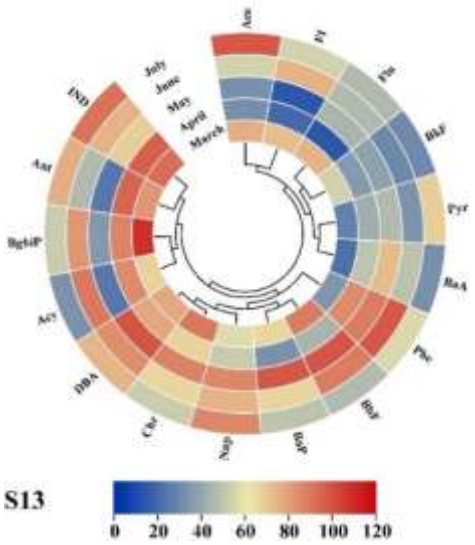

Figure 20 PAHs concentrations in water samples. The scale bar represents PAHs concentration range (ng/L).

5.2. PAHs concentrations in Euphrates River sediment

The spatial and temporal variations in PAHs concentrations in water and sediment samples are shown in Figure 21. The Figure demonstrates that in March, sediment samples from S5, S12, and S4 had the highest levels of 16 PAHs. In April, Site S5 remained the highest, followed by S12 and S8. In May, however, S12 recorded the highest PAHs levels, with S11 in second. Measurements conducted in June found that S12, S13, and S5 had the highest values of the 16 PAHs, while in the final month of sampling, S5 and S12 again exhibited the highest concentrations. Overall, S5 and S12 consistently showed the highest concentrations of the 16 PAHs along the main river course. The spatial variation of PAHs concentrations is clear, with levels generally increasing from upstream to downstream. However, Figure 21 does not reveal a consistent temporal trend in PAHs concentrations across different months in the water and sediment samples. This aligns with findings by Duodu et al. [122], who noted weak correlations between PAHs compounds, making it difficult to conclude any patterns in temporal variation across different months. Several factors complicate the understanding of PAHs spatial and temporal variation in the Euphrates River, including irregular wastewater discharge, industrial activities (e.g., oil and agriculture), the river's complex geology, and regional industrial practices. Additionally, climate change is a significant challenge in Iraq and the MENA region, with substantial negative impacts on the environment,

water resources, and the agricultural economy [146]. Reduced river flow, influenced by dam construction on major rivers and occasional droughts [147], leads to sediment accumulation throughout the river, potentially increasing PAHs levels.

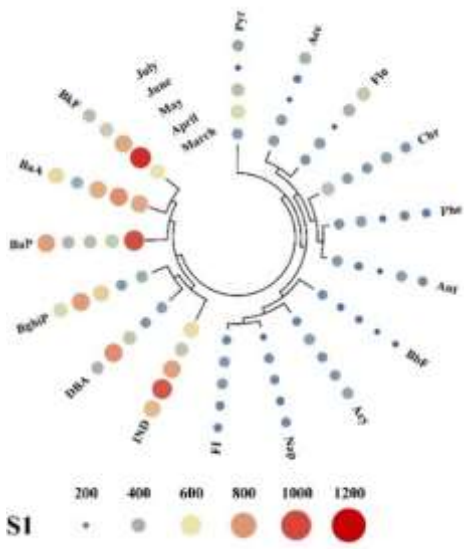
July
June
May
April
March
Pyr
Ace
Flu
Chr
Phe
Ant
BbF
Flt
IND
DBA
BghiP
BaP
BkF
BaA
200 400 600 800 1000 1200
S1

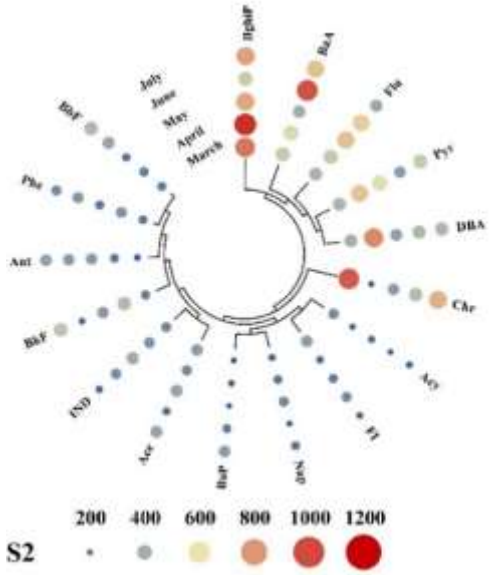
July
June
May
April
March
IghiP
BaA
Flu
Pyr
DBA
Chr
Acy
Flt
NAP
Ace
IND
BkF
Ant
Phe
BghiP
200 400 600 800 1000 1200
S2

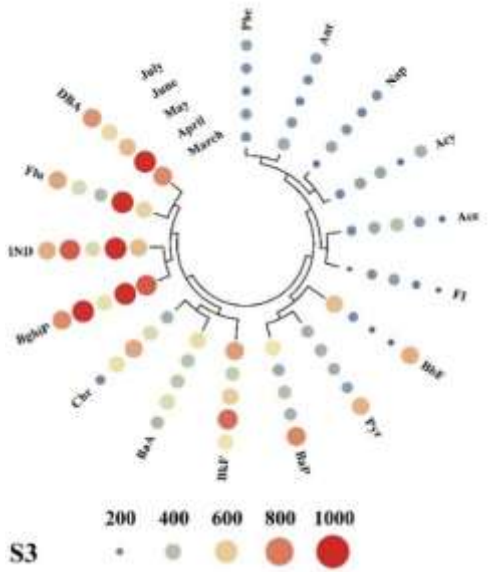
July
June
May
April
March
Phe
Ant
Nap
Acy
Ace
Flt
BbF
Pyr
BaP
BkF
BaA
Chr
BghiP
IND
DBA
200 400 600 800 1000
S3

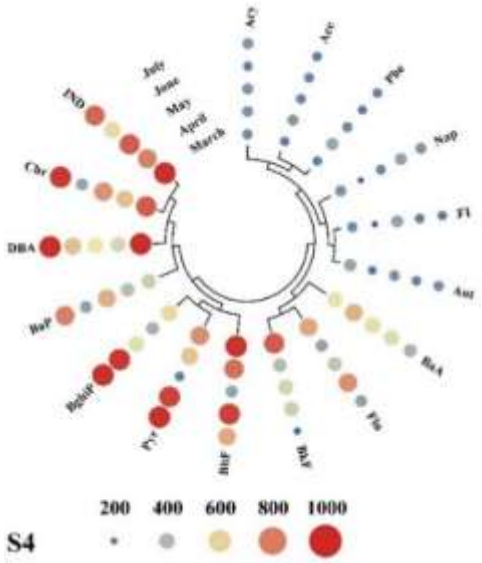
July
June
May
April
March
Acy
Ace
Phe
Nap
Flt
Ant
BaA
Flu
BbF
BkF
Pyr
BghiP
BaP
DBA
Chr
IND
200 400 600 800 1000
S4

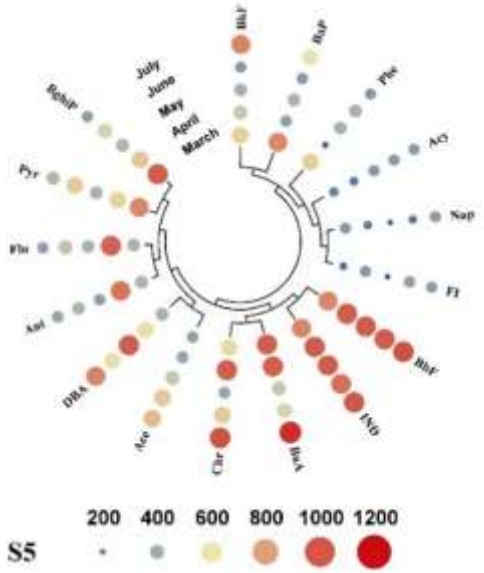
July
June
May
April
March
BkF
BaP
Phe
Acy
Nap
Flt
BbF
IND
BaA
Chr
Ace
DBA
Ant
Flu
BghiP
200 400 600 800 1000 1200
S5

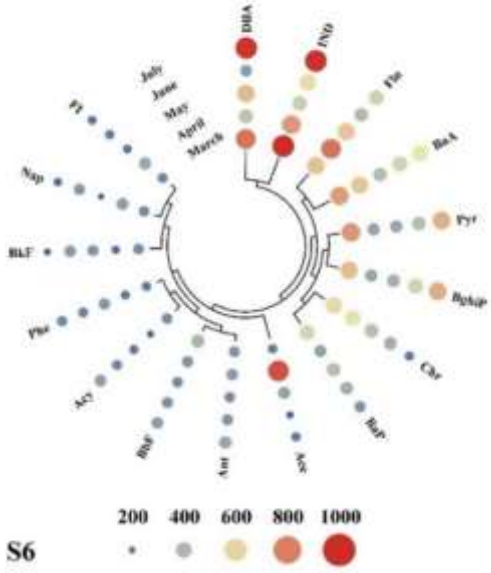
July
June
May
April
March
DBA
IND
Flu
BaA
Pyr
BghiP
Chr
BaP
Ace
Ant
BbF
Acy
Phe
Nap
Flt
200 400 600 800 1000
S6

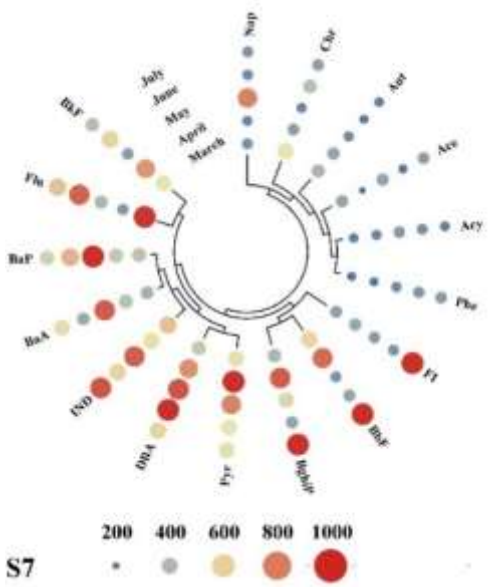

S7

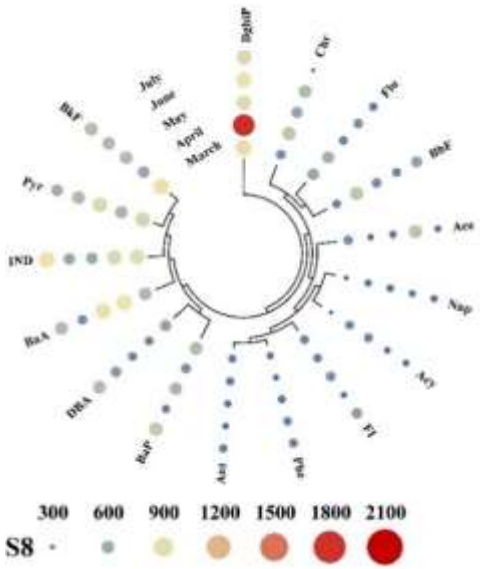

S8

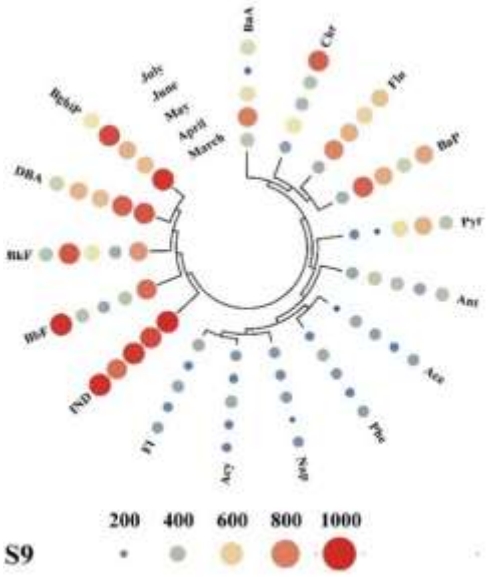

S9

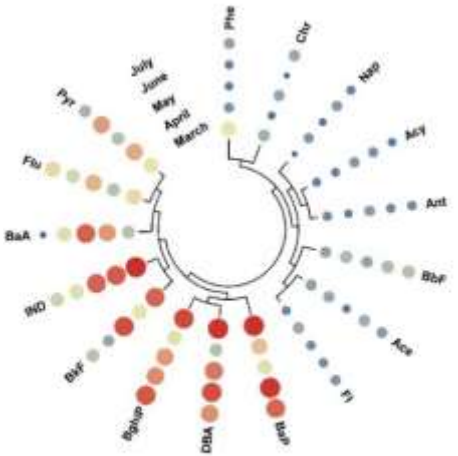

S10

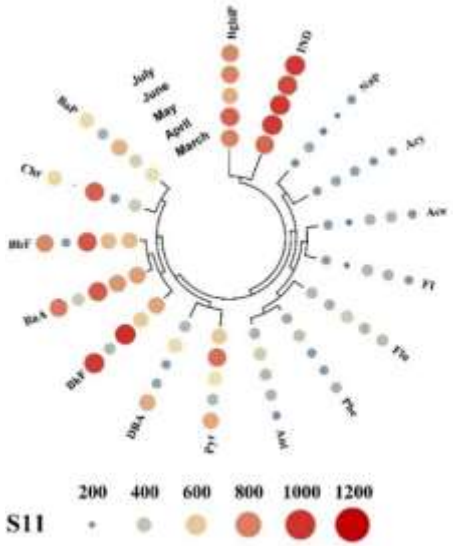

S11

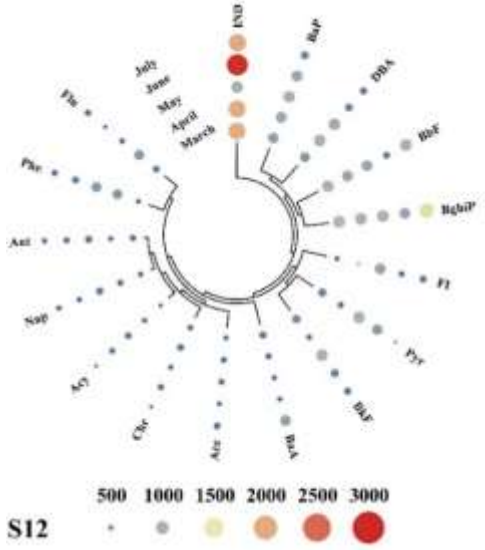

S12

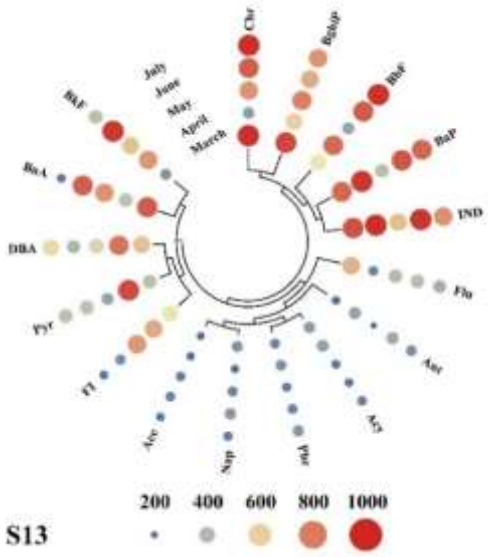

Figure 21 PAHs concentrations in sediment samples. The bubble bar represents PAHs concentration range (ng/g dw).

5.3. Overall PAHs concentrations in water and sediment along the Euphrates basin.

Figure 22 presents the mean concentrations of 16 PAHs detected in water (A) and sediment (B) samples. All targeted PAHs were detected at every sampling location along the river, with concentrations ranging from 464 to 992 ng/L in water samples and 5940 to 9723.9 ng/g dw in sediment samples. IND showed the highest average concentration in both water (65.22 ng/L) and sediment (863.30 ng/g dw) samples, accounting for approximately 9% and 11%, respectively, of the ∑ 16 PAHs. The lowest average concentration among all PAHs was recorded for Fl (34.30 ng/L) in water samples and Nap (247.34 ng/g dw) in sediment samples. Location 2 (Hit) exhibited the lowest ∑ 16 PAHs in both water (464.00 ng/L) and sediment (5940.00 ng/g dw) samples. In contrast, location 13 had the highest ∑ 16 PAHs in water samples (991.85 ng/L), while location 12 had the highest ∑ 16 PAHs in sediment samples (9723.9 ng/g dw). It was also observed that the ∑ 16 PAHs in upstream locations was lower than in downstream locations, likely due to the introduction of several pollution sources, both point and non-point, such as direct wastewater disposal and airborne dust, which increase PAHs levels in the river system [6], [148].

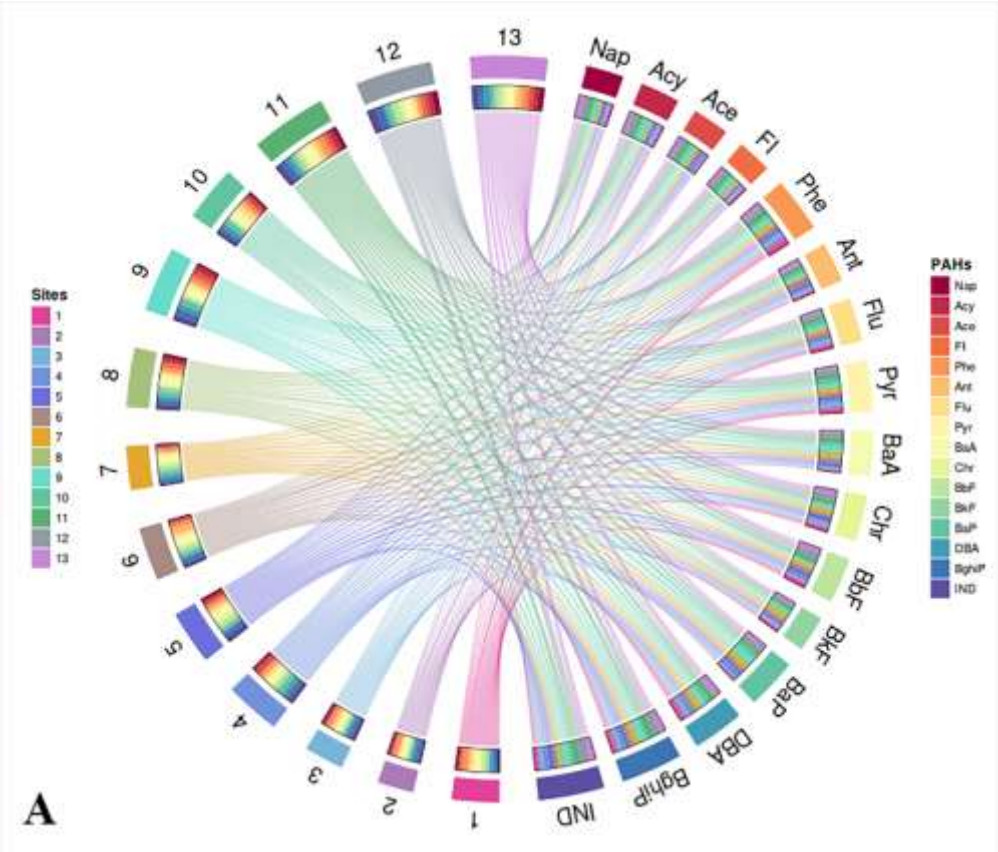

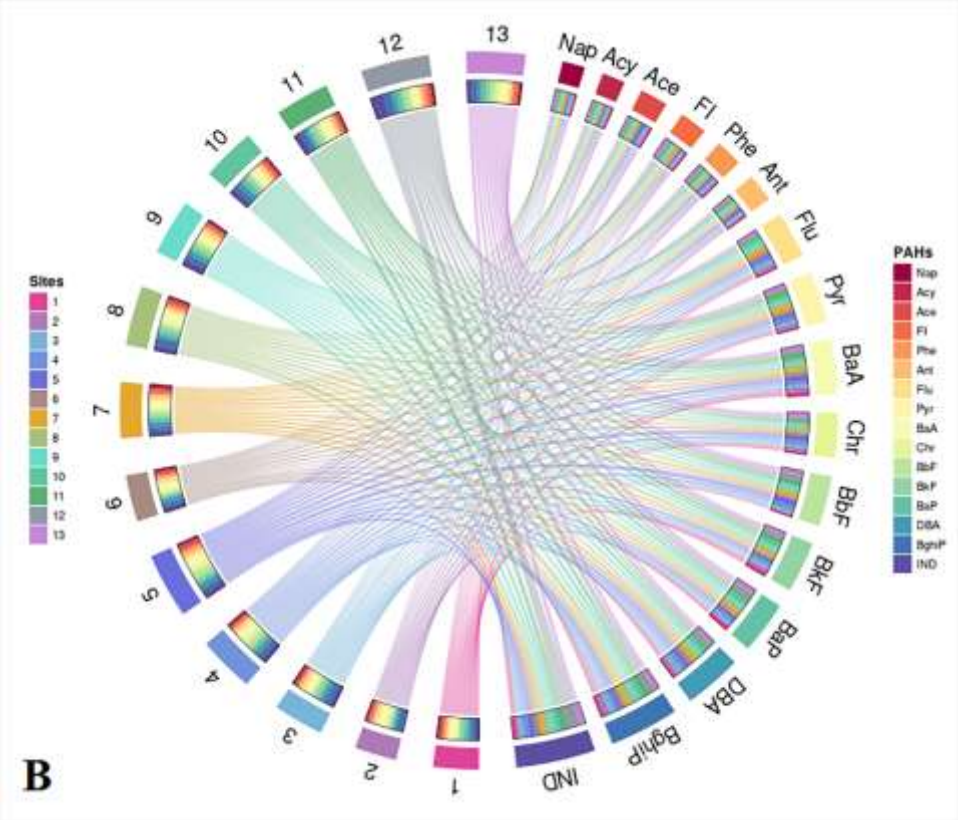

Figure 22 PAHs mean concentrations measured in (A) water samples (ng/L) and (B) sediment samples (ng/g dw) of all the sampling sites

The concentration range of ∑ 16 PAHs in the Euphrates River water (464–992 ng/L) is higher than that observed in the Yellow River Delta, China (64.8–335 ng/L) [149], the Shanghai River (46.53–222 ng/L[117], the Soan River in Pakistan (61–207 ng/L) [150], and surface waters of the Gulf of Gabes, Southern Mediterranean Sea, Tunisia (17.6–71.2 ng/L) [151]. It also surpasses PAHs levels measured in Tunisian coastal harbors along the Gulf of Tunis, with summer concentrations at 378.4 ng/L and winter concentrations reaching 703.1 ng/L [152]. In this study, PAHs levels in the Euphrates exceed those in the Al-Hussainya River (an estuary of the Euphrates), which ranged from 0.24 to 58.72 ng/L [153]. However, PAHs levels here are lower than those found in the Cauca River, Colombia (52.1–22,888 ng/L)[106] and the Daliao River, China (71.12–4255 ng/L) [124].

The PAHs concentration in sediment samples ranged from 5940 to 9723.9 ng/g dry weight (dw), with a mean of 7762.7 ng/g dw. According to the World Health Organization (WHO), the maximum allowable PAHs concentration in drinking water is 200 ng/L [128], [154], [155]. Thus, effective treatment is needed to reduce PAHs levels for safe drinking water, especially downstream where levels peak. Notably, seven commonly studied PAHs (Chr, BbF, BkF, BaA, BaP, IND, and

DBA) are classified as carcinogens by the US Environmental Protection Agency (USEPA). These compounds contribute about 46% of ∑ 16 PAHs in the water samples, a notably higher proportion than the 3.5%-28% range reported in seven major Chinese rivers [156]. Among these, BaP is recognized as highly carcinogenic, with a WHO guideline limit of 100 ng/L in drinking water [128]. In the Euphrates, BaP concentrations ranged from 9.918 to 85.54 ng/L (mean = 50.02 ng/L), lower than the WHO limit but exceeding Canada's drinking water guideline of 40 ng/L at some sampling sites [157]. Sites S4–S13 exceeded Canada's limit, while S1–S3 remained below it, highlighting potential health risks associated with using this water for fishing or consumption, as PAHs can enter the human body through ingestion [158].

The European WFD aims for "good status," combining "good chemical" and "good ecological" conditions [54], [55]. It mandates that EU Member States monitor Priority Substances (PS) in inland and coastal waters, with specific Environmental Quality Standards (EQS) set for each. Among PS, eight PAHs (naphthalene, anthracene, fluoranthene, benzo[b]fluoranthene, benzo[k]fluoranthene, benzo[a]pyrene, indeno[1,2,3-cd]pyrene, and benzo[ghi]perylene) are included. In this study, Nap, Ant, and Flu were within permissible limits across all sites, while BbF, BkF, BghiP, and IND exceeded allowable levels at every site. BaP concentrations were above limits at S4, S7–S10, S12, and S13, while other sites remained compliant.

The sedimentary ∑16 PAHs levels in this study (5940–9724 ng/g dw) are higher than those reported for the Brisbane River, Australia (148–3079 ng/g dw) [122], the river in Chongqing, China (221–3205 ng/g dw) [159], the Rizhao coastal area, China (79.3–853 ng/g dw) [160], the Gulf of Tunis, Tunisia (1294.6 ng/g dw) [152], Bizerte Lagoon, Tunisia (83.3–447.08 ng/g dw) [161], and Ghar El Melh Lagoon, Tunisia (39.59–655.28 ng/g dw) [162]. The current PAHs sediment load also exceeds values reported for the Euphrates in 2005–2006, which totaled 167 ng/g dw [163].

While sedimentary PAHs levels here are lower than those in Al-Hussainya River (0.36–119.06 µg/g dw), unit inconsistencies (µg/g dw in the abstract and ng/g in the Table) make comparisons challenging [153]. Globally, the PAHs levels are also below those found in Athabasca Lake, Canada (10.6–130,180 ng/g dw) [164], the Huai River, China (810–28,228 ng/g dw; [165], and coastal Bangladesh (200–17,089 ng/g dw) [166]. Carcinogenic PAHs contribute about 55% of the ∑16 PAHs in these sediments, surpassing levels found in the Brisbane River, Australia (46%) [122], and the Gao-ping River, Taiwan (22%) [167]. Although the Taiwan study was conducted 18 years ago, PAHs levels may have fluctuated over time. Baumard et al. [59]classified sediment

PAHs as low (0–100 ng/g), moderate (100–1000 ng/g), high (1001–5000 ng/g), and very contaminated (>5000 ng/g). By this classification, Euphrates sediments are highly contaminated and warrant intervention to reduce these elevated concentrations.

5.4. PAHs composition in water and sediment in Euphrates basin

The PAHs measured in this study were divided into three groups based on the number of rings in their structure: 2–3 rings (low molecular weight, LMW), 4 rings, and 5–6 rings (high molecular weight, HMW). The percentage contribution of each of these groups to the ΣPAHs in water and sediment samples is presented in Figure 23. Figure 24 shows ternary plots for water (A) and sediment samples (B).

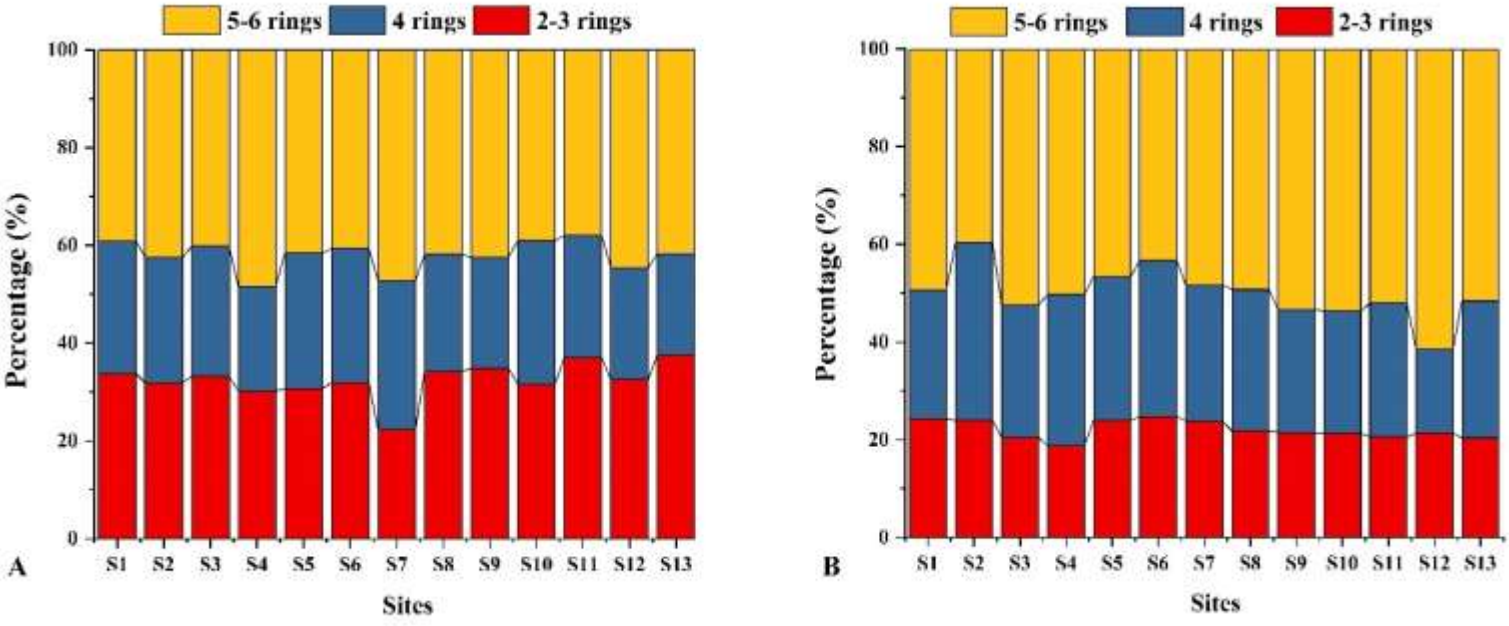

Figure 23 Percentage distribution of PAHs based on the number of rings for (A) water samples and (B) sediment samples.

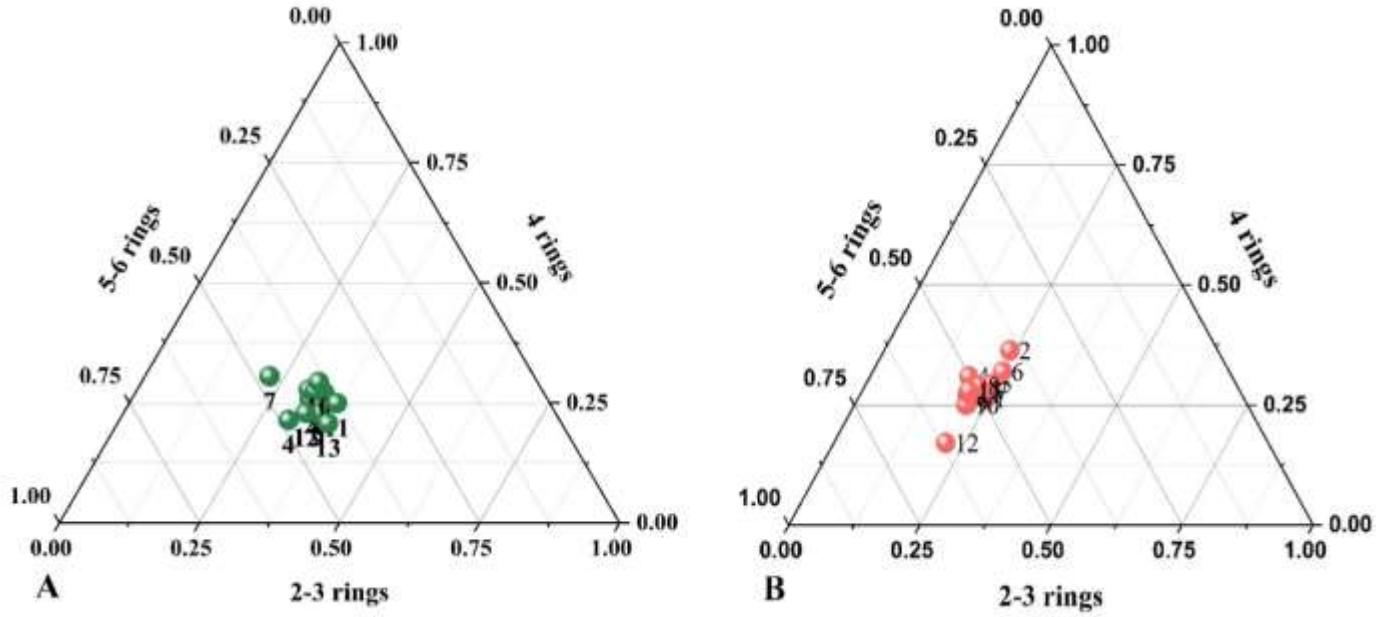

Figure 24 Ternary plots for water ng/L (A) and sediment samples ng/g dw (B).

The Euphrates water samples primarily consisted of 5–6 ring PAHs, accounting for 37.9% (S11) to 48.3% (S4) of Σ PAHs (average of 42%), followed by 2–3 ring PAHs, which accounted for 22.2% (S7) to 37.6% (S13) of Σ PAHs (average of 32%). The 4-ring PAHs accounted for 20.7% (S13) to 30.4% (S7) of Σ PAHs (average of 26%). The composition was slightly different in the sediment samples. In the Euphrates sediment samples, 5–6 ring PAHs predominated, accounting for 40% (S2) to 62% (S12) of Σ PAHs (average of 50%), followed by 4-ring PAHs, which accounted for 17.1% (S12) to 36.4% (S2) of Σ PAHs (average of 28%). The 2–3 ring PAHs accounted for 18.8% (S4) to 24.7% (S6) of Σ PAHs (average of 22%). Similar findings were reported in previous studies [117], [136], [168]. The high percentage of HMW PAHs in sediments may be attributed to their low solubility, leading to accumulation in sediment layers. The PAHs distribution in the Euphrates River resembled that of 9 out of 30 rivers monitored in Taiwan [136]. One of seven rivers assessed for PAHs in China also displayed a similar ring distribution to the Euphrates River [156]. HMW PAHs are more resistant to degradation, enabling them to be transported and deposited in sediments more efficiently. In contrast, LMW PAHs have higher water solubility and are more prone to benthic recycling, making them more prevalent in the dissolved phase [101]. LMW PAHs (2–3 rings) exhibit acute but relatively low toxicity, whereas HMW PAHs

(4–6 rings) pose chronic toxicity [132]. This implies that both water and sediment samples exhibit high toxicity due to the significant presence of HMW PAHs.

5.5. Principal components analysis (PCA) in water and sediment of Euphrates River

PCA has proven to be the multivariate analytical approach for identifying sources of PAHs in environmental source apportionment studies, transforming complex original data into several new factors or variables, each reflecting a group of correlated variables in the dataset (Anh et al., 2020). The sum of the principal components, also known as summary indices (PC-1, PC-2, …, PC-n), from a particular PCA always equals 100%, and the most significant components (PC1, PC2, etc.) are selected to explain the variances occurring in the original dataset.

The results of the PCA on water samples revealed three factors that explained 67.03% of the variation in the data. The largest portion of the overall variance was attributed to PC1, PC2, and PC3, as shown in Figure 25A, with variances of 41.59%, 13.91%, and 11.53%, respectively. Principal Component 1 (PC1), which represents LMW PAHs (Nap, Acy, Ace, and FI) and HMW PAHs (BaA, Chr, BbF, BaP, BghiP, IND), explained 41.59% of the overall variance. Nap is a major constituent of diesel fuels and gasoline and may be produced by incomplete combustion [88]. IND may be a byproduct of pyrolysis or incomplete fuel combustion [169]. BghiP is indicative of automobile emissions [170], while Chr indicates coal combustion; other PAHs, such as Flu, are mostly derived from the significant volume of vehicle emissions [171] . Principal Component 2 (PC2) and Principal Component 3 (PC3) represent the PAHs groups of Flu, Pyr, BaP, and DBA and Ant, Flu, Pyr, Chr, and BbF, respectively. Table 5 shows the eigenvectors and percentage of variance for the PCA analysis of water samples. Negative loadings, such as Nap, Chr, BbF, and BkF for PC2 and Acy, Fl, and BaA for PC3, suggest a negative relationship or correlation between these PAHs and others from which they originated. BaA and BbF primarily originate from vehicle emissions and the burning of fossil fuels [170]. Additionally, illegal waste (liquid and solid) dumping into the water system and direct wastewater discharge along the Euphrates River could contribute to higher PAHs concentrations. The atmospheric deposition of dust containing PAHs into the river system could also be a reason for elevated PAHs levels. The burning of fossil fuels, particularly in metropolitan areas, along with the use of private power generators, could further increase the concentration of these compounds in surrounding environments.

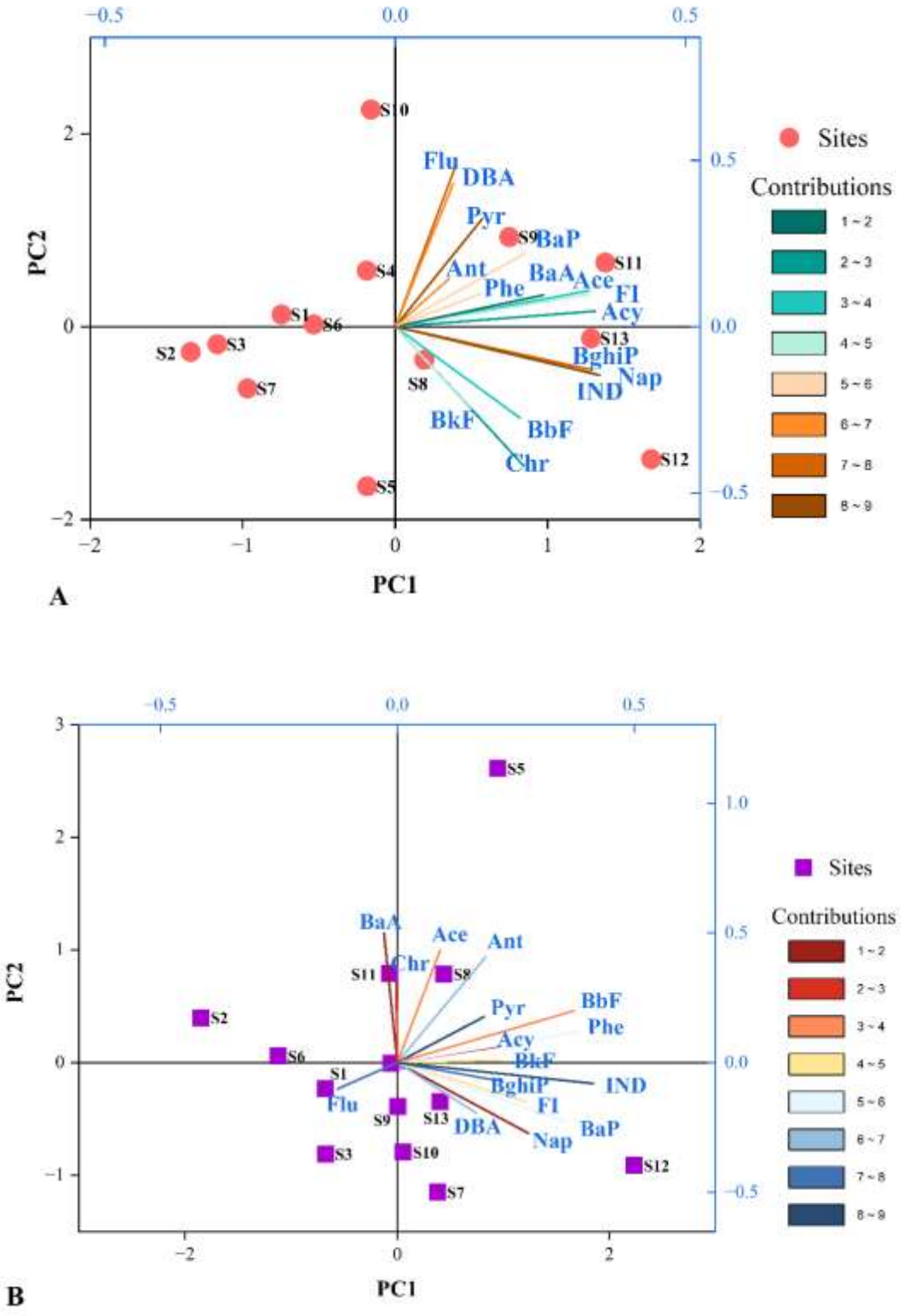

Figure 25 Biplots of the PCA analysis for (A) water and (B) sediment samples.

Table 5 Eigenvectors and percentage of variance for PC analysis of water samples.

Water	PC1	PC2	PC3
Nap	0.352	-0.145	0.061
Acy	0.344	0.046	-0.198
Ace	0.334	0.108	0.020
FI	0.332	0.097	-0.233
Phe	0.146	0.098	0.118
Ant	0.092	0.143	0.323
Flu	0.103	0.479	0.409
Pyr	0.150	0.324	0.334
BaA	0.255	0.094	-0.248
Chr	0.221	-0.417	0.288
BbF	0.214	-0.274	0.452
BkF	0.129	-0.245	-0.223
BaP	0.224	0.221	-0.289
DBA	0.099	0.429	-0.121
BghiP	0.338	-0.129	-0.070
IND	0.346	-0.142	0.028

The PCA biplot for sediment samples are shown in Figure 25 B, which depicts the PAHs loadings at PC1, PC2, and PC3. In the sediment samples, PC1 accounted for 26.60% of the variance, with representative PAHs including Nap, Acy, Ace, FI, BaA, Chr, BbF, BaP, BghiP, and IND. PC2 accounted for 18.55% of the variance, represented by PAHs such as Flu, Pyr, BaP, and DBA. PC3 was responsible for 15.83% of the variance in PAHs, including Ant, Flu, Pyr, Chr, and BbF. PC1 and PC3 exhibited greater loading of both LMW and HMW PAHs, whereas PC2 had a greater loading of HMW PAHs. Table 6 shows the extracted eigenvector values for sediment samples. Similar to the water samples, several negative correlations were detected between the assigned PAHs for each component. According to the PCA and diagnostic ratios, PAHs in the Euphrates River predominantly originates from coal and fuel combustion, petrogenic sources, and pyrolysis.

Table 6 Eigenvectors and percentage of variance for PC analysis of Sediment samples.

Sediment	PC1	PC2	PC3
Nap	0.276	-0.272	0.224
Acy	0.215	0.062	0.006
Ace	0.090	0.432	0.209
FI	0.272	-0.150	-0.10
Phe	0.383	0.119	-6.1E-4
Ant	0.186	0.407	0.229
Flu	-0.125	-0.101	0.527
Pyr	0.183	0.176	0.068
BaA	-0.027	0.499	-0.225
Chr	-0.001	0.312	0.103
BbF	0.372	0.199	0.165
BkF	0.218	0.009	-0.396
BaP	0.361	-0.231	-0.137
DBA	0.166	-0.194	0.492
BghiP	0.214	-0.070	-0.226
IND	0.413	-0.080	-0.016

5.6 Source identification and Pearson's correlation coefficient of PAHs of Euphrates basin

To manage the emission and release of PAHs with greater precision, it is essential to identify their sources of contamination to the fullest extent possible. In general, there are four main sources of PAHs: geogenic, petrogenic, pyrolytic, and biogenic [134]. Several diagnostic ratios for PAHs have been widely utilized to determine the likely source categories of PAHs in ecosystems [172]. HMW PAHs ratios, such as BaA/(BaA + Chr) and Flu/(Flu + Pyr), are typically preferred because they are more stable than LMW ratios. Therefore, to infer the potential origins of PAHs, the ratios of Ant/(Ant + Phe) and BaA/(BaA + Chr) against Flu/(Flu + Pyr) were graphed in Figure 26. According to results summarized by Yunker et al.[135], a BaA/(BaA + Chr) ratio of less than 0.2 indicates that oil emissions are the primary source of PAHs pollution, while a ratio greater than

0.35 indicates that combustion is the dominant source. A ratio between these two values indicates a mixture of oil and combustion pollution [135]. An Ant/(Ant + Phe) ratio of less than 0.1 suggests petroleum contamination, while a ratio greater than 0.1 indicates pyrogenic sources [136]. Conversely, a Flu/(Flu + Pyr) ratio of less than 0.4 indicates petroleum contamination or oil spills, while a ratio of 0.4 to 0.5 suggests petroleum combustion sources, and a Flu/(Flu + Pyr) ratio greater than 0.5 indicates biomass combustion sources [137]. The ratio of LMW/HMW and the proportion of isomers with similar physicochemical properties can qualitatively represent the characteristics of their contamination sources. An LMW/HMW ratio greater than 1.0 implies petroleum sources, whereas a ratio less than 1.0 indicates combustion sources [138]. The BaP/BghiP ratio can also be used to further confirm the estimation of PAHs sources. A BaP/BghiP ratio of less than 0.6 suggests that PAHs originated from non-traffic emissions, whereas a ratio greater than 0.6 indicates that the source is traffic emissions [139].

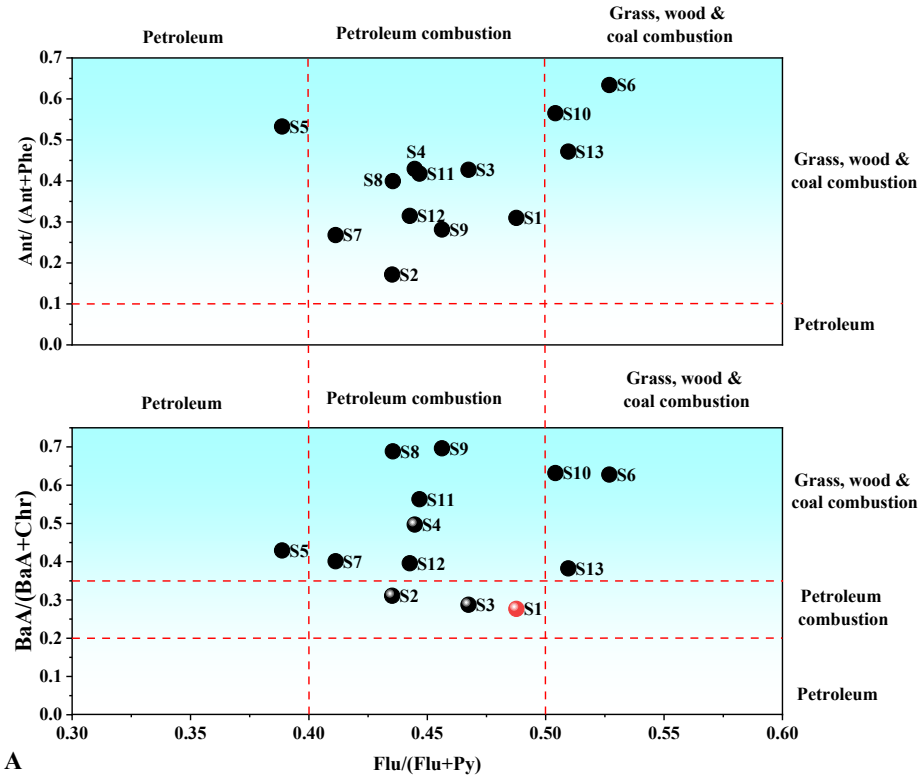

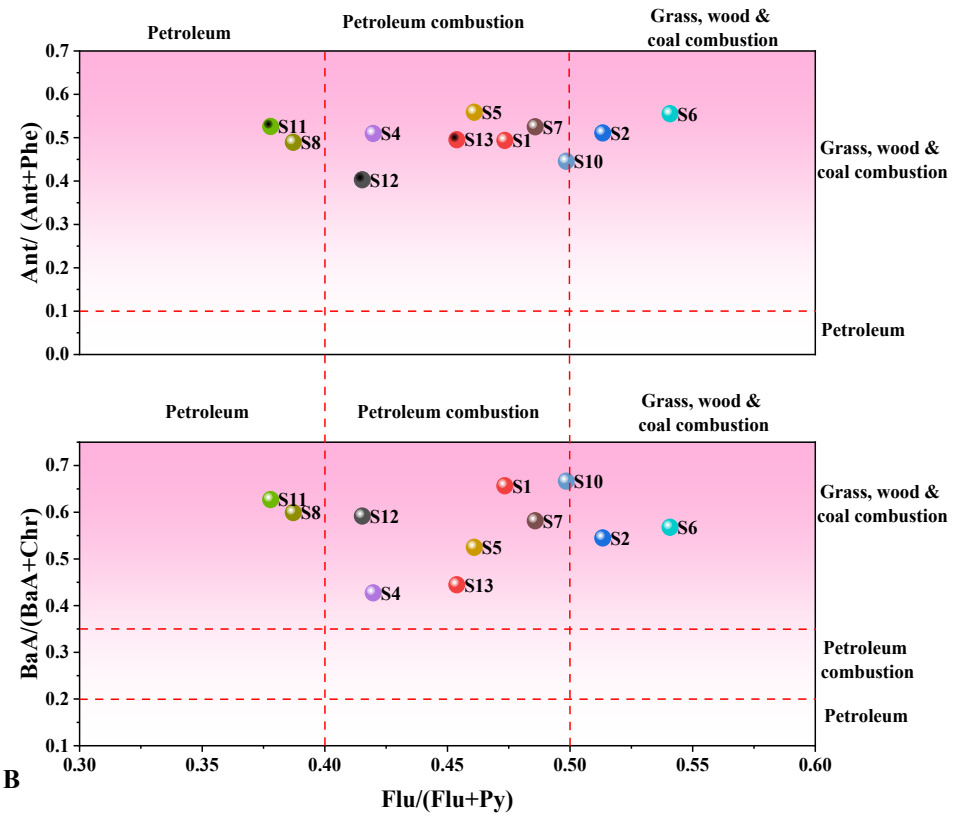

Figure 26 Cross plots of PAHs source identification for (A) water and (B) sediment samples

5.7 Source identification and Pearson's correlation coefficient of PAHs in Euphrates River water

In the water samples, except for S5, S6, S10, and S13, the sources of PAHs were primarily from petroleum combustion (0.4 < Flu/(Flu + Pyr) < 0.5) (Figure 27). S5 exhibited petroleum origin, while S6, S10, and S13 showed sources from biomass combustion. By applying the ratio BaA/(BaA + Chr) to the water samples, it can be concluded that the values for S1 to S3 fell between 0.2 and 0.35, indicating a mixture of oil and combustion pollution. In contrast, other sites (S4 to S13) indicated combustion as the dominant source, with ratios exceeding 0.35. Assessing the water samples along the entire river, an LMW/HMW ratio of less than one was found, suggesting that combustion is the primary source of PAHs compounds. Based on the BaP/BghiP ratio criteria, the PAHs in water samples S4, S10, S12, and S13 are likely derived from traffic emissions, while those from S1, S2, S3, and S11 originate from non-traffic emissions.

From the matrix of Pearson's correlation coefficients, it is evident that there is a positive association between the 2-3 ring PAHs ($R > 0.57$, $p < 0.05$) in the water samples. For instance,

Nap shows a strong positive correlation with Acy and FI. Additionally, the coefficients between 2-3 ring PAHs and 5-6 ring PAHs are notably positive, with r values exceeding 0.70. This is clearly illustrated by the positive correlation between Nap and Ace, as well as other 5-6 ring PAHs such as BbF and BghiP. Moreover, Acy (a 2-3 ring PAH) is positively correlated (R = 0.82) with 5-6 ring PAHs (BghiP and IND). It was also found that PAHs compounds with 4-ring structures, such as Chr, have very strong interactions with 5-6 ring PAHs like BbF, BghiP, and IND, with R-values of 0.81, 0.55, and 0.57, respectively. Among the 5-6 ring PAHs, IND shows a strong correlation with BghiP, with an R-value of 0.83.

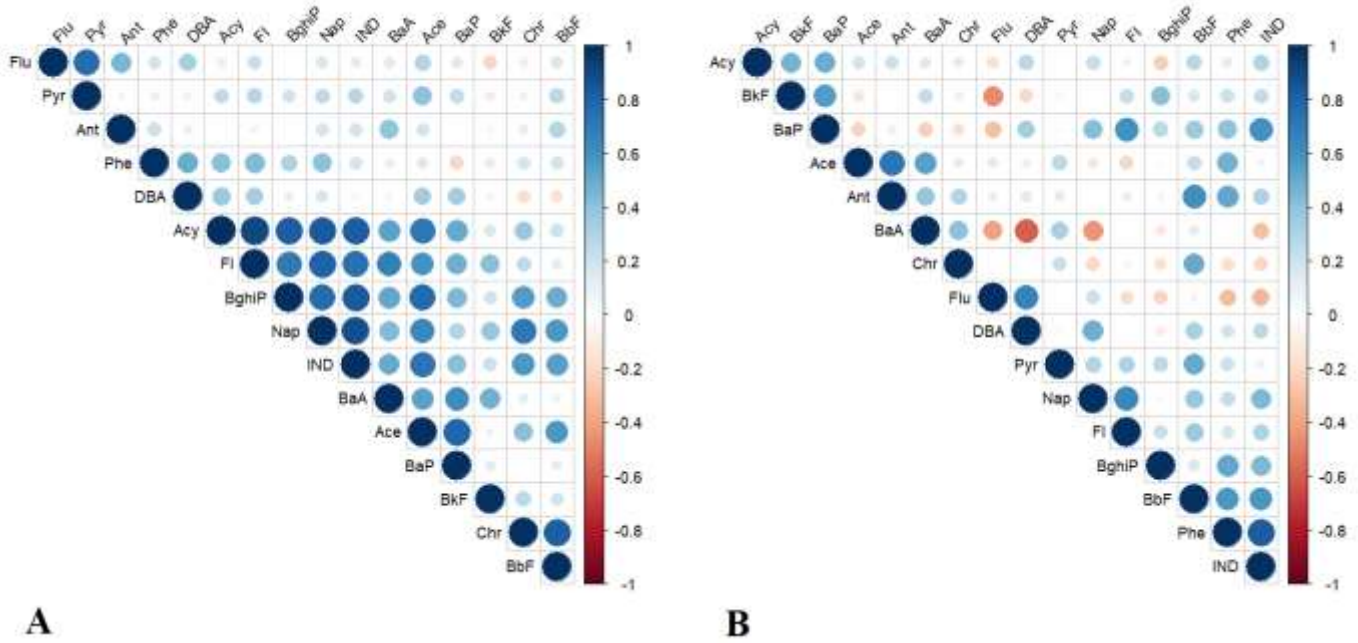

Figure 27 Pearson correlation coefficients of the 16 measured PAHs for water (A) and sediment (B) samples

5.8. Source identification of PAHs in Euphrates River sediment

In the sediment samples, PAHs in S1, S4, S5, S7, S12, and S13 are suggested to have originated mainly from petroleum combustion (0.4 < Flu/(Flu + Pyr) < 0.5), while S8 and S11 exhibited a petroleum origin, and other sites showed sources from biomass combustion(Figure 27). Moreover, the BaA/(BaA + Chr) ratio is greater than 0.35, indicating that combustion is the dominant source. When assessing the sediment samples along the entire river, an LMW/HMW ratio of less than 1

was found, suggesting that combustion is the main source of PAHs compounds. Regarding the BaP/BghiP ratio, S1, S4–S7, and S8–S13 had PAHs originating from traffic emissions, while PAHs in other sediment sites (S2, S3, and S8) were derived from non-traffic emissions. In terms of the Pearson correlation coefficient for sediment samples, Nap and FI, as well as Ace and Ant, exhibited positive interactions with R values of 0.64 and 0.72, respectively. Other 2-3 ring PAHs, such as Phe and Ant, showed a correlation with BbF. Furthermore, 4-ring PAHs like Flu demonstrated a positive interaction with 5-6 ring PAHs such as DBA. IND was positively correlated with other 4-5 ring PAHs, including BbF and DBA. Overall, the number of positive correlations between the PAHs groups is higher in water samples compared to sediment samples.

Based on the criteria mentioned above, it can be observed from Figures 26 and 27 that PAHs in both water and sediment samples are generally derived from pyrogenic sources. Pyrogenic PAHs are combustion byproducts primarily released into the atmosphere through the combustion of fossil fuels (coal, petroleum, and wood) and biomass (forest, grassland, or agricultural materials)[140]. Overall, the ratios indicate that pyrogenic sources dominate the production of the 16 PAHs in the Euphrates River system. This can be attributed to various observable sources, including emissions from significant traffic loads, gas and fuel combustion, home electricity generators, and the combustion of coal and wood.

5.9. Ecological risk assessment of Euphrates basin

The ecological risks posed by PAHs to the Euphrates River system were evaluated using water and sediment quality assessments. The USEPA surface water quality standards were adopted for this study, as the Iraqi standards were more generic and only specified limits for hydrocarbons (10 µg/L) [58], [84]. Appendix 7 shows the measured concentrations of PAHs at all locations, benchmarked against their counterparts in the USEPA surface water quality standards. Based on this benchmarking, the total concentration of the PAHs measured in the collected samples was found to be 8-18 times higher than the specified limits in the standards. This indicates a serious ecological risk to aquatic life in the Euphrates River. However, the EPA safe standard limits for human health protection from some individual PAHs, such as Ace, Ant, Flu, Fl, and Pyr, are in mg/L, which is higher than the highest detected concentration in the Euphrates River. This suggests that the river water might be safe for limited recreational activities but not for others. The ecological risk evaluation for sediment samples followed the procedure described by Ambade et al. [81]. The levels of PAHs in sediments were compared to sediment quality guidelines

(SQGs)[82]. Table 7 presents the concentration ranges of 16 individual PAHs along with toxicity guidelines. The concentrations of Acy, Ace, FI, Phe, Flu, BaA, and BghiP in sediments at all sites were above the ERL but below the ERM, indicating a possible effects range based on comparisons with SQGs. The concentration of Ant in the sediments at all sites was below the ERL, whereas DBA was higher than the ERM. Other PAHs, such as Pyr, Chr, BbF, BkF, and BaP, varied between a rare biological effect in some locations and occasional biological effects in others. The results indicate that there is a possible effects range with occasional biological effects for most of the measured PAHs in all sediment samples**.**

Table 7 Concentration range of 16 individual PAHs (ng/g dw) and toxicity guidelines

PAHs	**ERL-ERM**	**Concentration Range (ng/g dw)**	**<ERL**	**≥ERL and <ERM**	**≥ERM**
Nap	160–2100	195.3- 371.2	-	S1-S13	-
Acy	16–500	160.6- 300.2	-	S1-S13	-
Ace	44–640	201.2-530.1	-	S1-S13	-
FI	19–540	173.4-484	-	S1-S13	-
Phe	240–1500	242.8-486.6	-	S1-S13	-
Ant	600–5100	245.8-496.5	S1-S13	-	-
Flu	85.3–1100	321.3-632.2	-	S1-S13	-
Pyr	665–2500	357.5-733.6	S1-S3,S5, S6, S9-S13	S4, S7, S8	-
BaA	261–1600	426.5-821	-	S1-S13	-
Chr	384–2800	269.6-780.6	S1, S7, S10, S12	S2-S6, S8, S9, S11, S13	-
BbF	320–1880	173.8-969.8	S1, S2, S6	S3-S5, S7-S13	-
BkF	280–1620	235.2- 727.2	S6	S1-S5, S7-S13	-
BaP	430–1600	182.2- 822	S2, S6	S1, S3-S5, S7-S13	-
DBA	63.4–260	420.6-782.4	-	-	S1-S13

BghiP	430–1600	514.1- 1105	-	S1-S13	-
IND	240-	282.2-1986.5	-	-	-

5.10. Carcinogenic risk assessment and Incremental Lifetime Cancer Risk (ILCR) for Euphrates River sediment

It was found that the TEQ ranged between a minimum of 73.4 ng/L (S3) to a maximum of 171.3 ng/L (S13). The maximum and minimum values were present in S2 (838.9 ng/g dw) and S12 (1933 ng/g dw). The obtained TEQ values for both water and sediments samples were much higher than the reported values for rivers in other countries such as Australia, India, and Pakistan [122], [141], [150]. These elevated levels are alarming and a clear signal of the need for urgent environmental authorities' intervention. A risk assessment of human exposure to PAHs in the river sediments was conducted using the ILCR model of the USEPA, which considered three major routes of human exposure to contaminants (i.e., ingestion, dermal contact, and inhalation of vapor or sediment/dust) [83], [142]. The inhalation component of the ILCR was found to be insignificant ($< 10^6$), and hence it was removed. The ILCR levels for adults and children obtained for the Euphrates River sediment samples (Table 8) are significantly higher than those reported for Brisbane River in Australia [122]. If these levels are confirmed through long-term monitoring, the population living at the river basin needs to be made aware through and measures should be implemented to minimize human contact with the sediments.

Table 8 Calculated ILCR levels for adults and children exposed to the Euphrates River sediments (ng/g dw).

Sample	Adult			Children		
	Ingestion	Dermal	Total	Ingestion	Dermal	Total
1	3.78E-03	6.72E-03	1.05E-02	6.34E-03	7.90E-03	1.42E-02
2	2.40E-03	4.26E-03	6.65E-03	4.02E-03	5.01E-03	9.02E-03
3	4.13E-03	7.34E-03	1.15E-02	6.92E-03	8.63E-03	1.55E-02
4	4.42E-03	7.85E-03	1.23E-02	7.41E-03	9.23E-03	1.66E-02
5	4.50E-03	7.98E-03	1.25E-02	7.53E-03	9.39E-03	1.69E-02

6	3.53E-03	6.27E-03	9.80E-03	5.91E-03	7.37E-03	1.33E-02
7	4.53E-03	8.05E-03	1.26E-02	7.59E-03	9.47E-03	1.71E-02
8	3.91E-03	6.94E-03	1.08E-02	6.54E-03	8.16E-03	1.47E-02
9	4.58E-03	8.14E-03	1.27E-02	7.68E-03	9.57E-03	1.73E-02
10	5.23E-03	9.29E-03	1.45E-02	8.76E-03	1.09E-02	1.97E-02
11	3.53E-03	6.27E-03	9.80E-03	5.92E-03	7.37E-03	1.33E-02
12	5.52E-03	9.81E-03	1.53E-02	9.25E-03	1.15E-02	2.08E-02
13	4.80E-03	8.52E-03	1.33E-02	8.04E-03	1.00E-02	1.81E-02

6. Total organic matter (TOM) for the three rivers

Figure 28 illustrates the correlation between TOM contents (%) and total PAHs in sediments for the Danube River (A), Euphrates (B), and Tigris River (C). No correlation was found between TOM contents (%) and total PAHs in the Tigris River sediments, with an R-value of 0.098. A similar study found no statistically significant relationship in sediments sampled from Lake Balaton, Hungary [78], and likewise, no correlation was observed between total PAHs levels and TOM in sediments from Yemen's Hadhramout coast [173]. This suggests that PAHs concentrations and their distribution in the Tigris River sediments were primarily influenced by direct inputs rather than the intrinsic sediment characteristics, confirming pollution from oil refineries in the Tigris River. In contrast, a strong correlation was observed for the Danube and Euphrates Rivers, with R-values of 0.932 and 0.950, respectively, indicating a mix of pollution sources.

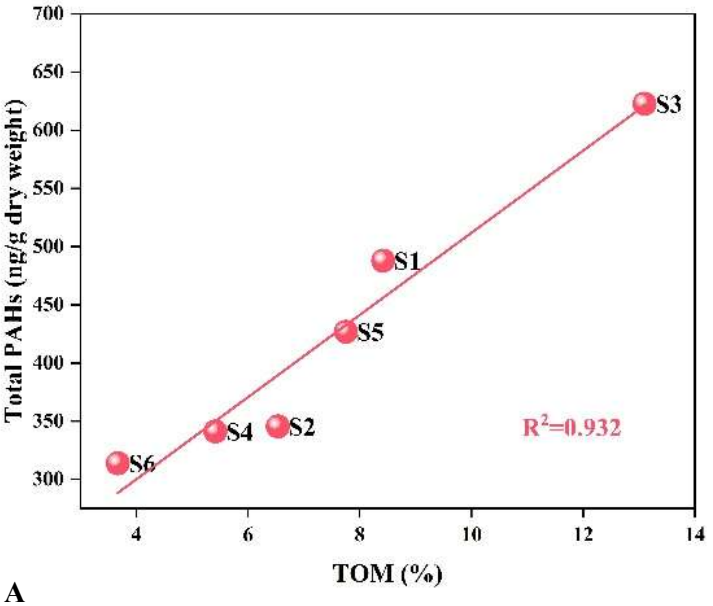

A

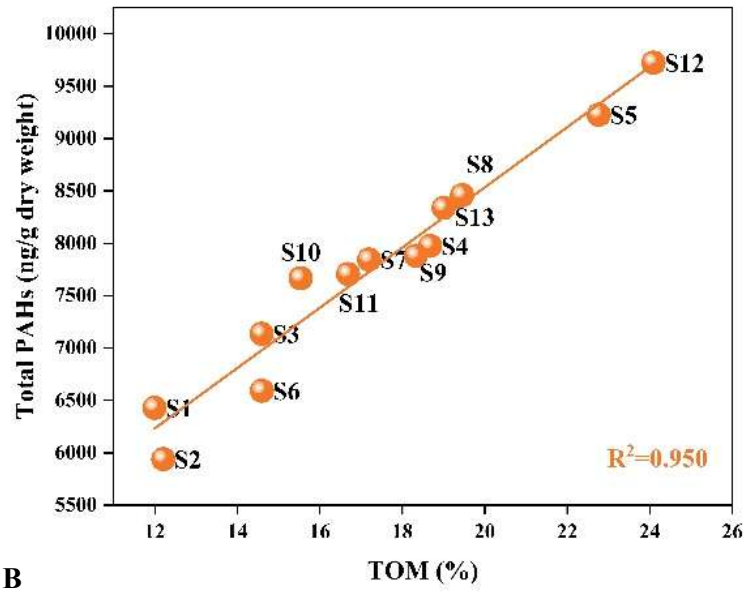

B

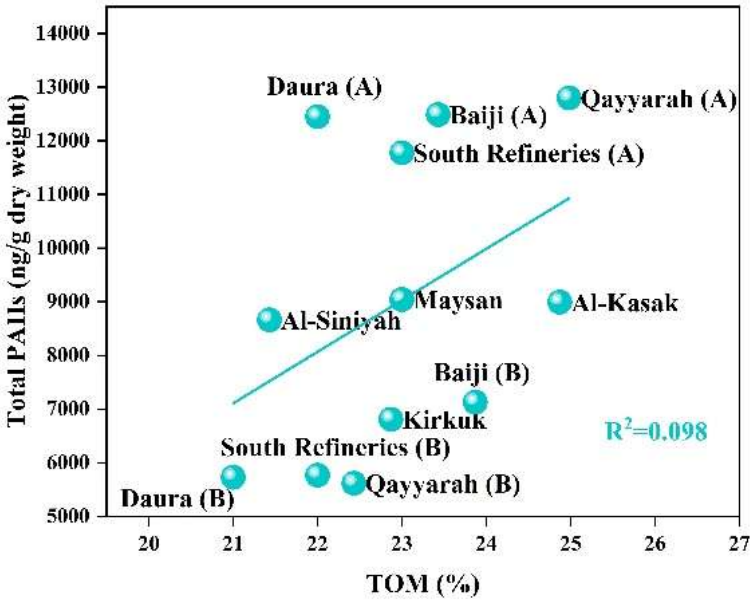

C

Figure 28 correlation between TOM contents (%) and total PAHs in sediments for Danube River (A), Euphrates (B) and Tigris River (C)

7.Uncertainty and limitations

In PAHs analysis, GC techniques are common because of their higher selectivity, sensitivity and resolution in comparison to liquid chromatography techniques. Separation and retention of PAHs could be influenced via a variety of parameters, for instance, solvent effect, temperature programs, stationary phases, injection conditions, etc., which consequently impact the analysis precision and accuracy [29]. Among these parameters, the stationary phase of GC is an essential component that has been studied. Although DB-5MS is one of the most commonly utilized capillary columns for PAHs analysis, GC capillary columns with a higher phenyl content, such as a DB-17MS column with 50% phenyl-substituted methylpolysiloxane, demonstrated enhanced separation of HMWPAHs [29], [174]. For example, it was stated that a DB-17MS column of 30 m was adequate for the separation of the majority of HMWPAHs, but a column of 60 m may be required for the separation of certain critical isomers [174]. In this investigation, PAHs compounds were measured using an HP-5MS capillary column of 30 m, rather than HP-5MS column of 60 m due to the 60 m column's extended analysis duration. In addition, liquid chromatography with fluorescence detectors could be a replacement technique because of its own unique fluorescence properties [175].

It should be noted that there were some limitations in isomeric ratios; for instance, in real multimedia environments, the paired isomers were (bio)degraded and transformed to various extents during the transport process, resulting in an overestimate of source allocation. Zhang and co-workers [176] proposed an application of the multimedia fugacity model to calibrate isomeric ratio deviations. Their attempt was to quantify potential changes in PAHs ratios from sources to bulk media, including PAHs ratios on particles in air, sediment, suspended solids, and soil. This model requires comprehensive information on all source types and the chemical composition profile for each source, which is generally unavailable. Furthermore, the local combustion process affects both the isomer ratios and chemical composition profiles that are essential in receptor models. Ratios or profiles from various regions could be significantly different and unrepresentative of one another. Adding to that, due to the extremely high cost of multimedia sampling in a large area, like our study along the entire Tigris River, as well as some limitations on the pretreatment and analytical conditions, we used the specific ratios of paired isomeric species to diagnose the local emission sources of PAHs in this study. Furthermore, PCA was utilized to aid in source identification.

8- Suggested methods for PAHs detection development

PAHs can be identified using various analytical techniques. However, traditional detection methods exhibit certain limitations. For instance, HPLC requires a complex pretreatment process, while capillary electrophoresis still lacks sufficient sensitivity and necessitates further enhancement [31]. Additionally, some advanced analytical techniques have yet to be fully utilized. An example is comprehensive two-dimensional gas chromatography coupled with mass spectrometry (GC×GC-MS), which extends data representation into an additional dimension. This makes it particularly suitable for investigating intricate interrelations among multiple factors, such as synergistic competition or higher-order interactions. Nevertheless, despite its significance in environmental monitoring, GC×GC-MS has not yet achieved a major breakthrough in PAH analysis [31], [177]. In addition, hybrid analytical techniques, such as gas chromatography coupled with tandem mass spectrometry (GC-MS/MS), have emerged as indispensable tools for the extraction and characterization of PAHs in environmental samples. These advanced methodologies integrate the exceptional separation efficiency of chromatography with the high detection precision of mass spectrometry, facilitating the accurate identification and quantification of PAHs even within complex matrices. GC-MS/MS enhances both sensitivity and specificity, allowing for the differentiation of isomeric compounds and the detection of PAHs at trace levels. The application of these analytical techniques significantly enhances the precision, sensitivity, and reproducibility of PAH analysis. This, in turn, contributes to a more comprehensive understanding of their distribution, sources, and environmental impact.

Moreover, emerging analytical methodologies, including microfluidics, chemometrics, and machine learning [31], [178], offer substantial potential for analyzing complex matrix samples and could be effectively applied to PAH detection. However, their application in PAH-related studies remains limited. Achieving real-time and online PAH detection requires several key advancements, such as direct sample injection, atmospheric pressure ionization, and the miniaturization of mass spectrometers. Ambient mass spectrometry effectively addresses the constraints of conventional mass spectrometry by eliminating the need for extensive sample pretreatment and high-vacuum ionization. It enables rapid, high-throughput analysis of trace compounds in complex matrices. A particularly promising development in this domain is MPT mass spectrometry, which has recently been introduced for PAHs analysis [31]. Initial findings suggest that MPT mass spectrometry is exceptionally suited for direct PAH studies, with the potential to elucidate dynamic processes such

as sequential hydrogenation, Birch reduction, and molecular stability. Furthermore, it presents a promising avenue for the rapid and direct detection of PAHs isomers, paving the way for future advancements in this field. Another notable mass spectrometric technique, mass spectrometry imaging (MSI), holds significant promise in advancing PAH research [179], [180]. Unlike conventional mass spectrometry methods, MSI not only quantifies PAHs across an entire sample but also maps their spatial distribution on a given surface. This capability provides valuable two-dimensional data, greatly enhancing investigations into PAH migration, aggregation, formation, and transformation across different media.

9. Conclusions

In Hungary, PAHs level in Danube River highlighted a broad variance range of 16 PAHs contents in water with total concentrations of PAHs ranging from 283.1-541.9, 198.6-404.3, 160.0-324.6, and 228.2-378.1 ng/L for winter, spring, summer, and autumn, respectively. Sediment samples showed PAHs ranging from 313.7-622.7, 312.7-595.4, 215.1-465.4, and 311.3-491.7 ng/g for winter, spring, summer, and autumn, respectively. The overall analysis of the results indicates that the putative anthropogenic sources of PAHs were verified to be both pyrogenic (incomplete combustion of biomass and coal) and pyrolytic (incomplete combustion of liquid fossil fuels and vehicle exhaust emissions); with pyrogenic origins predominating over pyrolytic sources. This might suggest that the industries essentially utilize fossil fuels, which would increase the PAHs emissions in the study area. Generally, except for Acy and FI concentrations, the eco-toxicological assessment of the Danube River environment showed no significant PAHs pollutants in sediments, suggesting a low chance for negative biological impacts and low ecological risk. The total ILCR in both children and adults were calculated to be more than $1/10^4$ in all seasons, with the highest values recorded in spring and followed by winter, which constitutes a concerning issue. Continuous monitoring of the PAHs would offer better insight into the scale of the pollution, which would help in devising effective mitigation strategies.

On the other side, both Tigris and Euphrates River in Iraq showed high level of PAHs compounds. For Tigris River, the level of 16 PAHs near Iraqi oil refineries were monitored for six months. Most of these refineries are located near the Tigris River and its estuaries, one of Iraq's most important sources of potable water and irrigation. The refineries examined were Baiji, Kirkuk, Al-Siniyah, Qayyarah, Al-Kasak, Daura, South Refineries Company, and the Maysan oil refinery. The 16 PAHs concentration in water varied from 567.8 to 3750.7 ng/L, whereas the

concentration in sediment ranged from 5619.2 to 12795.0 ng/g, which registered a very high load of PAHs compounds compared to other regions in the world. The PAHs concentration in the downstream sites of the refineries Baiji, Qayyarah, Daura, and South Refineries Company was double the values of the upstream. The HMWPAHs accounted for 49.41% - 81.67 % and 39.06% - 89.39% of the total 16 PAHs in Tigris water and sediment samples, respectively. The 16 PAHs detected in water and sediment samples from the Tigris River originated from pyrogenic sources. All sites indicated high ILCR values which exceeded the ILCR reported elsewhere. In Euphrates River, the PAHs pollutions for both water and sediment increase along the river. IND was the most prominent PAHs compound in water and sediment samples across all 13 sampling locations. Some measured PAHs concentrations were significantly higher than reported levels in other countries in Asia. Source identification suggests that PAHs pollution primarily originates from petroleum product consumption, which is expected given the increasing use of private cars and home electricity generators. The measured PAHs in water and sediment samples predominantly consisted of larger molecules with 5-6 rings in their structure. The elevated levels of PAHs detected in the Euphrates River system, especially the carcinogenic compounds, pose potential ecological and health risks.

10-Recommendations and Future Outlook

1. Long-Term and Comprehensive Monitoring in Iraq and Other Polluted Regions

- Given the direct impact of oil refineries on both human health and the environment, it is crucial to conduct extensive, long-term studies on PAH contamination across different environmental media (air, water, soil, and biota) near refineries.

- Future research should include seasonal variations to understand fluctuations in PAHs concentrations over time.

- Studies should extend beyond industrial zones to assess PAH dispersion patterns in urban, suburban, and rural areas and their impact on human exposure and ecological health.

2. Development of Advanced Analytical Methods

- Expanding analytical methods to detect non-priority and emerging PAHs, which may pose previously unrecognized health and environmental risks.

- Enhancing the sensitivity and selectivity of detection techniques, particularly two-dimensional gas chromatography (GC×GC), high-resolution mass spectrometry (HRMS), and liquid chromatography-tandem mass spectrometry (LC-MS/MS), to improve the identification of PAHs in complex matrices.

- Further research into green and sustainable extraction methods (e.g., solvent-free or minimal-solvent approaches) to reduce environmental impact while improving efficiency.

3. Integration of Portable and Automated Technologies

- The development of portable, miniaturized, and lab-on-a-chip systems can enable real-time, on-site PAH analysis, reducing reliance on extensive sample storage and transportation.

- Increasing automation in sample preparation and analysis can minimize human error, enhance reproducibility, and improve throughput for large-scale monitoring programs.

- Adoption of remote sensing and sensor networks for continuous PAHs surveillance in air, water, and soil environments.

4. Health Risk Assessment and Toxicological Studies

- Conducting comprehensive health risk assessments to evaluate the chronic and acute exposure effects of PAHs on different population groups, particularly vulnerable populations (e.g., children, pregnant women, and workers in high-exposure occupations).

- Expanding research into the metabolism and bioaccumulation of PAHs in humans and wildlife to better understand their long-term biological effects.

- Investigating the synergistic toxicity of PAHs with other pollutants, such as heavy metals and persistent organic pollutants (POPs), to assess combined exposure risks.

5. Regulatory Frameworks and Environmental Policies

- Strengthening environmental regulations and standards for PAH emissions and contamination levels, particularly in regions with high industrial activity.

- Promoting international collaboration for data-sharing and harmonization of PAH monitoring protocols.

- Encouraging industry compliance with best practices in pollution control, including cleaner production techniques and emissions reduction strategies.

6. Source Apportionment and Modeling Approaches

- Utilizing advanced source apportionment techniques such as positive matrix factorization (PMF) and chemical mass balance (CMB) to identify and quantify PAH sources.

- Implementing atmospheric and hydrological modeling to predict PAH dispersion, deposition, and degradation under different environmental conditions.

- Developing geospatial mapping and risk prediction tools to visualize PAH hotspots and their potential impact on communities.

7. Public Awareness and Community Engagement

- Enhancing public awareness campaigns about PAHs exposure risks and mitigation strategies.

- Involving local communities and stakeholders in environmental monitoring through participatory research programs.

- Promoting citizen science initiatives, where individuals can contribute to PAH data collection using low-cost monitoring devices.

11. Thesis points

In the Danube River, I found the following points:

- I observed significant seasonal fluctuations in PAHs concentrations in water, ranging from 224.8 ng/L in summer to 365.8 ng/L in winter. Similarly, PAHs concentrations in sediment samples varied, from 316.7 ng/g (dry weight) in summer to 422.9 ng/g (dry weight) in winter.
- According to the European Drinking Water Directive, PAHs levels exceeded the permitted limit of 100 ng/L, showing a 124.8% increase in summer and a 265.8% increase in winter.
- I concluded that the primary sources of PAHs were anthropogenic, mainly from pyrolytic and pyrogenic processes, with pyrogenic sources being more dominant.
- Except for Acy and FI concentrations, the eco-toxicological assessment of the Danube River environment showed no significant PAHs pollution in sediments, suggesting a low likelihood of negative biological impacts and a low ecological risk.
- ILCR for both children and adults marginally higher than the limit ($1/10^4$) in all seasons, with the highest values recorded in spring, followed by winter, indicating a concerning public health issue.

In the Tigris River, I found the following results:

- The 16 PAHs concentrations ranged from 567.8 to 3750.7 ng/L in water and from 5619.2 to 12795.0 ng/g in sediment. Water samples near the South Refineries Company recorded the highest PAHs concentrations, while sediment samples from the Baiji oil refinery showed the highest levels.
- I observed that HMWPAHs (5-6 rings) had the highest percentages in both water and sediment samples, ranging from 49.41% to 81.67% for water and from 39.06% to 89.39% for sediment.
- I concluded that the majority of the 16 PAHs measured in water and sediment samples from the Tigris River were derived from pyrogenic sources.
- For Sediment Quality Guidelines (SQGs), most sites showed a possible effect range with occasional biological impacts due to elevated PAHs concentrations in sediment samples.

The calculated ILCR value indicated a high risk, with potential adverse health effects, including cancer.

In the Euphrates River, I found the following points:

- I observed that PAHs contamination increased along the river's flow direction due to rising non-point source pollution.
- I found that 5-6 ring PAHs were dominant in water and sediment samples, with averages of 42% and 50%, respectively.
- Carcinogenic PAHs constituted 46% and 55% of the total measured compounds in water and sediment samples, respectively, highlighting potential ecological and human health risks.
- For Sediment Quality Guidelines (SQGs), most sites exhibited an effect range between low and medium. The calculated ILCR for adults and children was in the range of 10^{-2} to 10^{-3}, which is 3-6 times higher than reported in the literature.
- I concluded that PAHs source identification suggests the PAHs pollution originates from petroleum product consumption, which is expected given the increasing use of private cars and home electricity generators

References

[1] M. Rodell *et al.*, "Emerging trends in global freshwater availability," *Nature*, vol. 557, no. 7707, pp. 651–659, May 2018, doi: 10.1038/s41586-018-0123-1.

[2] B. O. Botwe, P. Kelderman, E. Nyarko, and P. N. L. Lens, "Assessment of DDT, HCH and PAH contamination and associated ecotoxicological risks in surface sediments of coastal Tema Harbour (Ghana)," *Mar. Pollut. Bull.*, vol. 115, no. 1–2, pp. 480–488, Feb. 2017, doi: 10.1016/j.marpolbul.2016.11.054.

[3] S. Mitra, S. Corsolini, K. Pozo, O. Audy, S. K. Sarkar, and J. K. Biswas, "Characterization, source identification and risk associated with polyaromatic and chlorinated organic contaminants (PAHs, PCBs, PCBzs and OCPs) in the surface sediments of Hooghly estuary, India," *Chemosphere*, vol. 221, pp. 154–165, Apr. 2019, doi: 10.1016/j.chemosphere.2018.12.173.

[4] M. Honda and N. Suzuki, "Toxicities of Polycyclic Aromatic Hydrocarbons for Aquatic Animals," *Int. J. Environ. Res. Public. Health*, vol. 17, no. 4, p. 1363, Feb. 2020, doi: 10.3390/ijerph17041363.

[5] F. Jesus *et al.*, "A review on polycyclic aromatic hydrocarbons distribution in freshwater ecosystems and their toxicity to benthic fauna," *Sci. Total Environ.*, vol. 820, p. 153282, May 2022, doi: 10.1016/j.scitotenv.2022.153282.

[6] R. A. Grmasha, O. J. Al-sareji, J. M. Salman, and K. S. Hashim, "Polycyclic aromatic hydrocarbons (PAHs) in urban street dust within three land-uses of Babylon governorate, Iraq: Distribution, sources, and health risk assessment," *J. King Saud Univ. - Eng. Sci.*, vol. 34, no. 4, pp. 231–239, May 2022, doi: 10.1016/j.jksues.2020.11.002.

[7] A. Binelli *et al.*, "A comparison of sediment quality guidelines for toxicity assessment in the Sunderban wetlands (Bay of Bengal, India)," *Chemosphere*, vol. 73, no. 7, pp. 1129–1137, Oct. 2008, doi: 10.1016/j.chemosphere.2008.07.019.

[8] M. Andersson, M. Klug, O. A. Eggen, and R. T. Ottesen, "Polycyclic aromatic hydrocarbons (PAHs) in sediments from lake Lille Lungegårdsvannet in Bergen, western Norway; appraising pollution sources from the urban history," *Sci. Total Environ.*, vol. 470–471, pp. 1160–1172, Feb. 2014, doi: 10.1016/j.scitotenv.2013.10.086.

[9] M. A. Mallah *et al.*, “Polycyclic aromatic hydrocarbon and its effects on human health: An overeview,” *Chemosphere*, vol. 296, p. 133948, Jun. 2022, doi: 10.1016/j.chemosphere.2022.133948.

[10] J. T. Andersson and C. Achten, “Time to Say Goodbye to the 16 EPA PAHs? Toward an Up-to-Date Use of PACs for Environmental Purposes,” *Polycycl. Aromat. Compd.*, vol. 35, no. 2–4, pp. 330–354, Mar. 2015, doi: 10.1080/10406638.2014.991042.

[11] T. Wenzl, R. Simon, E. Anklam, and J. Kleiner, “Analytical methods for polycyclic aromatic hydrocarbons (PAHs) in food and the environment needed for new food legislation in the European Union,” *TrAC Trends Anal. Chem.*, vol. 25, no. 7, pp. 716–725, Jul. 2006, doi: 10.1016/j.trac.2006.05.010.

[12] B. A. Alaidaroos, “Advancing Eco-Sustainable Bioremediation for Hydrocarbon Contaminants: Challenges and Solutions,” *Processes*, vol. 11, no. 10, p. 3036, Oct. 2023, doi: 10.3390/pr11103036.

[13] I. C. T. Nisbet and P. K. LaGoy, “Toxic equivalency factors (TEFs) for polycyclic aromatic hydrocarbons (PAHs),” *Regul. Toxicol. Pharmacol.*, vol. 16, no. 3, pp. 290–300, Dec. 1992, doi: 10.1016/0273-2300(92)90009-X.

[14] A. Mojiri, J. L. Zhou, A. Ohashi, N. Ozaki, and T. Kindaichi, “Comprehensive review of polycyclic aromatic hydrocarbons in water sources, their effects and treatments,” *Sci. Total Environ.*, vol. 696, p. 133971, Dec. 2019, doi: 10.1016/j.scitotenv.2019.133971.

[15] M. Vijayanand *et al.*, “Polyaromatic hydrocarbons (PAHs) in the water environment: A review on toxicity, microbial biodegradation, systematic biological advancements, and environmental fate,” *Environ. Res.*, vol. 227, p. 115716, Jun. 2023, doi: 10.1016/j.envres.2023.115716.

[16] K. Srogi, “Monitoring of environmental exposure to polycyclic aromatic hydrocarbons: a review,” *Environ. Chem. Lett.*, vol. 5, no. 4, pp. 169–195, Nov. 2007, doi: 10.1007/s10311-007-0095-0.

[17] K. Ravindra, E. Wauters, and R. Van Grieken, “Variation in particulate PAHs levels and their relation with the transboundary movement of the air masses,” *Sci. Total Environ.*, vol. 396, no. 2–3, pp. 100–110, Jun. 2008, doi: 10.1016/j.scitotenv.2008.02.018.

[18] A. Gupte, A. Tripathi, H. Patel, D. Rudakiya, and S. Gupte, “Bioremediation of Polycyclic Aromatic Hydrocarbon (PAHs): A Perspective,” *Open Biotechnol. J.*, vol. 10, no. 1, pp. 363–378, Nov. 2016, doi: 10.2174/1874070701610010363.

[19] A. R. Johnsen and U. Karlson, “Diffuse PAH contamination of surface soils: environmental occurrence, bioavailability, and microbial degradation,” *Appl. Microbiol. Biotechnol.*, vol. 76, no. 3, pp. 533–543, Sep. 2007, doi: 10.1007/s00253-007-1045-2.

[20] H. I. Abdel-Shafy and M. S. M. Mansour, “A review on polycyclic aromatic hydrocarbons: Source, environmental impact, effect on human health and remediation,” *Egypt. J. Pet.*, vol. 25, no. 1, pp. 107–123, Mar. 2016, doi: 10.1016/j.ejpe.2015.03.011.

[21] C. R. Marris *et al.*, “Polyaromatic hydrocarbons in pollution: a heart-breaking matter,” *J. Physiol.*, vol. 598, no. 2, pp. 227–247, Jan. 2020, doi: 10.1113/JP278885.

[22] IARC, “(International Agency for Research on Cancer), Some non-heterocyclic polycyclic aromatic hydrocarbons and some related exposures, Monogr Eval Carcinog Risks Hum 92 (2010) 765–771.”

[23] “An Assessment of Occupational Exposure to Polycyclic Aromatic Hydrocarbons in the UK,” *Ann. Occup. Hyg.*, Mar. 2006, doi: 10.1093/annhyg/mel010.

[24] D. L. Diggs *et al.*, “Polycyclic Aromatic Hydrocarbons and Digestive Tract Cancers: A Perspective,” *J. Environ. Sci. Health Part C*, vol. 29, no. 4, pp. 324–357, Oct. 2011, doi: 10.1080/10590501.2011.629974.

[25] P. B. Bach, M. J. Kelley, R. C. Tate, and D. C. McCrory, “Screening for Lung Cancer*,” *Chest*, vol. 123, no. 1, pp. 72S-82S, Jan. 2003, doi: 10.1378/chest.123.1_suppl.72S.

[26] US EPA, “Environmental Protection Agency). Polycyclic aromatic hydrocarbons (PAHs) — EPA fact sheet. Washington (DC): National Center for Environmental Assessment,” Office of Research and Development; 2008.

[27] A. O. Adeniji, O. O. Okoh, and A. I. Okoh, “Analytical Methods for Polycyclic Aromatic Hydrocarbons and their Global Trend of Distribution in Water and Sediment: A Review,” in *Recent Insights in Petroleum Science and Engineering*, M. Zoveidavianpoor, Ed., InTech, 2018. doi: 10.5772/intechopen.71163.

[28] A. O. Adeniji, O. O. Okoh, and A. I. Okoh, “Analytical Methods for the Determination of the Distribution of Total Petroleum Hydrocarbons in the Water and Sediment of Aquatic Systems: A Review,” *J. Chem.*, vol. 2017, pp. 1–13, 2017, doi: 10.1155/2017/5178937.

[29] D. L. Poster, M. M. Schantz, L. C. Sander, and S. A. Wise, “Analysis of polycyclic aromatic hydrocarbons (PAHs) in environmental samples: a critical review of gas chromatographic (GC) methods,” *Anal. Bioanal. Chem.*, vol. 386, no. 4, pp. 859–881, Oct. 2006, doi: 10.1007/s00216-006-0771-0.

[30] E. Gilgenast, G. Boczkaj, A. Przyjazny, and M. Kamiński, “Sample preparation procedure for the determination of polycyclic aromatic hydrocarbons in petroleum vacuum residue and bitumen,” *Anal. Bioanal. Chem.*, vol. 401, no. 3, pp. 1059–1069, Aug. 2011, doi: 10.1007/s00216-011-5134-9.

[31] Y. Zhang *et al.*, “Contemporary Research Progress on the Detection of Polycyclic Aromatic Hydrocarbons,” *Int. J. Environ. Res. Public. Health*, vol. 19, no. 5, p. 2790, Feb. 2022, doi: 10.3390/ijerph19052790.

[32] Q. Zhang, P. Liu, S. Li, X. Zhang, and M. Chen, “Progress in the analytical research methods of polycyclic aromatic hydrocarbons (PAHs),” *J. Liq. Chromatogr. Relat. Technol.*, vol. 43, no. 13–14, pp. 425–444, Aug. 2020, doi: 10.1080/10826076.2020.1746668.

[33] L. E. Blue *et al.*, “Recent advances in capillary ultrahigh pressure liquid chromatography,” *J. Chromatogr. A*, vol. 1523, pp. 17–39, Nov. 2017, doi: 10.1016/j.chroma.2017.05.039.

[34] P. Rocío-Bautista, V. Pino, J. H. Ayala, J. Pasán, C. Ruiz-Pérez, and A. M. Afonso, “A magnetic-based dispersive micro-solid-phase extraction method using the metal-organic framework HKUST-1 and ultra-high-performance liquid chromatography with fluorescence detection for determining polycyclic aromatic hydrocarbons in waters and fruit tea infusions,” *J. Chromatogr. A*, vol. 1436, pp. 42–50, Mar. 2016, doi: 10.1016/j.chroma.2016.01.067.

[35] C. Hutzler, A. Luch, and J. G. Filser, “Analysis of carcinogenic polycyclic aromatic hydrocarbons in complex environmental mixtures by LC-APPI-MS/MS,” *Anal. Chim. Acta*, vol. 702, no. 2, pp. 218–224, Sep. 2011, doi: 10.1016/j.aca.2011.07.003.

[36] Y. Nolvachai, C. Kulsing, C. S. Hawes, S. R. Batten, D. R. Turner, and P. J. Marriott, “Selectivity differences of coordination compound stationary phases for polyaromatic hydrocarbons and polar analytes in gas and liquid phases,” *J. Chromatogr. A*, vol. 1500, pp. 167–171, Jun. 2017, doi: 10.1016/j.chroma.2017.04.037.

[37] J. Fan, M. Qi, R. Fu, and L. Qu, “Performance of graphene sheets as stationary phase for capillary gas chromatographic separations,” *J. Chromatogr. A*, vol. 1399, pp. 74–79, Jun. 2015, doi: 10.1016/j.chroma.2015.04.030.

[38] Y. Zheng, M. Qi, and R. Fu, “Graphitic carbon nitride as high-resolution stationary phase for gas chromatographic separations,” *J. Chromatogr. A*, vol. 1454, pp. 107–113, Jul. 2016, doi: 10.1016/j.chroma.2016.05.073.

[39] Y. Saito, A. Tahara, M. Imaizumi, T. Takeichi, H. Wada, and K. Jinno, “Polymer-Coated Fibrous Materials as the Stationary Phase in Packed Capillary Gas Chromatography,” *Anal. Chem.*, vol. 75, no. 20, pp. 5525–5531, Oct. 2003, doi: 10.1021/ac030052h.

[40] C. Saridara and S. Mitra, “Chromatography on Self-Assembled Carbon Nanotubes,” *Anal. Chem.*, vol. 77, no. 21, pp. 7094–7097, Nov. 2005, doi: 10.1021/ac050812j.

[41] X. Han, H. Wang, X. He, B. Wang, and B. Wu, “7,10-Diphenylfluoranthene grafted polysiloxane as a highly selective stationary phase for gas chromatography,” *J. Chromatogr. A*, vol. 1468, pp. 192–199, Oct. 2016, doi: 10.1016/j.chroma.2016.09.063.

[42] G. A. Odugbesi, H. Nan, M. Soltani, J. H. Davis, and J. L. Anderson, “Ultra-high thermal stability perarylated ionic liquids as gas chromatographic stationary phases for the selective separation of polyaromatic hydrocarbons and polychlorinated biphenyls,” *J. Chromatogr. A*, vol. 1604, p. 460466, Oct. 2019, doi: 10.1016/j.chroma.2019.460466.

[43] X. Han, X. He, H. Wang, B. Wang, and B. Wu, “Fluoro-substituted tetraphenyl–phenyl grafted polysiloxanes as highly selective stationary phases for gas chromatography,” *J. Chromatogr. A*, vol. 1449, pp. 118–128, Jun. 2016, doi: 10.1016/j.chroma.2016.04.073.

[44] C. Emmenegger, M. Kalberer, V. Samburova, and R. Zenobi, “Analysis of size-segregated aerosol-bound polycyclic aromatic hydrocarbons with high time resolution using two-step laser mass spectrometry,” *The Analyst*, vol. 129, no. 5, p. 416, 2004, doi: 10.1039/b401201a.

[45] R. Zimmermann, T. Ferge, M. Gälli, and R. Karlsson, “Application of single-particle laser desorption/ionization time-of-flight mass spectrometry for detection of polycyclic aromatic hydrocarbons from soot particles originating from an industrial combustion process,” *Rapid Commun. Mass Spectrom.*, vol. 17, no. 8, pp. 851–859, Apr. 2003, doi: 10.1002/rcm.979.

[46] M. Guo *et al.*, “Quantitative analysis of polycyclic aromatic hydrocarbons (PAHs) in water by surface-enhanced Raman spectroscopy (SERS) combined with Random Forest,” *Spectrochim. Acta. A. Mol. Biomol. Spectrosc.*, vol. 287, p. 122057, Feb. 2023, doi: 10.1016/j.saa.2022.122057.

[47] X. Zhao *et al.*, “Magnetic solid phase extraction coupled to HPLC-UV for highly sensitive analysis of mono-hydroxy polycyclic aromatic hydrocarbons in urine,” *Anal. Chim. Acta*, vol. 1285, p. 342020, Jan. 2024, doi: 10.1016/j.aca.2023.342020.

[48] T. M. Mogashane, L. Mokoena, and J. Tshilongo, “A Review on Recent Developments in the Extraction and Identification of Polycyclic Aromatic Hydrocarbons from Environmental Samples,” *Water*, vol. 16, no. 17, p. 2520, Sep. 2024, doi: 10.3390/w16172520.

[49] H. Chen, G. Gao, P. Liu, R. Pan, X. Liu, and C. Lu, “Determination of 16 Polycyclic Aromatic Hydrocarbons in Tea by Simultaneous Dispersive Solid-Phase Extraction and Liquid–Liquid Extraction Coupled with gas Chromatography–Tandem Mass Spectrometry,” *Food Anal. Methods*, vol. 9, no. 8, pp. 2374–2384, Aug. 2016, doi: 10.1007/s12161-016-0427-4.

[50] L. Zhang, W. Li, and S. Wu, “Rapid Determination of Oxygenated and Parent Polycyclic Aromatic Hydrocarbons in Milk Using Supercritical Fluid Chromatography-Mass Spectrometry,” *Foods*, vol. 11, no. 24, p. 3980, Dec. 2022, doi: 10.3390/foods11243980.

[51] NIOSH, “(National Institute for Occupational Safety and Healt,” 2010. [Online]. Available: http://www.cdc.gov/niosh/about.html

[52] US EPA, . “Deposition of air pollutants to the great waters: third report to congress. Office of Air Quality Planning and Standards. EPA-453/R-00-0005.” [Online]. Available: http://www.epa.gov/air/oaqps/gr8water/3rdrpt/ index.html

[53] World Health Organization, “Polynuclear aromatic hydrocarbons in drinking-water. Background document for development of WHO guidelines for drinking-water quality. Geneva: World Health Organization,” 2003.

[54] WFD, “European Commission, Directive 2000/60/EC of the European Parliament and of the Council of 23 October 2000 establishing a framework for Community action in the field of water policy, Off. J. Eur. Commun. L 327.” 2000.

[55] L. Jones Antoin Lawlor, Michael Cahill, Brian Kinsella, Ken Forde, Ambrose Furey, and Fiona Regan., “Priority and hazardous substances." (2011).” [Online]. Available: https://doras.dcu.ie/18646/1/Lisa_3.pdf

[56] SCHEER, “Final Opinion on Draft Environmental Quality Standards for Priority Substances under the WaterFramework Directive" - PAHs,” Mar. 2023. [Online]. Available: https://health.ec.europa.eu/system/files/2023-03/scheer_o_061.pdf

[57] S. Felemban, P. Vazquez, and E. Moore, “Future Trends for In Situ Monitoring of Polycyclic Aromatic Hydrocarbons in Water Sources: The Role of Immunosensing Techniques,” *Biosensors*, vol. 9, no. 4, p. 142, Dec. 2019, doi: 10.3390/bios9040142.

[58] IQS, *I.S. 2009. Iraqi Standard of Drinking Water No. 417 Second modification*.

[59] P. Baumard, H. Budzinski, P. Garrigues, J. C. Sorbe, T. Burgeot, and J. Bellocq, “Concentrations of PAHs (polycyclic aromatic hydrocarbons) in various marine organisms in

relation to those in sediments and to trophic level," *Mar. Pollut. Bull.*, vol. 36, no. 12, pp. 951–960, Dec. 1998, doi: 10.1016/S0025-326X(98)00088-5.

[60] CCME, "Canadian soil quality guide- lines for potentially carcinogenic and other PAHs: scientific criteria document. Win- nipeg: CCME; 2010."

[61] E. Szalinska, "Water Quality and Management Changes Over the History of Poland," *Bull. Environ. Contam. Toxicol.*, vol. 100, no. 1, pp. 26–31, Jan. 2018, doi: 10.1007/s00128-017-2226-z.

[62] C. L. Chiţescu, A. Ene, E.-I. Geana, A. M. Vasile, and C. T. Ciucure, "Emerging and Persistent Pollutants in the Aquatic Ecosystems of the Lower Danube Basin and North West Black Sea Region—A Review," *Appl. Sci.*, vol. 11, no. 20, p. 9721, Oct. 2021, doi: 10.3390/app11209721.

[63] R. A. Grmasha *et al.*, "Temporal and spatial distribution of polycyclic aromatic hydrocarbons (PAHs) in the Danube River in Hungary," *Sci. Rep.*, vol. 14, no. 1, p. 8318, Apr. 2024, doi: 10.1038/s41598-024-58793-2.

[64] E. UN, "UN-ESCWA and BGR (United Nations Economic and Social Commission for Western Asia; Bundesanstalt für Geowissenschaften und Rohstoffe). Inventory of Shared Water Resources in Western Asia. Beirut." 2013. [Online]. Available: https://waterinventory.org/sites/waterinventory.org/files/chapters/Chapter-03-Tigris_River-Basin-web_0.pdf

[65] T. AL-Saadi, A. Cherepovitsyn, and T. Semenova, "Iraq Oil Industry Infrastructure Development in the Conditions of the Global Economy Turbulence," *Energies*, vol. 15, no. 17, p. 6239, Aug. 2022, doi: 10.3390/en15176239.

[66] U.S. Energy Information Administration, "Background Reference: Iraq," Mar. 2021. [Online]. Available: https://www.eia.gov/international/content/analysis/countries_long/Iraq/iraq_bkgd.pdf

[67] B. UN-ESCWA, "(United Nations Economic and Social Commission for Western Asia; Bundesanstalt für Geowissenschaften und Rohstoffe," Inventory of Shared Water Resources in Western Asia. Beirut., 2013.

[68] G. Mezősi, *The Physical Geography of Hungary*. in Geography of the Physical Environment. Cham: Springer International Publishing, 2017. doi: 10.1007/978-3-319-45183-1.

[69] L. Van, G. Sipos, J. Lábdy, M. Baksa, and Z. Tobak, “River ice monitoring of the Danube and Tisza rivers using Sentinel-1 radar data,” *Geogr. Pannonica*, vol. 26, no. 3, pp. 215–229, 2022, doi: 10.5937/gp26-39962.

[70] ICPDR, “The International Commission for the Protection of the Danube River 2023, Hungary,” Jan. 2024. [Online]. Available: https://www.icpdr.org/danube-basin/countries/hungary

[71] R. A. Grmasha *et al.*, “Polycyclic aromatic hydrocarbons in the surface water and sediment along Euphrates River system: Occurrence, sources, ecological and health risk assessment,” *Mar. Pollut. Bull.*, vol. 187, p. 114568, Feb. 2023, doi: 10.1016/j.marpolbul.2022.114568.

[72] L. Lin *et al.*, “Distribution and sources of polycyclic aromatic hydrocarbons and phthalic acid esters in water and surface sediment from the Three Gorges Reservoir,” *J. Environ. Sci.*, vol. 69, pp. 271–280, Jul. 2018, doi: 10.1016/j.jes.2017.11.004.

[73] R. A. Grmasha *et al.*, “Ecological and human health risk assessment of polycyclic aromatic hydrocarbons (PAH) in Tigris river near the oil refineries in Iraq,” *Environ. Res.*, vol. 227, p. 115791, Jun. 2023, doi: 10.1016/j.envres.2023.115791.

[74] C.-F. Chen *et al.*, “Distribution, sources, and behavior of PAHs in estuarine water systems exemplified by Salt River, Taiwan,” *Mar. Pollut. Bull.*, vol. 154, p. 111029, May 2020, doi: 10.1016/j.marpolbul.2020.111029.

[75] B. Han *et al.*, “Spatial distribution, source analysis, and ecological risk assessment of polycyclic aromatic hydrocarbons (PAHs) in the sediments from rivers emptying into Jiaozhou Bay, China,” *Mar. Pollut. Bull.*, vol. 168, p. 112394, Jul. 2021, doi: 10.1016/j.marpolbul.2021.112394.

[76] L. Dong *et al.*, “PAHs in the surface water and sediments of the middle and lower reaches of the Han River, China: Occurrence, source, and probabilistic risk assessment,” *Process Saf. Environ. Prot.*, vol. 164, pp. 208–218, Aug. 2022, doi: 10.1016/j.psep.2022.06.009.

[77] E. Ternon and I. Tolosa, “Comprehensive analytical methodology to determine hydrocarbons in marine waters using extraction disks coupled to glass fiber filters and compound-specific isotope analyses,” *J. Chromatogr. A*, vol. 1404, pp. 10–20, Jul. 2015, doi: 10.1016/j.chroma.2015.05.029.

[78] R. A. Grmasha *et al.*, “Seasonal variation and concentration of PAHs in Lake Balaton sediment: A study on molecular weight distribution and sources of pollution,” *Mar. Pollut. Bull.*, vol. 202, p. 116333, May 2024, doi: 10.1016/j.marpolbul.2024.116333.

[79] Y. Zhu, Y. Yang, M. Liu, M. Zhang, and J. Wang, “Concentration, Distribution, Source, and Risk Assessment of PAHs and Heavy Metals in Surface Water from the Three Gorges Reservoir, China,” *Hum. Ecol. Risk Assess. Int. J.*, vol. 21, no. 6, pp. 1593–1607, Aug. 2015, doi: 10.1080/10807039.2014.962315.

[80] Y. Wang, C. Shen, Z. Shen, D. Zhang, and J. C. Crittenden, “Spatial variation and sources of polycyclic aromatic hydrocarbons (PAHs) in surface sediments from the Yangtze Estuary, China,” *Environ. Sci. Process. Impacts*, vol. 17, no. 7, pp. 1340–1347, 2015, doi: 10.1039/C5EM00077G.

[81] B. Ambade, S. S. Sethi, S. Kurwadkar, A. Kumar, and T. K. Sankar, “Toxicity and health risk assessment of polycyclic aromatic hydrocarbons in surface water, sediments and groundwater vulnerability in Damodar River Basin,” *Groundw. Sustain. Dev.*, vol. 13, p. 100553, May 2021, doi: 10.1016/j.gsd.2021.100553.

[82] E. R. Long, D. D. Macdonald, S. L. Smith, and F. D. Calder, “Incidence of adverse biological effects within ranges of chemical concentrations in marine and estuarine sediments,” *Environ. Manage.*, vol. 19, no. 1, pp. 81–97, Jan. 1995, doi: 10.1007/BF02472006.

[83] USEPA, *Risk Assessment Guidance for Superfund. Vol. 1: Human Health Evaluation Manual (F, Supplemental Guidance for InhalationRisk Assessment) EPA/540/R/070/002; Office of Superfund Remediation and Technology Innovation*.

[84] USEPA, *US Environmental Protection Agency). Risk Assessment Guidance for Superfund, Vol. 1: Human Health Evaluation ManualEPA/se0/1-89/002; Office of Solid Waste and Emergency Response: Washington, DC, USA, 1989.*

[85] NYS DOH, “New York States Department of Health). Hopewell precision area contamination: Appendix C-NYS DOH. In Procedure for Evaluating Potential Health Risks for Contaminants of Concern; States Department of Health: New York, NY, USA, 2007.” [Online]. Available: http://www.health.ny.gov/environmental/investigations/hopewell/appendc.htm

[86] M. Chen, P. Huang, and L. Chen, “Polycyclic aromatic hydrocarbons in soils from Urumqi, China: distribution, source contributions, and potential health risks,” *Environ. Monit. Assess.*, vol. 185, no. 7, pp. 5639–5651, Jul. 2013, doi: 10.1007/s10661-012-2973-6.

[87] US EPA, *Exposure Factors Handbook. 2011 ed., Final Report. Environmental Protection Agency, Washington, DC EPA/600/R-09/052F.* 2011.

[88] N. Soltani *et al.*, “Ecological and human health hazards of heavy metals and polycyclic aromatic hydrocarbons (PAHs) in road dust of Isfahan metropolis, Iran,” *Sci. Total Environ.*, vol. 505, pp. 712–723, Feb. 2015, doi: 10.1016/j.scitotenv.2014.09.097.

[89] U.S. Environmental Protection Agency, “Human health evaluation manual, supplemental guidance: update of standard default exposure factors. OSWER Directive 9200 1–120.” 2014.

[90] K. Alboukadel, “‘ggpubr:’ggplot2’based publication ready plots.’ R package version (2018): 2.”

[91] T. Wei, “Simko, V. R., Levy, M., Xie, Y., Jin, Y., & Zemla, J. (2021). package ‘corrplot’: Visualization of a Correlation Matrix. 2017. Version 0.84.,” 2017.

[92] M. Marquès *et al.*, “Climate change impact on the PAH photodegradation in soils: Characterization and metabolites identification,” *Environ. Int.*, vol. 89–90, pp. 155–165, Apr. 2016, doi: 10.1016/j.envint.2016.01.019.

[93] C. Teodora Ciucure, E.-I. Geana, C. Lidia Chitescu, S. Laurentiu Badea, and R. Elena Ionete, “Distribution, sources and ecological risk assessment of polycyclic aromatic hydrocarbons in waters and sediments from Olt River dam reservoirs in Romania,” *Chemosphere*, vol. 311, p. 137024, Jan. 2023, doi: 10.1016/j.chemosphere.2022.137024.

[94] A. Visca *et al.*, “Legacy and Emerging Pollutants in an Urban River Stretch and Effects on the Bacterioplankton Community,” *Water*, vol. 13, no. 23, p. 3402, Dec. 2021, doi: 10.3390/w13233402.

[95] A. Nagy, G. Simon, and I. Vass, “Monitoring of Polycyclic Aromatic Hydrocarbons (Pahs) in Surface Water of the Hungarian Upper Section of the Danube River,” *Nova Biotechnol. Chim.*, vol. 11, no. 1, Jan. 2012, doi: 10.2478/v10296-012-0003-2.

[96] A. S. Nagy, J. Szabó, and I. Vass, “Occurrence and distribution of polycyclic aromatic hydrocarbons in surface water and sediments of the Danube River and its tributaries, Hungary,” *J. Environ. Sci. Health Part A*, vol. 49, no. 10, pp. 1134–1141, Aug. 2014, doi: 10.1080/10934529.2014.897155.

[97] A. Szabó Nagy, J. Szabó, and I. Vass, “An Assessment Of Water And Sediment Quality Of The Danube River: Polycyclic Aromatic Hydrocarbons And Trace Metals,” Feb. 2018, doi: 10.5281/ZENODO.1316073.

[98] A. Barra Caracciolo *et al.*, “Chemical mixtures and autochthonous microbial community in an urbanized stretch of the River Danube,” *Microchem. J.*, vol. 147, pp. 985–994, Jun. 2019, doi: 10.1016/j.microc.2019.04.021.

[99] A. S. Nagy, J. Szabó, and I. Vass, “Occurrence and distribution of polycyclic aromatic hydrocarbons in surface water of the Raba River, Hungary,” *J. Environ. Sci. Health Part A*, vol. 48, no. 10, pp. 1190–1200, Aug. 2013, doi: 10.1080/10934529.2013.776455.

[100] F. Liu, Q. Yang, Y. Hu, H. Du, and F. Yuan, “Distribution and transportation of polycyclic aromatic hydrocarbons (PAHs) at the Humen river mouth in the Pearl River delta and their influencing factors,” *Mar. Pollut. Bull.*, vol. 84, no. 1–2, pp. 401–410, Jul. 2014, doi: 10.1016/j.marpolbul.2014.04.045.

[101] P. Montuori, S. Aurino, F. Garzonio, P. Sarnacchiaro, A. Nardone, and M. Triassi, “Distribution, sources and ecological risk assessment of polycyclic aromatic hydrocarbons in water and sediments from Tiber River and estuary, Italy,” *Sci. Total Environ.*, vol. 566–567, pp. 1254–1267, Oct. 2016, doi: 10.1016/j.scitotenv.2016.05.183.

[102] M. Qiao, L. Fu, Z. Li, D. Liu, Y. Bai, and X. Zhao, “Distribution and ecological risk of substituted and parent polycyclic aromatic hydrocarbons in surface waters of the Bai, Chao, and Chaobai rivers in northern China,” *Environ. Pollut.*, vol. 257, p. 113600, Feb. 2020, doi: 10.1016/j.envpol.2019.113600.

[103] Y. Chen, C. Sun, J. Zhang, and F. Zhang, “Assessing 16 Polycyclic Aromatic Hydrocarbons(PAHs) in River Basin Water and SedimentRegarding Spatial-Temporal Distribution,Partitioning, and Ecological Risks,” *Pol. J. Environ. Stud.*, vol. 27, no. 2, pp. 579–589, Jan. 2018, doi: 10.15244/pjoes/75827.

[104] B. Barhoumi *et al.*, “Occurrence, distribution and ecological risk of trace metals and organic pollutants in surface sediments from a Southeastern European river (Someşu Mic River, Romania),” *Sci. Total Environ.*, vol. 660, pp. 660–676, Apr. 2019, doi: 10.1016/j.scitotenv.2018.12.428.

[105] F. Wang *et al.*, “Spatial and vertical distribution, composition profiles, sources, and ecological risk assessment of polycyclic aromatic hydrocarbon residues in the sediments of an urban tributary: A case study of the Songgang River, Shenzhen, China,” *Environ. Pollut.*, vol. 266, p. 115360, Nov. 2020, doi: 10.1016/j.envpol.2020.115360.

[106] R. Sarria-Villa, W. Ocampo-Duque, M. Páez, and M. Schuhmacher, “Presence of PAHs in water and sediments of the Colombian Cauca River during heavy rain episodes, and implications for risk assessment,” *Sci. Total Environ.*, vol. 540, pp. 455–465, Jan. 2016, doi: 10.1016/j.scitotenv.2015.07.020.

[107] Y. Sheng *et al.*, "The partitioning behavior of PAHs between settled dust and its extracted water phase: Coefficients and effects of the fluorescent organic matter," *Ecotoxicol. Environ. Saf.*, vol. 223, p. 112573, Oct. 2021, doi: 10.1016/j.ecoenv.2021.112573.

[108] Y. Dong, Z. Yan, H. Wu, G. Zhang, H. Zhang, and M. Yang, "Polycyclic Aromatic Hydrocarbons in Sediments from Typical Algae, Macrophyte Lake Bay and Adjoining River of Taihu Lake, China: Distribution, Sources, and Risk Assessment," *Water*, vol. 13, no. 4, p. 470, Feb. 2021, doi: 10.3390/w13040470.

[109] J. Salmela, S. Saarni, L. Blåfield, M. Katainen, E. Kasvi, and P. Alho, "Comparison of cold season sedimentation dynamics in the non-tidal estuary of the Northern Baltic Sea," *Mar. Geol.*, vol. 443, p. 106701, Jan. 2022, doi: 10.1016/j.margeo.2021.106701.

[110] J. Beyer, A. Goksøyr, D. Ø. Hjermann, and J. Klungsøyr, "Environmental effects of offshore produced water discharges: A review focused on the Norwegian continental shelf," *Mar. Environ. Res.*, vol. 162, p. 105155, Dec. 2020, doi: 10.1016/j.marenvres.2020.105155.

[111] S. Mukhopadhyay, R. Dutta, and P. Das, "A critical review on plant biomonitors for determination of polycyclic aromatic hydrocarbons (PAHs) in air through solvent extraction techniques," *Chemosphere*, vol. 251, p. 126441, Jul. 2020, doi: 10.1016/j.chemosphere.2020.126441.

[112] D. M. González-Pérez, G. Garralón, F. Plaza, J. I. Pérez, B. Moreno, and M. A. Gómez, "Removal of low concentrations of phenanthrene, fluoranthene and pyrene from urban wastewater by membrane bioreactors technology," *J. Environ. Sci. Health Part A*, vol. 47, no. 14, pp. 2190–2197, Dec. 2012, doi: 10.1080/10934529.2012.707496.

[113] X. Zhang *et al.*, "The fate and enhanced removal of polycyclic aromatic hydrocarbons in wastewater and sludge treatment system: A review," *Crit. Rev. Environ. Sci. Technol.*, vol. 49, no. 16, pp. 1425–1475, Aug. 2019, doi: 10.1080/10643389.2019.1579619.

[114] Q. Liu, X. Xu, L. Lin, and D. Wang, "Occurrence, distribution and ecological risk assessment of polycyclic aromatic hydrocarbons and their derivatives in the effluents of wastewater treatment plants," *Sci. Total Environ.*, vol. 789, p. 147911, Oct. 2021, doi: 10.1016/j.scitotenv.2021.147911.

[115] F. Kafilzadeh, "Distribution and sources of polycyclic aromatic hydrocarbons in water and sediments of the Soltan Abad River, Iran," *Egypt. J. Aquat. Res.*, vol. 41, no. 3, pp. 227–231, 2015, doi: 10.1016/j.ejar.2015.06.004.

[116] I. Tongo, L. Ezemonye, and K. Akpeh, “Levels, distribution and characterization of Polycyclic Aromatic Hydrocarbons (PAHs) in Ovia river, Southern Nigeria,” *J. Environ. Chem. Eng.*, vol. 5, no. 1, pp. 504–512, Feb. 2017, doi: 10.1016/j.jece.2016.12.035.

[117] S. Liu *et al.*, “Levels, sources and risk assessment of PAHs in multi-phases from urbanized river network system in Shanghai,” *Environ. Pollut.*, vol. 219, pp. 555–567, Dec. 2016, doi: 10.1016/j.envpol.2016.06.010.

[118] A. Motelay-Massei, D. Ollivon, B. Garban, M. J. Teil, M. Blanchard, and M. Chevreuil, “Distribution and spatial trends of PAHs and PCBs in soils in the Seine River basin, France,” *Chemosphere*, vol. 55, no. 4, pp. 555–565, Apr. 2004, doi: 10.1016/j.chemosphere.2003.11.054.

[119] J. C. Otte *et al.*, “Contribution of Priority PAHs and POPs to Ah Receptor-Mediated Activities in Sediment Samples from the River Elbe Estuary, Germany,” *PLoS ONE*, vol. 8, no. 10, p. e75596, Oct. 2013, doi: 10.1371/journal.pone.0075596.

[120] F. Di Duca, P. Montuori, U. Trama, A. Masucci, G. Borrelli, and M. Triassi, “Health Risk Assessment of PAHs from Estuarine Sediments in the South of Italy,” *Toxics*, vol. 11, no. 2, p. 172, Feb. 2023, doi: 10.3390/toxics11020172.

[121] N. Yavar Ashayeri, B. Keshavarzi, F. Moore, M. Kersten, M. Yazdi, and A. R. Lahijanzadeh, “Presence of polycyclic aromatic hydrocarbons in sediments and surface water from Shadegan wetland – Iran: A focus on source apportionment, human and ecological risk assessment and Sediment-Water Exchange,” *Ecotoxicol. Environ. Saf.*, vol. 148, pp. 1054–1066, Feb. 2018, doi: 10.1016/j.ecoenv.2017.11.055.

[122] G. O. Duodu, K. N. Ogogo, S. Mummullage, F. Harden, A. Goonetilleke, and G. A. Ayoko, “Source apportionment and risk assessment of PAHs in Brisbane River sediment, Australia,” *Ecol. Indic.*, vol. 73, pp. 784–799, Feb. 2017, doi: 10.1016/j.ecolind.2016.10.038.

[123] J.-H. Sun, G.-L. Wang, Y. Chai, G. Zhang, J. Li, and J. Feng, “Distribution of polycyclic aromatic hydrocarbons (PAHs) in Henan Reach of the Yellow River, Middle China,” *Ecotoxicol. Environ. Saf.*, vol. 72, no. 5, pp. 1614–1624, Jul. 2009, doi: 10.1016/j.ecoenv.2008.05.010.

[124] B. Zheng, L. Wang, K. Lei, and B. Nan, “Distribution and ecological risk assessment of polycyclic aromatic hydrocarbons in water, suspended particulate matter and sediment from Daliao River estuary and the adjacent area, China,” *Chemosphere*, vol. 149, pp. 91–100, Apr. 2016, doi: 10.1016/j.chemosphere.2016.01.039.

[125] M. Keshavarzifard *et al.*, "Polycyclic Aromatic Hydrocarbons (PAHs) in Sediments from Prai and Malacca Rivers, Peninsular Malaysia," in *From Sources to Solution*, A. Z. Aris, T. H. Tengku Ismail, R. Harun, A. M. Abdullah, and M. Y. Ishak, Eds., Singapore: Springer Singapore, 2014, pp. 415–420. doi: 10.1007/978-981-4560-70-2_75.

[126] W. A.-M. Omar and H. M. Mahmoud, "Risk assessment of polycyclic aromatic hydrocarbons (PAHs) in River Nile up- and downstream of a densely populated area," *J. Environ. Sci. Health Part A*, vol. 52, no. 2, pp. 166–173, Jan. 2017, doi: 10.1080/10934529.2016.1240488.

[127] Z. Li, W. Zhang, and B. Shan, "Effects of organic matter on polycyclic aromatic hydrocarbons in riverine sediments affected by human activities," *Sci. Total Environ.*, vol. 815, p. 152570, Apr. 2022, doi: 10.1016/j.scitotenv.2021.152570.

[128] N. R. Ekere, N. M. Yakubu, T. Oparanozie, and J. N. Ihedioha, "Levels and risk assessment of polycyclic aromatic hydrocarbons in water and fish of Rivers Niger and Benue confluence Lokoja, Nigeria," *J. Environ. Health Sci. Eng.*, vol. 17, no. 1, pp. 383–392, Jun. 2019, doi: 10.1007/s40201-019-00356-z.

[129] W. Yu, R. Liu, F. Xu, and Z. Shen, "Environmental risk assessments and spatial variations of polycyclic aromatic hydrocarbons in surface sediments in Yangtze River Estuary, China," *Mar. Pollut. Bull.*, vol. 100, no. 1, pp. 507–515, Nov. 2015, doi: 10.1016/j.marpolbul.2015.09.004.

[130] A. O. Adeniji, O. O. Okoh, and A. I. Okoh, "Levels of Polycyclic Aromatic Hydrocarbons in the Water and Sediment of Buffalo River Estuary, South Africa and Their Health Risk Assessment," *Arch. Environ. Contam. Toxicol.*, vol. 76, no. 4, pp. 657–669, May 2019, doi: 10.1007/s00244-019-00617-w.

[131] B. Han *et al.*, "Characterization of PM10 fraction of road dust for polycyclic aromatic hydrocarbons (PAHs) from Anshan, China," *J. Hazard. Mater.*, vol. 170, no. 2–3, pp. 934–940, Oct. 2009, doi: 10.1016/j.jhazmat.2009.05.059.

[132] M. C. Kennicutt, T. L. Wade, B. J. Presley, A. G. Requejo, J. M. Brooks, and G. J. Denoux, "Sediment contaminants in Casco Bay, Maine: inventories, sources, and potential for biological impact," *Environ. Sci. Technol.*, vol. 28, no. 1, pp. 1–15, Jan. 1994, doi: 10.1021/es00050a003.

[133] A. Ramzi, K. Habeeb Rahman, T. R. Gireeshkumar, K. K. Balachandran, C. Jacob, and N. Chandramohanakumar, "Dynamics of polycyclic aromatic hydrocarbons (PAHs) in surface

sediments of Cochin estuary, India," *Mar. Pollut. Bull.*, vol. 114, no. 2, pp. 1081–1087, Jan. 2017, doi: 10.1016/j.marpolbul.2016.10.015.

[134] L. Traven, "Sources, trends and ecotoxicological risks of PAH pollution in surface sediments from the northern Adriatic Sea (Croatia)," *Mar. Pollut. Bull.*, vol. 77, no. 1–2, pp. 445–450, Dec. 2013, doi: 10.1016/j.marpolbul.2013.08.043.

[135] M. B. Yunker, R. W. Macdonald, R. Vingarzan, R. H. Mitchell, D. Goyette, and S. Sylvestre, "PAHs in the Fraser River basin: a critical appraisal of PAH ratios as indicators of PAH source and composition," *Org. Geochem.*, vol. 33, no. 4, pp. 489–515, Apr. 2002, doi: 10.1016/S0146-6380(02)00002-5.

[136] C.-C. Lee, C. S. Chen, Z.-X. Wang, and C.-J. Tien, "Polycyclic aromatic hydrocarbons in 30 river ecosystems, Taiwan: Sources, and ecological and human health risks," *Sci. Total Environ.*, vol. 795, p. 148867, Nov. 2021, doi: 10.1016/j.scitotenv.2021.148867.

[137] J. F. Ontiveros-Cuadras *et al.*, "Recent history of persistent organic pollutants (PAHs, PCBs, PBDEs) in sediments from a large tropical lake," *J. Hazard. Mater.*, vol. 368, pp. 264–273, Apr. 2019, doi: 10.1016/j.jhazmat.2018.11.010.

[138] H. H. Soclo, P. Garrigues, and M. Ewald, "Origin of Polycyclic Aromatic Hydrocarbons (PAHs) in Coastal Marine Sediments: Case Studies in Cotonou (Benin) and Aquitaine (France) Areas," *Mar. Pollut. Bull.*, vol. 40, no. 5, pp. 387–396, May 2000, doi: 10.1016/S0025-326X(99)00200-3.

[139] G. Gbeddy, P. Egodawatta, A. Goonetilleke, E. Akortia, and E. T. Glover, "Influence of photolysis on source characterization and health risk of polycyclic aromatic hydrocarbons (PAHs), and carbonyl-, nitro-, hydroxy- PAHs in urban road dust," *Environ. Pollut.*, vol. 269, p. 116103, Jan. 2021, doi: 10.1016/j.envpol.2020.116103.

[140] A. L. C. Lima, J. W. Farrington, and C. M. Reddy, "Combustion-Derived Polycyclic Aromatic Hydrocarbons in the Environment—A Review," *Environ. Forensics*, vol. 6, no. 2, pp. 109–131, Jun. 2005, doi: 10.1080/15275920590952739.

[141] S. Kurwadkar, S. S. Sethi, P. Mishra, and B. Ambade, "Unregulated discharge of wastewater in the Mahanadi River Basin: Risk evaluation due to occurrence of polycyclic aromatic hydrocarbon in surface water and sediments," *Mar. Pollut. Bull.*, vol. 179, p. 113686, Jun. 2022, doi: 10.1016/j.marpolbul.2022.113686.

[142] USEPA, *Risk Assessment Guidance for Superfund, Vol. 1: Human Health Evaluation Manual EPA/se0/1-89/002; Office of Solid Waste and Emergency Response: Washington, DC, USA*, 1989.

[143] L. Wang *et al.*, "Polycyclic Aromatic Hydrocarbons in Urban Soil in the Semi-arid City of Xi'an, Northwest China: Composition, Distribution, Sources, and Relationships with Soil Properties," *Arch. Environ. Contam. Toxicol.*, vol. 75, no. 3, pp. 351–366, Oct. 2018, doi: 10.1007/s00244-018-0522-1.

[144] O. C. Ihunwo, M. U. Ibezim-Ezeani, and T. A. DelValls, "Human health and ecological risk of polycyclic aromatic hydrocarbons (PAHs) in sediment of Woji creek in the Niger Delta region of Nigeria," *Mar. Pollut. Bull.*, vol. 162, p. 111903, Jan. 2021, doi: 10.1016/j.marpolbul.2020.111903.

[145] X. Miao, Y. Hao, J. Cai, Y. Xie, and J. Zhang, "The distribution, sources and health risk of polycyclic aromatic hydrocarbons (PAHs) in sediments of Liujiang River Basin: A field study in typical karstic river," *Mar. Pollut. Bull.*, vol. 188, p. 114666, Mar. 2023, doi: 10.1016/j.marpolbul.2023.114666.

[146] R. Namdar, E. Karami, and M. Keshavarz, "Climate Change and Vulnerability: The Case of MENA Countries," *ISPRS Int. J. Geo-Inf.*, vol. 10, no. 11, p. 794, Nov. 2021, doi: 10.3390/ijgi10110794.

[147] A. Moridnejad, N. Karimi, and P. A. Ariya, "Newly desertified regions in Iraq and its surrounding areas: Significant novel sources of global dust particles," *J. Arid Environ.*, vol. 116, pp. 1–10, May 2015, doi: 10.1016/j.jaridenv.2015.01.008.

[148] Al Bomola, A, "Temporal and spatial changes in water quality of the Euphrates river-Iraq." TVVR11/5013., 2011.

[149] L. Wang, Z. Yang, J. Niu, and J. Wang, "Characterization, ecological risk assessment and source diagnostics of polycyclic aromatic hydrocarbons in water column of the Yellow River Delta, one of the most plenty biodiversity zones in the world," *J. Hazard. Mater.*, vol. 169, no. 1–3, pp. 460–465, Sep. 2009, doi: 10.1016/j.jhazmat.2009.03.125.

[150] F. Aziz *et al.*, "Occurrence of polycyclic aromatic hydrocarbons in the Soan River, Pakistan: Insights into distribution, composition, sources and ecological risk assessment," *Ecotoxicol. Environ. Saf.*, vol. 109, pp. 77–84, Nov. 2014, doi: 10.1016/j.ecoenv.2014.07.022.

[151] H. Zaghden *et al.*, "Occurrence, origin and potential ecological risk of dissolved polycyclic aromatic hydrocarbons and organochlorines in surface waters of the Gulf of Gabès (Tunisia,

Southern Mediterranean Sea)," *Mar. Pollut. Bull.*, vol. 180, p. 113737, Jul. 2022, doi: 10.1016/j.marpolbul.2022.113737.

[152] N. Mzoughi and L. Chouba, "Distribution and partitioning of aliphatic hydrocarbons and polycyclic aromatic hydrocarbons between water, suspended particulate matter, and sediment in harbours of the West coastal of the Gulf of Tunis (Tunisia)," *J. Environ. Monit.*, vol. 13, no. 3, p. 689, 2011, doi: 10.1039/c0em00616e.

[153] F. M. Hassan, A. H. M. J. Alobaidy, J. M. Salman, and S. H. Abdulameer, "Distribution of Polycyclic Aromatic Hydrocarbons in Water and Sediments in the Euphrates River, Iraq," *Iraqi J. Sci.*, pp. 2572–2582, Dec. 2019, doi: 10.24996/ijs.2019.60.12.5.

[154] A. N. Ekanem, V. N. Osabor, and B. O. Ekpo, "Polycyclic aromatic hydrocarbons (PAHs) contamination of soils and water around automobile repair workshops in Eket metropolis, Akwa Ibom State, Nigeria," *SN Appl. Sci.*, vol. 1, no. 5, p. 447, May 2019, doi: 10.1007/s42452-019-0397-4.

[155] WHO, "Polynuclear aromatic hydrocarbons. In: Guidelines for Drinking-Water Quality, 2nd editionAddendum to Vol.2 Health Criteria and Other SupportingInformation." World Health Organization, Geneva, pp. 123–152., 1998.

[156] H. Yu *et al.*, "Polycyclic aromatic hydrocarbons in surface waters from the seven main river basins of China: Spatial distribution, source apportionment, and potential risk assessment," *Sci. Total Environ.*, vol. 752, p. 141764, Jan. 2021, doi: 10.1016/j.scitotenv.2020.141764.

[157] Health Canada F. P. T. C. o. D. W. o. t. F. P. T. C. o. H. a. t. E, "Guidelines for Canadian drinking water quality summary table: water and air quality bureau, healthy environments and consumer safety branch, Health Canada, Ottawa, Ontario." 2019. [Online]. Available: https://www.canada.ca/en/health-canada/services/environmental-workplace-health/reports-publications/water-quality.html

[158] WHO, "Chapter 5.9, Polycyclic aromatic hydrocarbons (PAHs)." 2000. [Online]. Available: https://www.euro.who.int/__data/assets/pdf_file/0015/123063/AQG2ndEd_5_9PAH.pdf

[159] P. Lei, K. Pan, H. Zhang, and J. Bi, "Pollution and Risk of PAHs in Surface Sediments from the Tributaries and Their Relation to Anthropogenic Activities, in the Main Urban Districts of Chongqing City, Southwest China," *Bull. Environ. Contam. Toxicol.*, vol. 103, no. 1, pp. 28–33, Jul. 2019, doi: 10.1007/s00128-018-2411-8.

[160] H. Chen, Y. Teng, and J. Wang, “Source apportionment of polycyclic aromatic hydrocarbons (PAHs) in surface sediments of the Rizhao coastal area (China) using diagnostic ratios and factor analysis with nonnegative constraints,” *Sci. Total Environ.*, vol. 414, pp. 293–300, Jan. 2012, doi: 10.1016/j.scitotenv.2011.10.057.

[161] B. Barhoumi *et al.*, “Polycyclic aromatic hydrocarbons (PAHs) in surface sediments from the Bizerte Lagoon, Tunisia: levels, sources, and toxicological significance,” *Environ. Monit. Assess.*, vol. 186, no. 5, pp. 2653–2669, May 2014, doi: 10.1007/s10661-013-3569-5.

[162] W. B. Ameur, S. Trabelsi, and M. R. Driss, “Polycyclic Aromatic Hydrocarbons in Superficial Sediments from Ghar El Melh Lagoon, Tunisia,” *Bull. Environ. Contam. Toxicol.*, vol. 85, no. 2, pp. 184–189, Aug. 2010, doi: 10.1007/s00128-010-0044-7.

[163] A. B. Mohammed Al-Taee, M. M. and Hassan, F. M. ,., “The study of some PAH compounds in Euphrates River sediment from Al-Hindiya Barrageto Al-Kifil city, Iraq.” . In Scientific Conference, College of 4th Science, Babylon University. CSASC English Ver (Vol. 4, p. 216).

[164] M. Evans *et al.*, “PAH distributions in sediments in the oil sands monitoring area and western Lake Athabasca: Concentration, composition and diagnostic ratios,” *Environ. Pollut.*, vol. 213, pp. 671–687, Jun. 2016, doi: 10.1016/j.envpol.2016.03.014.

[165] J. Zhang, G. Liu, R. Wang, and H. Huang, “Polycyclic aromatic hydrocarbons in the water-SPM-sediment system from the middle reaches of Huai River, China: Distribution, partitioning, origin tracing and ecological risk assessment,” *Environ. Pollut.*, vol. 230, pp. 61–71, Nov. 2017, doi: 10.1016/j.envpol.2017.06.012.

[166] Md. Habibullah-Al-Mamun, Md. Kawser Ahmed, A. Hossain, and S. Masunaga, “Distribution, Source Apportionment, and Risk Assessment of Polycyclic Aromatic Hydrocarbons (PAHs) in the Surficial Sediments from the Coastal Areas of Bangladesh,” *Arch. Environ. Contam. Toxicol.*, vol. 76, no. 2, pp. 178–190, Feb. 2019, doi: 10.1007/s00244-018-0571-5.

[167] R. Doong and Y. Lin, “Characterization and distribution of polycyclic aromatic hydrocarbon contaminations in surface sediment and water from Gao-ping River, Taiwan,” *Water Res.*, vol. 38, no. 7, pp. 1733–1744, Apr. 2004, doi: 10.1016/j.watres.2003.12.042.

[168] J. Li, X. Shang, Z. Zhao, R. L. Tanguay, Q. Dong, and C. Huang, “Polycyclic aromatic hydrocarbons in water, sediment, soil, and plants of the Aojiang River waterway in Wenzhou,

China," *J. Hazard. Mater.*, vol. 173, no. 1–3, pp. 75–81, Jan. 2010, doi: 10.1016/j.jhazmat.2009.08.050.

[169] Y.-F. Jiang *et al.*, "Levels, composition profiles and sources of polycyclic aromatic hydrocarbons in urban soil of Shanghai, China," *Chemosphere*, vol. 75, no. 8, pp. 1112–1118, May 2009, doi: 10.1016/j.chemosphere.2009.01.027.

[170] Y. Liu, L. Chen, Q. Huang, W. Li, Y. Tang, and J. Zhao, "Source apportionment of polycyclic aromatic hydrocarbons (PAHs) in surface sediments of the Huangpu River, Shanghai, China," *Sci. Total Environ.*, vol. 407, no. 8, pp. 2931–2938, Apr. 2009, doi: 10.1016/j.scitotenv.2008.12.046.

[171] S. B. Tavakoly Sany, R. Hashim, A. Salleh, M. Rezayi, A. Mehdinia, and O. Safari, "Polycyclic Aromatic Hydrocarbons in Coastal Sediment of Klang Strait, Malaysia: Distribution Pattern, Risk Assessment and Sources," *PLoS ONE*, vol. 9, no. 4, p. e94907, Apr. 2014, doi: 10.1371/journal.pone.0094907.

[172] V. Kapsimalis *et al.*, "Organic contamination of surface sediments in the metropolitan coastal zone of Athens, Greece: Sources, degree, and ecological risk," *Mar. Pollut. Bull.*, vol. 80, no. 1–2, pp. 312–324, Mar. 2014, doi: 10.1016/j.marpolbul.2013.12.051.

[173] A. R. Mostafa, T. L. Wade, S. T. Sweet, A. K. A. Al-Alimi, and A. O. Barakat, "Distribution and characteristics of polycyclic aromatic hydrocarbons (PAHs) in sediments of Hadhramout coastal area, Gulf of Aden, Yemen," *J. Mar. Syst.*, vol. 78, no. 1, pp. 1–8, Aug. 2009, doi: 10.1016/j.jmarsys.2009.02.002.

[174] P. Schubert, M. M. Schantz, L. C. Sander, and S. A. Wise, "Determination of Polycyclic Aromatic Hydrocarbons with Molecular Weight 300 and 302 in Environmental-Matrix Standard Reference Materials by Gas Chromatography/Mass Spectrometry," *Anal. Chem.*, vol. 75, no. 2, pp. 234–246, Jan. 2003, doi: 10.1021/ac0259111.

[175] J. Sauvain and T. Vu Duc, "Approaches to identifying and quantifying polycyclic aromatic hydrocarbons of molecular weight 302 in diesel particulates," *J. Sep. Sci.*, vol. 27, no. 1–2, pp. 78–88, Jan. 2004, doi: 10.1002/jssc.200301620.

[176] X. L. Zhang, S. Tao, W. X. Liu, Y. Yang, Q. Zuo, and S. Z. Liu, "Source Diagnostics of Polycyclic Aromatic Hydrocarbons Based on Species Ratios: A Multimedia Approach," *Environ. Sci. Technol.*, vol. 39, no. 23, pp. 9109–9114, Dec. 2005, doi: 10.1021/es0513741.

[177] M. S. Alam and R. M. Harrison, "Recent advances in the application of 2-dimensional gas chromatography with soft and hard ionisation time-of-flight mass spectrometry in

environmental analysis," *Chem. Sci.*, vol. 7, no. 7, pp. 3968–3977, 2016, doi: 10.1039/C6SC00465B.

[178] K. Kaufmann *et al.*, "Crystal symmetry determination in electron diffraction using machine learning," *Science*, vol. 367, no. 6477, pp. 564–568, Jan. 2020, doi: 10.1126/science.aay3062.

[179] E. Solon *et al.*, "Imaging Mass Spectrometry (IMS) for drug discovery and development survey: Results on methods, applications and regulatory compliance," *Drug Metab. Pharmacokinet.*, vol. 43, p. 100438, Apr. 2022, doi: 10.1016/j.dmpk.2021.100438.

[180] N. Ogrinc *et al.*, "Robot-Assisted SpiderMass for *In Vivo* Real-Time Topography Mass Spectrometry Imaging," *Anal. Chem.*, vol. 93, no. 43, pp. 14383–14391, Nov. 2021, doi: 10.1021/acs.analchem.1c01692.

[181] A. Baran *et al.*, "Distribution of polycyclic aromatic hydrocarbons (PAHs) in the bottom sediments of a dam reservoir, their interaction with organic matter and risk to benthic fauna," *J. Soils Sediments*, vol. 21, no. 6, pp. 2418–2431, Jun. 2021, doi: 10.1007/s11368-021-02968-1.

Appendix 1 Danube sampling coordinates

Sites	Latitude (N)	Longitude (E)
S1	47.788016	19.114344
S2	47.680858	19.125760
S3	47.523438	19.049630
S4	47.248683	18.910842
S5	46.912084	18.964844
S6	46.616233	18.858203

Appendix *2* Tigris Site's locations

Site*	Latitudes (N)	Longitudes (E)	Oil refinery
S1	36.494376	42.755748	Al-Kasak
S2	35.788080	43.292380	Qayyarah
S3	35.784016	43.287928	Qayyarah
S4	35.655453	44.058611	Kirkuk
S5	34.901388	43.499173	Al-siniyah
S6	35.050725	43.555699	Baiji (Before)
S7	34.937740	43.511217	Baiji (After)
S8	33.274830	44.400752	Daura Refineries (Before)
S9	33.284691	44.421569	Daura Refineries (After)
S10	31.845809	47.399335	Maysan
S11	30.489322	47.737841	South Refineries Company (Before)
S12	30.463533	47.749310	South Refineries Company (After)

*The sites were chosen with the closest possible point to the oil refineries (some of them are far from the oil refinery).

Appendix 3 Euphrates Sampling sites latitudes and longitude

Euphrates Sampling sites latitudes and longitude

No	Name	Latitude (N)	Longitude (E)
1	Haditha (related to Al-Anbar)	34.120401	42.387498
2	Hit (Al-Anbar)	33.6572154	42.813924
3	Ramadi (capital of Al Anbar Governorate)	33.462656	43.254828
4	Al-Fallujah (Al-Anbar)	33.346458	43.715164
5	Jorf Al-Sakhar (related to Babylon)	32.884892	44.204238
6	Musayyib (related to Babylon)	32.784594	44.290283
7	Hindiyah	32.537369	44.229300
8	Kefel (related to Babylon)	32.235363	44.361694
9	Najaf	31.916232	44.491813
10	Al-Qadisiyyah	31.711897	44.484604
11	Samawah	31.323116	45.279991
12	Nasiriyah	31.044193	46.241727
13	Basrah	30.951577	47.147543

- Note: The city or province names are taken from Google maps directly. It can be varied in different research, but overall, the names should at least match the written names here.

Appendix 4 Recoveries of the PAHs compounds and surrogate recoveries (%) for the analyzed PAHs in Euphrates River

PAHs	**Recoveries (%) Water**	**Recoveries (%) Sediment**	**Selected deuterated surrogate**	**Surrogate Recovery (%) Water**	**Surrogate Recovery (%) Sediment**
Nap	93.74 ± 2.70	81.40 ± 1.20	naphthalene-d_8	94.61 ± 3.73	85.40 ± 4.13
Acy	92.94 ± 0.68	94.14 ± 2.08	anthracene-d_{10}	92.60 ± 3.83	85.38 ± 4.14
Ace	96.31 ± 3.40	84.43 ± 3.98		94.62 ± 3.14	85.39± 4.13
Fl	90.40 ± 0.10	93.55 ± 4.01		94.62 ± 3.14	85.38 ± 4.12
Phe	95.94 ± 4.69	90.83 ± 5.29		94.62 ± 3.15	85.39 ± 4.13
Ant	96.74 ± 4.94	87.04 ± 5.24		94.62 ± 3.14	85.39 ± 4.13
Flu	93.45 ± 3.39	89.25 ± 0.79	fluoranthene-d_{10}	96.83 ± 3.28	91.66 ± 5.11
Pyr	96.14 ± 0.96	84.19 ± 3.46		95.82 ± 3.31	91.66 ± 5.30
BaA	91.33 ± 1.78	93.29 ± 2.41		96.82 ± 3.27	91.65 ± 5.28
Chr	94.34 ± 3.15	90.88 ± 3.82		96.83 ± 3.28	91.66 ± 5.29
BbF	97.67 ± 3.27	94.57 ± 2.29	perylene-d_{12}	98.79 ± 2.16	95.30 ± 3.30
BkF	97.14± 3.25	85.91± 4.11		98.82 ± 2.15	95.29 ± 2.28
BaP	92.28 ± 4.23	89.78 ± 3.03		99.84 ± 2.17	95.30 ± 2.27
DBA	93.73 ± 0.31	88.70 ± 2.31		101.81 ± 2.16	95.29 ± 3.30
BghiP	96.78 ± 4.12	97.60 ± 0.12		98.81 ± 2.16	94.29 ± 3.16
IND	100.00 ± 0.40	94.22 ± 1.40		106.80 ±3.16	95.29 ±3.30

Appendix 5 Sources diagnostic ratios of PAHs in water Explanation of PAHs diagnostic ratios

.

Ratio	Range	Source	Calculated Ratios	References
LMW/HMW	>1	Petrogenic inputs (liquid fuel discharges)	Winter = 2.26 > 1 Spring = 1.70 > 1 Summer = 0.48 < 1 autumn= 1.60 >1	[181]
	<1	Pyrogenic - Combustion of solid fuel - natural sources such as biomass (grass and wood) and coal		
Flu/(Flu+Pyr)	<0.4	Petrogenic inputs (liquid fuel discharges)	Winter = 0.42 (0.4-0.5) Spring = 0.49 (0.4-0.5) Summer = 0.36 < 0.4 Autumn = 0.45 (0.4-0.5)	[124]
	0.4-0.5	Pyrolytic (burning of liquid fossil fuels and crude oil. vehicles)		
	>0.5	Pyrogenic - Combustion of solid fuel - natural sources such as biomass (grass and wood) and coal		
IND/(IND+BghiP)	<0.2	Petrogenic inputs (liquid fuel discharges)	Winter = 0.48 (0.2-0.5) Spring = 0.58 > 0.5 Summer = 0.35 (0.2-0.5) Autumn = 0.41 (0.2-0.5)	[135], [181]
	0.2-0.5	Pyrolytic (burning of liquid fossil fuels and crude oil. vehicles)		
	>0.5	Pyrogenic - Combustion of solid fuel - natural sources such as biomass (grass and wood) and coal		
BaA/(BaA+Chr)	<0.2	Petrogenic inputs (liquid fuel discharges)	Winter = 0.37 > 0.35 Spring = 0.45 > 0.35	[130], [181]
		Mixed sources (petrogenic / pyrogenic)		

	0.2-0.35		Summer = 0.44 > 0.35 Autumn = 0.48 > 0.35	
	>0.35	Pyrogenic - Combustion of solid fuel - natural sources such as biomass (grass and wood) and coal		
BaP/(BaP+Chr)	<0.4	Petrogenic inputs (liquid fuel discharges)	Winter = 0.35 < 0.4 Spring = 0.49 > 0.4 Summer = 0.62 > 0.4 Autumn = 0.55 > 0.4	[135]
	>0.4	Pyrogenic - Combustion of solid fuel - natural sources such as biomass (grass and wood) and coal		
BaP/BghiP	>0.6	Petrogenic inputs (liquid fuel discharges)	Winter = 0.95 > 0.6 Spring = 0.78 > 0.6 Summer = 0.68 > 0.6 Autumn = 1.19 >0.6	[104]
	<0.6 (non-traffic emission)	Pyrogenic - Combustion of solid fuel - natural sources such as biomass (grass and wood) and coal		

Appendix 6 Sources diagnostic ratios of PAHs in sediments Explanation of PAHs diagnostic ratios

Ratio	Range	Source	Calculated Ratios	References
LMW/HMW	>1	Petrogenic inputs (liquid fuel discharges)	Winter = 0.34 < 1 Spring = 0.43 < 1 Summer = 0.39 < 1 autumn= 0.39 < 1	[181]
	<1	Pyrogenic - Combustion of solid fuel - natural sources such as biomass (grass and wood) and coal		
Flu/(Flu+Pyr)	<0.4	Petrogenic inputs (liquid fuel discharges)	Winter = 0.32 < 0.4 Spring = 0.37 < 0.4 Summer =0.43 (0.4-0.5) Autumn = 0.54 > 0.5	[129]
	0.4-0.5	Pyrolytic (burning of liquid fossil fuels and crude oil. vehicles)		
	> 0.5	Pyrogenic - Combustion of solid fuel - natural sources such as biomass (grass and wood) and coal		
IND/(IND+BghiP)	<0.2	Petrogenic inputs (liquid fuel discharges)	Winter = 0.53 > 0.5 Spring = 0.37 (0.2-0.5) Summer = 0.51 > 0.5 Autumn = 0.57 > 0.5	[129]
	0.2-0.5	Pyrolytic (burning of liquid fossil fuels and crude oil. vehicles)		
	>0.5	Pyrogenic - Combustion of solid fuel - natural sources such as biomass (grass and wood) and coal		
BaA/(BaA+Chr)	<0.2	Petrogenic inputs (liquid fuel discharges)	Winter = 0.39 > 0.35 Spring = 0.51 > 0.35	[135], [181]
		Mixed sources (petrogenic / pyrogenic)		

	0.2-0.35		Summer=0.28 (0.2-0.35) Autumn = 0.55 > 0.35	
	>0.35	Pyrogenic - Combustion of solid fuel - natural sources such as biomass (grass and wood) and coal		
BaP/(BaP+Chr)	<0.4	Petrogenic inputs (liquid fuel discharges)	Winter = 0.39 < 0.4 Spring = 0.68 > 0.4 Summer = 0.52 > 0.4 Autumn = 0.70 > 0.4	[135]
	>0.4	Pyrogenic - Combustion of solid fuel - natural sources such as biomass (grass and wood) and coal		
BaP/BghiP	> 0.6	Petrogenic inputs (liquid fuel discharges)	Winter = 1.70 > 0.6 Spring = 1.1 > 0.6 Summer = 2.45 > 0.6 Autumn = 5.10 > 0.6	[104]
	< 0.6 (non-traffic emission)	Pyrogenic - Combustion of solid fuel - natural sources such as biomass (grass and wood) and coal		

Appendix 7 Measured PAHs vs standard limits set by USEPA

Sample location	**∑PAHs***
	Measured value (ng/L)
S1	318.1
S2	243.0
S3	253.5
S4	403.9
S5	402.5
S6	375.0
S7	355.5
S8	421.8
S9	458.1
S10	357.2
S11	500.6
S12	562.7

* ∑ PAHs = Acy, BaA, BaP, BbF, BghiP, BkF, Chr, DBA, IND, and Phe (USEPA standard limit ≤ 31 ng/L)